WMO

INTERGOVERNMENTAL PANEL ON CLIMATE CHANGE

UNEP

## IPCC Working Group I

# Workshop on Climate Sensitivity

École Normale Supérieure
Paris, France
26–29 July, 2004

## Workshop Materials and Extended Abstracts

**IPCC Working Group I**

# Workshop on Climate Sensitivity

École Normale Supérieure, Paris, France, July 26–29, 2004

## WGI Co-Chairs

Susan Solomon (NOAA Aeronomy Laboratory, USA)
Qin Dahe (China Meteorological Administration, China)

## Scientific Steering Committee

### *Co-Chairs*

Sandrine Bony (Laboratoire de Météorologie Dynamique du CNRS, France)
Bryant McAvaney (Bureau of Meteorology Research Centre, Australia)
Gerald Meehl (National Center for Atmospheric Research, USA)

### *Committee Members*

George Boer (Canadian Centre for Climate Modelling and Analysis, Canada)
Chen Dehui (China Meteorological Administration, China)
William Collins (National Center for Atmospheric Research, USA)
Ulrich Cubasch (Freie Universität Berlin, Germany)
Jonathan Gregory (University of Reading, UK)
Sylvie Joussaume (National Institute for Sciences of the Universe, France)
Jean Jouzel (Institut Pierre Simon Laplace, France)
Akio Kitoh (Meteorological Research Institute, Japan)
Hervé Le Treut (Laboratoire de Météorologie Dynamique du CNRS, France)
Luo Yong (China Meteorological Administration, China)
Valentin Meleshko (Voeikov Main Geophysical Observatory, Russia)
V. Ramaswamy (NOAA Geophysical Fluid Dynamics Laboratory, USA)
Catherine Senior (Hadley Centre for Climate Prediction and Research, Met Office, UK)

## Acknowledgements

This workshop has been generously supported by the Institut Pierre Simon Laplace (PSL), École Normale Supérieure (ENS) and the Mission Interministérielle pour l'Effet de Serre (MIES).

## Local Organizers

Sandrine Bony (Laboratoire de Météorologie Dynamique du CNRS, France)
Jean Jouzel (Institut Pierre Simon Laplace, France)
Hervé Le Treut (Laboratoire de Météorologie Dynamique du CNRS, France)
Armella Longrez (Institut Pierre Simon Laplace, France)

## IPCC Working Group I Technical Support Unit

Martin Manning
Tahl Kestin
Scott Longmore
Melinda Tignor

# Contents

# Scoping Document for the IPCC Working Group I Workshop on Climate Sensitivity

IPCC Working Group I (WG I) will hold a workshop on the topic of Climate Sensitivity in 2004 as a major keystone in activities preparing for the WG I contribution to the IPCC Fourth Assessment Report (AR4).

## Background

One of the most important parameters in climate science is the 'climate sensitivity', broadly defined as the global mean temperature change (°C) for a given forcing, often that of a doubling of atmospheric carbon dioxide. Climate sensitivity has played a central role throughout the history of IPCC in interpretation of model outputs, in evaluation of future climate changes expected from various scenarios, and it is closely linked to attribution of currently observed climate changes. An ongoing challenge to models and to climate projections has been to better define this key parameter, and to understand the differences in computed values between various models. Throughout the last three IPCC assessments this basic parameter of the Earth's climate system has been estimated as being in the range 1.5 to 4.5°C (i.e., uncertain by a factor of three), making this parameter central to discussions of uncertainty in climate change.

WG I is concerned to sharpen understanding of the differences between general circulation models used in climate change research.

Currently the primary reason for the substantial range in model based estimates of climate sensitivity is widely believed to be differences in their treatment of feedbacks – particularly cloud feedbacks, but systematic intercomparisons have not been done to confirm that this is so for the current generation of models. Within international climate modeling projects, the development of new models together with both formal and informal model intercomparison exercises that are currently taking place by various groups suggest that a renewed focus on the reasons for different model estimates of climate sensitivity may be particularly useful at this time.

In addition, some recent studies suggest that new insights into the likely range of climate sensitivity may be possible through comparisons of models and observational data – both contemporary and historical or paleoclimatic. Observation/model intercomparisons will be a special focus of this workshop.

Other recent studies raise issues regarding the limitations of applicability of forcing/response relationships in the climate system - such as questions regarding the degree of predictability of climate and its relevance for estimates of climate sensitivity, and the degree to which forcings such as those due to solar, well-mixed greenhouse gases, or aerosols may produce different responses. A review of these questions about the interpretation of climate sensitivity could also sharpen scientific understanding and would hence be of benefit to the WG I AR4.

In summary, there is broad interest for a carefully planned workshop on climate sensitivity. Given the importance of the climate sensitivity parameter, it is likely that the outcome of this workshop will provide a major focus for the discussion and treatment of climate models in the WG I contribution to AR4.

## Aims

The aims of the climate sensitivity workshop would be to:

- Evaluate a range of climate model results so as to relate different climate sensitivity estimates to differences descriptions of physical processes, particularly those related to atmospheric water vapor, clouds, lapse rate changes, ocean heat uptake, treatment of evapotranspiration, land-atmosphere coupling, etc.;

- Obtain a more comprehensive picture of the relationships between climate sensitivity and other model features such as resolution, numerical approach, radiative transfer parameters, etc.;

- Consider how current, historical, and/or paleoclimatic data can aid in the determination of the likely range of climate sensitivity;

- Improve the understanding of the interpretation and limits of the climate sensitivity concept, including for example possible dependencies upon different forcing agents, predictability questions, and transient and steady-state responses;

- Start a process towards objective assessment to critically determine whether the range 1.5 to 4.5°C remains appropriate in the AR4 – e.g. by defining criteria that may assist in the evaluation of results from many different climate models.

## Approach and Timetable

Given the range of issues to be considered and the commitment that would be required from major modeling groups around the world, the process will be structured by a broad-based scientific steering group. Planning for the workshop will be carried out by the steering group. Organizational support for the meetings, and production of a workshop report will be carried out by the WG I TSU.

In order to include a carefully constructed intercomparison of climate model results as part of the proposed workshop, a preliminary expert meeting will foster explicit analysis of feedbacks, in collaboration with WCRP activities on this topic. The expert meeting is currently planned for April 2004 in Exeter, UK.

The workshop will take place on July 26-29, 2004 in Paris, France.

## Program Overview

Note: participants will receive the full program separately

### DAY 1: Monday, 26 July

*Introduction and Overview Session*

*Climate Sensitivity from Models*

### DAY 2: Tuesday, 27 July

*Radiation Code Intercomparisons and Climate Sensitivity*

*Climate Sensitivity PDFs and Measures*

*Paleoclimatic Observations and Climate Sensitivity*

### DAY 3: Wednesday, 28 July

*Modern Observations and Deduced Climate Sensitivity*

*Breakout Session 1*

BG 1: Climate sensitivity from models (Leaders: G. Meehl, B. McAvaney)
Short presentations on equilibrium sensitivity and TCR from each modelling group, and how these relate to IPCC TAR numbers; what are the new ranges for equilibrium and TCR and why have these ranges changed.

BG 2: Climate sensitivity from observations (Leaders: S. Bony, J. Gregory)
Specify the best estimate and range for climate sensitivity from observations and recommend a preliminary database of observations.

### DAY 4: Thursday, 29 July

*Breakout Session 2*

BG 3: Radiative transfer and forcing (Leaders: W. Collins, V. Ramaswamy)
Compare and assess radiation codes and forcings used in GCMs, including globally averaged and geographic patterns of forcings.

BG 4: Probabilistic approaches to climate sensitivity (Leaders: C. Senior, G. Boer)
Assess techniques to formulate probabilistic estimates of climate sensitivity and propose an approach to climate sensitivity evaluation (including pdfs) for the AR4.

*Closing Plenary*

# Introduction to Breakout Groups

## Breakout Group 1: Climate Sensitivity from Models

*Chairs: G. Meehl and B. McAvaney*

The breakout session will include short presentations by representatives of each modeling group on equilibrium sensitivity and TCR, how these relate to IPCC TAR numbers, the new ranges for equilibrium and TCR, and why these ranges have changed.

The representatives have been asked to specifically address the following questions:

1. What is the equilibrium sensitivity of your model (surface air $\Delta T$ equilibrium $2XCO_2$ minus control with atmosphere coupled to slab ocean)?

2. What is the transient climate response (TCR) of your model (surface air $\Delta T$ for years 61-80 of a transient 1% per year $CO_2$ increase minus control, where $CO_2$ doubles around year 70)?

3. What is the percent change in globally averaged precipitation in your equilibrium 2XCO2 simulation compared to control with atmosphere coupled to slab ocean?

4. What is the percent change in globally averaged precipitation in your 1% $CO_2$ simulation (percent change for years 61-80 of a transient 1% per year $CO_2$ increase compared to control)?

5. How do these compare to previous versions of your model, and to the numbers given in the TAR (e.g. Fig. 9.18)?

6. Why have these changed (e.g. what factors have the greatest influence on sensitivity in your model)?

## Breakout Group 2: Climate Sensitivity from Observations

*Chairs: S. Bony and J. Gregory*

Climate sensitivity, that characterizes the link between forcing and response in climate, critically depends on the sign and on the magnitude of feedback processes. These processes differ among models, and this presumably explains a large part of uncertainties associated with the magnitude and rate of climate change projections. Observations may help to constrain climate sensitivity and thereby reduce these uncertainties.

The main objectives of that breakout group will be:

- **To point out key physical mechanisms thought to be critical for climate sensitivity that may be constrained by available observations.**
    - put particular attention on mechanisms related to water vapor, clouds and sea-ice feedbacks, as well as to the ocean heat uptake.
    - invoke suggestions from theory, simple climate models, analysis of GCM simulations (of current, past or future climate) and observations.
    - suggest specific analyses or diagnostics that can be applied both to observations and to model simulations, and to past and future climate change simulations.
    - consider the definition of a set of observed diagnostic tests or metrics related to feedback processes against which climate models may be evaluated. This discussion will be developed in BOG4, in particular the methods whereby that metrics may be used to interpret and to narrow the range of models climate sensitivity.
- **To estimate a range for global climate sensitivity derived (primarily) from observations.**
    - Based on observations of paleoclimate changes, last several centuries proxies, 20th century climate evolution, and volcanic eruptions.
    - Based on the combined use of observations and simple models.
    - These discussions will be developed in BOG4.

A brief introduction will be followed by discussions (illustrated eventually by 1 or 2 transparencies from contributors) among people from different communities (theory, models, observations, future climate changes, past climate changes).

Anticipated products:

- the identification of observations relevant to constraining climate sensitivity.
- the proposition of a set of observed diagnostic tests, or metrics, that may be used to assess the feedbacks produced by climate models.

## Breakout Group 3: Radiative Transfer and Forcing

*Chairs: W. Collins and V. Ramaswamy*

BOG3 will focus on two principal issues:

1) Radiative forcing intercomparison. This will be comprised of a comparison of various line-by-line computations that have been performed as part of the IPCC intercomparison project that Bill and I are leading. Also, as part of the comparison, the results from the GCM codes will be evaluated, with the line-by-line results considered to be the "benchmarks". We will determine the extent of the agreements, and attempt to evaluate the reasons for the differences amongst models and between models and LBLs. We will also place the results in the context of the forcing values documented in TAR. Also of note is the particular model experiment related to influence of water vapor change on the forcing. We hope to address the issue of how comparable and reliable are radiation codes for evaluating the forcing, and water vapor's influence on the forcing by the well-mixed gases. (See Annex 2 for the letter that was sent to the modeling groups regarding the intercomparison project.)

2) We will rely on the results of the ongoing AEROCOM project to deal with the issue of intercomparison of the radiative forcing due to sulfate aerosols. AEROCOM has undertaken an intercomparison of burdens, optical depths and flux changes associated with sulfate aerosols. We hope to get geographical maps and address the question of how comparable are radiative codes and forcing in the case of sulfate aerosols.

## Breakout Group 4: Probabilistic Estimates of Climate Sensitivity

*Chairs: C. Senior and G. Boer*

### *Introduction*

Many recent studies have addressed the possibility of producing probability based estimates of climate sensitivity, in terms of it probability distribution function $p(s)$ to reflect the uncertainty in this parameter in a more quantitative way. In this BOG we will deal with estimates of $p(s)$ based on observations, simple models and full GCMs. We will also investigate the possibility of applying observational constraints on $p(s)$ and other variables. BOG4 will deal broadly with:

- Estimates of sensitivity s and its probability distribution $p(s)$ based on a combination of observations and models
- Methods of constraining $s$, $p(s)$ and $T$

The investigation of sensitivity $s$ and its pdf $p(s)$ will include:

- studies based on the instrumental record, paleoclimate information and special events such as the Pinatubo eruption in conjunction with simple models (e.g. Gregory et al., 2002; Andronova and Schlesinger, 2001; Forest et al., 2002, 2001, 2000; Knutti et al., 2002; Soden et al., 2002; Forster and Collins, 2004[1])
- estimates of $s$ and $p(s)$ based on available coupled models results and ensembles of results obtained by perturbing physical processes (e.g. Murphy et al., 2004; Stainforth et al., 2004; Raisanen and Palmer, 2001)

The use of observations and simple models to constrain climate sensitivity will refer to the parallel discussions in BOG2. BOG4 will also focus on:

- methods of constraining $s$ and estimating $p(s)$ using the diagnostics and climate metrics developed from the investigation of physical mechanisms of importance to climate (ref. BOG2, Wielicki et al. in Senior et al., 2004 (Annex 1 in this volume)
- constraints on the evolution of temperature and other variables (Allen, pers com)

### *Program*

Brief introductions will be followed by discussions (illustrated by 1 or 2 transparencies from contributors)

[1] See Annex 1 in this volume for a list of the references cited here.

## Extended Abstracts

* Speaker

**IPCC Workshop on Climate Sensitivity**
Paris, France, July 26–29, 2004
*Pre-Conference Volume*

# Water Vapour Feedback Observations and Climate Sensitivity

Richard P. Allan

*Environmental Systems Science Centre (ESSC), University of Reading*

The response of atmospheric moisture to changes in surface temperature (Ts) determines to a large extent the sensitivity of the climate system to a radiative perturbation. Aside from the indirect influence of moisture changes on cloud feedbacks, a primary component of the direct water vapour feedback ($\beta_{wv}$) is encapsulated by,

$$\beta_{wv} \approx \left( \frac{\partial OLR_C}{\partial WV} \right) \left( \frac{\partial WV}{\partial Ts} \right), \quad (1)$$

where *OLRc* is the clear-sky outgoing longwave radiation and *WV* is a generic water vapour variable. An important step in diagnosing water vapour feedback from observations is therefore to establish a relationship between water vapour concentrations and the surface temperature. Although it is only possible to measure *dWV/dTs* rather than *∂WV/∂Ts*, it is possible to reduce this difference by removing the effects of the large scale circulation on the local changes in *WV*. This may be achieved by subsampling dynamical regimes (e.g. Bony *et al.* (1997), Allan *et al.* (2002c)) or by averaging over the large-scale circulation systems (e.g. Allan *et al.* (2002a)).

An important theoretical constraint on the water vapour feedback is the Clausius Clapeyron equation which predicts an approximately exponential increase in water vapour with temperature where relative humidity (*RH*) is conserved (e.g. Raval and Ramanathan (1989)). Wentz and Schabel (2000) demonstrated an observed increase in column integrated water vapour (*CWV*) with *Ts* of about 9% $K^{-1}$, close to that predicted by the Clausius Clapeyron equation, by analysing trends over the ocean. In Fig. 1a-b both models and satellite observations show excellent agreement in the relationship between *CWV* and *Ts* over a decadal time-scale (see also Soden (2000)) with *dCWV/dTs* = 3.5 kg $m^{-2}$ (≈ 9% $K^{-1}$).

Given the strong coupling between ocean surface temperature and boundary layer water vapour, which is the primary determinant of *CWV*, it would be surprising if the relationship between marine *CWV* and *Ts* did not hold. However, *OLRc* is sensitive to humidity changes throughout the troposphere (e.g. Allan *et al.* (1999)) so it is therefore important also to evaluate the free tropospheric moisture changes simulated by models. One possibility is to use reanalyses which assimilate a variety of observations into an atmospheric model and output variables such as the vertical profiles of atmospheric water vapour globally. However, the changing quality of the observational input to reanalyses render the presently available products unsuitable for the analysis of water vapour feedback (Trenberth *et al.* (2001), Allan *et al.* (2002b), Allan *et al.* (2004)).

Because *OLRc* is highly sensitive to humidity throughout the troposphere it is feasible to use *dOLRc/dTs* as a proxy for $\beta_{wv}$ (e.g. Raval and Ramanathan (1989), Slingo *et al.* (2000)). Cess *et al.* (1990) demonstrated good agreement between model *dOLRc/dTs* and interpreted this as consistency in water vapour feedback. Agreement between observed and simulated variations in *OLRc* (Soden (2000), Allan and Slingo (2002)) suggest that the simulated water vapour feedback is realistic. For example, Fig. 1c shows reasonable agreement between observed and model simulated normalised greenhouse trapping, $g_a = 1 - (\sigma Ts^4/OLRc)$, with increased greenhouse trapping during warm events, symptomatic of positive water vapour feedback (Allan *et al.* (2003)). However, as demonstrated in Fig. 1c (dashed line), $g_a$ is also sensitive to forcings such as greenhouse gas concentration changes and volcanic aerosols which may confuse the diagnosis of water vapour feedback from analysing broadband radiative fluxes. In addition to this limitation, similarity in *dOLRc/dTs* does not necessarily indicate consistency in water vapour feedback. For example, Allan *et al.* (2002a) showed that 2 models with identical forcings produced a similar sensitivity, *dOLRc/dTs* ≈ 2 W $m^{-2}$ $K^{-1}$, but contained rather different temperature and water vapour profile responses to *Ts* over an interannual time-scale. The discrepancy, which was ascribed to differences in the model convection parametrizations, raises questions as how best to diagnose water vapour feedback (see also Held and Soden (2000)) and how the water vapour, temperature lapse rate and cloud feedbacks may interact.

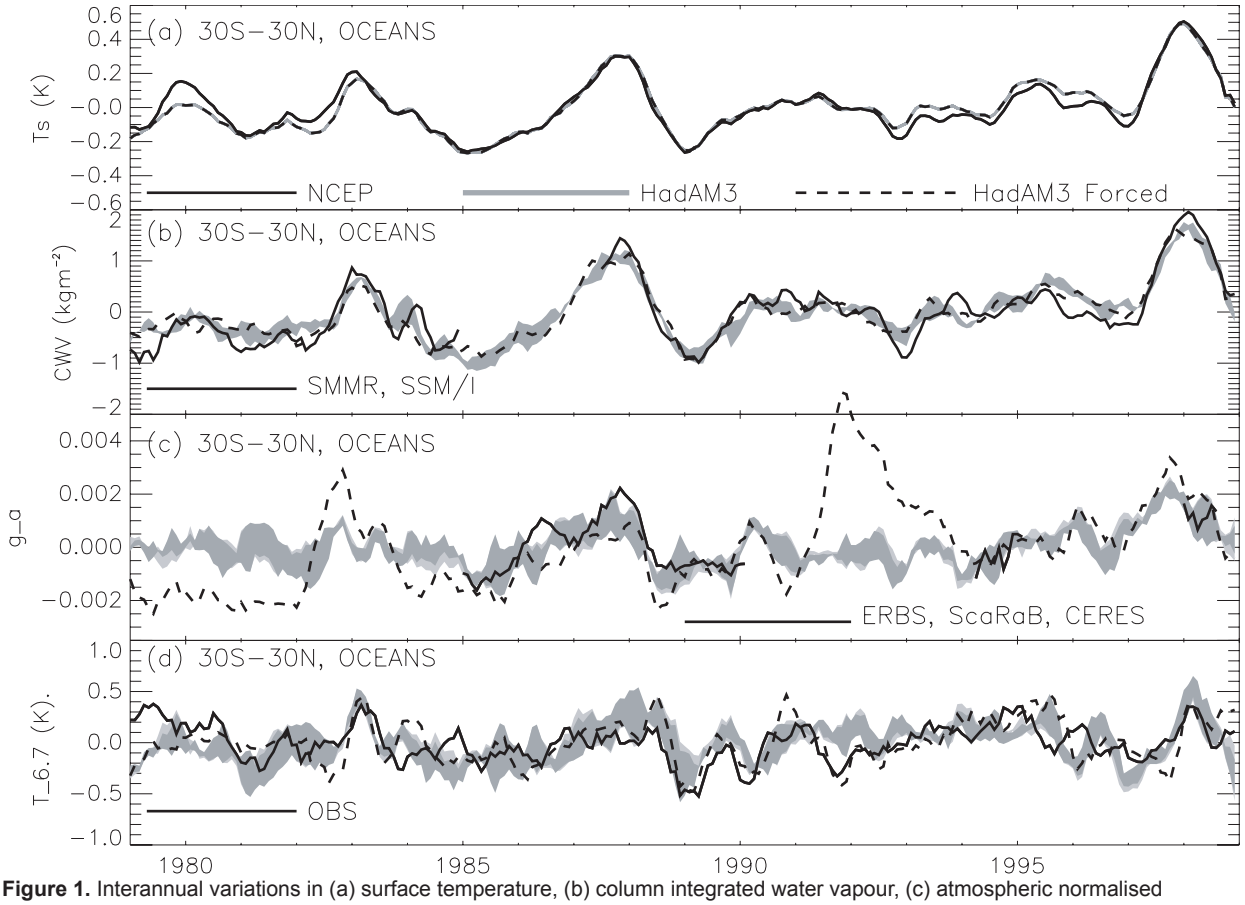


**Figure 1.** Interannual variations in (a) surface temperature, (b) column integrated water vapour, (c) atmospheric normalised greenhouse trapping and (d) 6.7 μm brightness temperature for sea surface temperature (SST) forced model (shaded), model with all known forcings (dashed) and observations (solid) (from Allan *et al.* (2003).

Colman (2003) compared climate feedbacks from a variety of models and found a large compensation between water vapour and temperature lapse rate feedback, consistent with the analysis of Allan *et al.* (2002a). Based on the apparent robust nature of modelled and observed constant relative humidity water vapour feedback feedback (e.g. Ingram (2002), Soden *et al.* (2002)) it seems reasonable to check for departure from this theoretical relationship by measuring the feedback, if any, involving relative humidity. An additional benefit of this approach is the potential applicability to cloud feedbacks given the strong relationship between *RH* and cloudiness (e.g. J. M. Slingo (1980)). Thus it is important to evaluate the sensitivity of *OLRc* to *RH* ($\partial OLRc/\partial RH$) and to diagnose the changes in *RH* in response to *Ts*.

Figure 2 illustrates a technique to estimate $\partial OLRc/\partial RH$ by computing *dOLRc/dUTH* using the results of Allan *et al.* (2003). Here, *dOLRc/dUTH* is calculated at each tropical grid-point from interannual monthly anomalies, plotted as a function of mean *UTH* where *UTH* is estimated from observations *and* simulations of 6.7 μm radiances. The increasingly negative *dOLRc/dUTH* with decreasing humidity is consistent with previous studies (e.g. Spencer and Braswell (1997)) although the model appears to overestimate the magnitude of this sensitivity, especially at low humidities compared with the combined ERBS and HIRS satellite observations. Regardless of the approximate relationship, $dOLRc/dUTH \approx 0.5\%\ K^{-1}$, the departure from a constant relative humidity water vapour feedback appears small on the interannual time-scale because changes in 6.7 μm radiance (or equivalent brightness temperature, $T_{6.7}$) are small and not significantly correlated with *Ts* (Fig. 1d; Allan *et al.* (2003)). Although $T_{6.7}$ does not appear to be directly influenced by additional forcings (see dashed line in Fig. 1d) the relationship between $T_{6.7}$ and *UTH* may not be robust on interannual time-scales where temperature changes may also influence changes in $T_{6.7}$ (Allan *et al.* 2003). Therefore, these techniques may need to be further refined. Finally, understanding the links between *Ts*, *RH*, cloudiness and the large-scale dynamics may improve our understanding of climate feedbacks and how they interact with one another (e.g. Hartmann *et al.* (2001)).

**References**


Allan, R. P. and Slingo, A. (2002). Can current climate model forcings explain the spatial and temporal signatures of decadal OLR variations? *Geophys. Res. Lett.,* **29,** 0.1029/2001GL014620.

Allan, R. P., Shine, K. P., Slingo, A., and Pamment, J. A. (1999). The dependence of clear-sky outgoing longwave radiation on surface temperature and relative humidity. *Quart. J. Roy. Meteorol. Soc.,* **125,** 2103–2126.

Allan, R. P., Ramaswamy, V., and Slingo, A. (2002a). A diagnostic analysis of atmospheric moisture and clear-sky radiative feedback in the Hadley Centre and Geophysical Fluid Dynamics Laboratory (GFDL) climate models. *J. Geophys. Res.,* pages 4329, doi 10.1029/2001JD001131.

Allan, R. P., Slingo, A., and Ramaswamy, V. (2002b). Analysis of moisture variability in the European Centre for Medium-Range Weather Forecasts 15-year reanalysis over the tropical oceans. *J. Geophys. Res.,* **107,** 4230, doi 10.1029/2001JD001132.

Allan, R. P., Slingo, A., and Ringer, M. A. (2002c). Influence of dynamics on the changes in tropical cloud radiative forcing during the 1998 El Niño. *J. Climate,* **15,** 1979–1986.

Allan, R. P., Ringer, M. A., and Slingo, A. (2003). Evaluation of moisture in the Hadley Centre climate model using simulations of HIRS water-vapour channel radiances. *Quart. J. Roy. Meteorol. Soc.,* **129,** 3371–3389.

Allan, R. P., Ringer, M. A., Pamment, J. A., and Slingo, A. (2004). Simulation of the Earth's radiation budget by the European Centre for Medium Range Weather Forecasts 40-year reanalysis (ERA40). *J. Geophys. Res.,* **accepted.**

Bony, S., Lau, K., and Sud, Y. C. (1997). Sea surface temperature and large-scale circulation influences on tropical greenhouse effect and cloud radiative forcing. *J. Climate,* **10,** 2055–2077.

Cess, R. D., and coauthors (1990). Intercomparison and interpretation of climate feedback processes in 19 atmospheric general circulation models. *J. Geophys. Res.,* **95,** 16601–16615.

Colman, R. (2003). A comparison of climate feedbacks in general circulation models. *Climate Dynamics,* **20,** 865–873.

Hartmann, D. L., Moy, L. A., and Fu, Q. (2001). Tropical convection and the energy balance at the top of the atmosphere. *J. Climate,* **14,** 4495–4511.

Held, I. and Soden, B. J. (2000). Water vapor feedback and global warming. *Ann. Rev. Energy Environ.,* **25,** 441–475.


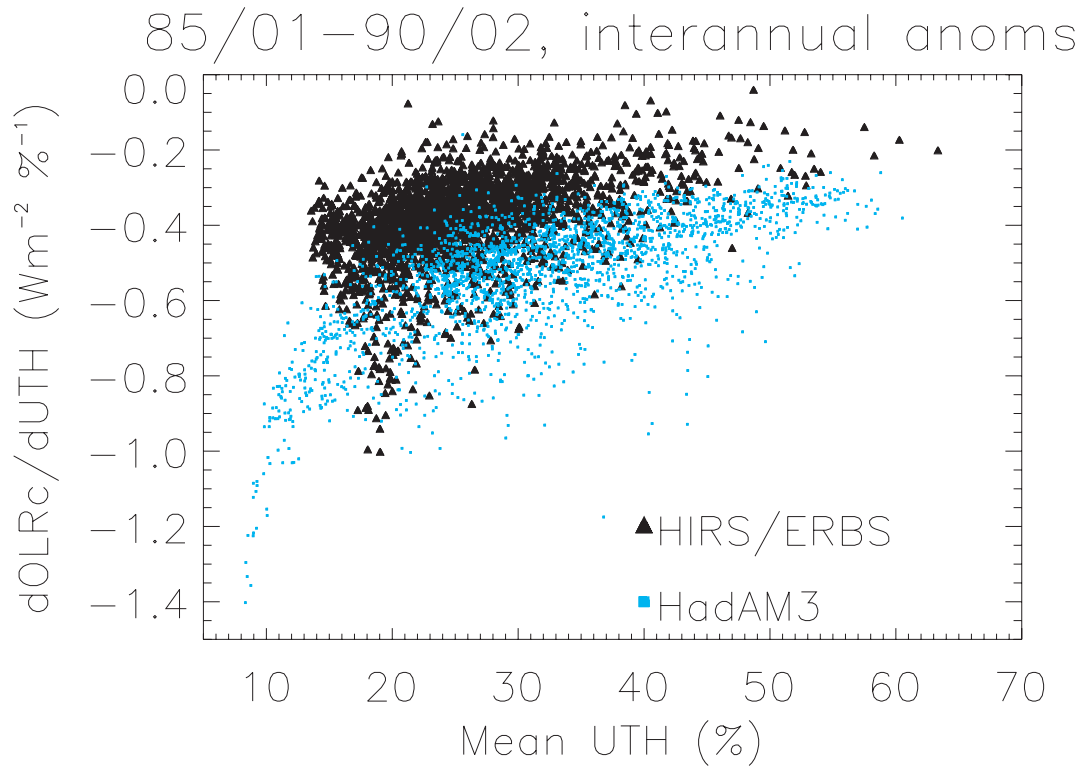


**Figure 2.** Sensitivity of clear-sky OLR to upper tropospheric humidity (UTH) as a function of mean UTH for the HadAM3 model and satellite observations.

Ingram, W. J. (2002). On the robustness of the water vapor feedback: GCM vertical resolution and formulation. *J. Climate,* **15,** 917–921.

Raval, A. and Ramanathan, V. (1989). Observational determination of the greenhouse effect. *Nature,* **342,** 758–761.

Slingo, A., Pamment, J. A., Allan, R. P., and Wilson, P. (2000). Water vapour feedbacks in the ECMWF Re-Analyses and Hadley Centre climate model. *J. Climate,* **13,** 3080–3098.

Slingo, J. M. (1980). A cloud parameterization scheme derived from GATE data for use with a numerical model. *Quart. J. Roy. Meteorol. Soc.,* **106,** 747–770.

Soden, B. J. (2000). The sensitivity of the tropical hydrological cycle to ENSO. *J. Climate,* **13,** 538–549.

Soden, B. J., Wetherald, R. T., Stenchikov, G. L., and Robock, A. (2002). Global cooling after the eruption of Mount Pinatubo: a test of climate feedback by water vapor. *Science,* **296,** 727–730.

Spencer, R. W. and Braswell, W. D. (1997). How dry is the tropical free troposphere? Implications for global warming theory. *Bull. Amer. Met. Soc.,* **78,** 1097–1106.

Trenberth, K. E., Stepaniak, D. P., Hurrell, J. W., and Fiorino, M. (2001). Quality of reanalyses in the tropics. *J. Climate,* **14,** 1499–1510.

Wentz, F. J. and Schabel, M. (2000). Precise climate monitoring using complementary satellite data sets. *Nature,* **403,** 414–416.

**IPCC Workshop on Climate Sensitivity**
Paris, France, July 26–29, 2004
*Pre-Conference Volume*

# Observational Constraints and Prior Assumptions on Climate Sensitivity

David Frame and Myles Allen

*Atmospheric, Oceanic and Planetary Physics, University of Oxford, Clarendon Laboratory, Parks Road, Oxford OX1 3PU, UK*

**Abstract:** The commitment to "stabilise atmospheric greenhouse gas concentrations" below a "dangerous" level appears to require an objective range of uncertainty in equilibrium climate sensitivity (ECS). We find that any such range depends critically on subjective prior assumptions regarding the distribution of ECS before any physical or observational constraints are applied. This is particularly true of the likelihood assigned to the high sensitivity values that are most relevant to any assessment of whether a given stabilisation level is considered "dangerous". Indefinite stabilisation is, however, an unrealistic scenario. We argue that objective ranges of uncertainty on scientific inputs to most policy-relevant questions require a constraint on the transient climate response (TCR), not on ECS. These inputs include predicted transient 1990-2100 warming under the full range of emissions scenarios, peak warming assuming a realistic decline in greenhouse gas levels after the 21st century and the warming commitment due to greenhouse gas emissions to date. TCR is well constrained by the warming attributable to greenhouse gases over the 20th century, providing a robust and objective constraint on policy-relevant questions, bypassing the need for an objective range on ECS. The inherent difficulty in placing objective upper bounds on ECS means that policies aiming to avoid dangerous anthropogenic interference in the climate system may need to be formulated in terms of a peak concentration and subsequent minimum rate of decline rather than indefinite stabilisation.

All studies attempting to constrain sensitivity objectively can be couched in a Bayesian formulation in which the "posterior distribution", *P(ECS|data)*, is proportional to the "likelihood" of the data assuming a given value of ECS (specifically, the likelihood of obtaining a model consistent with observations and with this particular value of ECS, *P(data|ECS)*) multiplied by the "prior", *P(ECS)*. Recent studies [1,2,3] using the combination of observed warming over the 20th century and estimates of the recent rise in ocean heat content [4] to constrain ECS have arrived at highly asymmetric posterior distributions, assigning a relatively high likelihood to high sensitivities. The reason is the well-documented non-linear relationship between ECS and observed greenhouse-induced warming under almost any transient forcing scenario [5,6]: sensitive climates take longer to reach equilibrium, making it difficult to place an upper bound on ECS based on transient warming to date.

This point is illustrated in the figure (a) on the next page, which shows the relationship between ECS (colour coding), warming attributable to greenhouse gases over the 20th century (vertical axis) and effective heat capacity of the atmosphere/ocean system (horizontal axis) in a simple climate model driven with observed greenhouse gas forcing. Although ECS has been sampled uniformly over the range 0.17 to 20K, the diamonds are not distributed uniformly in the vertical because of the non-linear relationship between ECS and transient response.

The black ellipse in figure (a) encloses the region consistent, at the 95% level, with the combination of warming attributable to greenhouse gases over the 20th century [7] and the effective heat capacity implied by observations of surface and subsurface temperature change over the 1957-1997 period [4]. The ellipse is based on published estimates of uncertainty in greenhouse and other forcings as well as surface and subsurface temperature trends: although contentious, these do not affect our basic point. If, following refs. [1-3], we assume a uniform ("neutral") prior in ECS and heat capacity (all diamonds equally likely before the comparison with observations is made) and subsequently weight the diamonds by the likelihood of the observations given each particular combination of ECS and heat capacity, the resulting distribution *P(ECS|data)* is shown as the red curve in figure (c). The "fat tail" extending out to high sensitivities arises from the fact that the ellipse in figure (a) includes a region (upper right quadrant) where the prior density, *P(ECS)*, is very high in the space defined by the observable quantities used to constrain the forecast.

A very different approach is taken by ref. [8], who perturb parameters in a climate model, weight the members of the resulting "perturbed-physics ensemble"

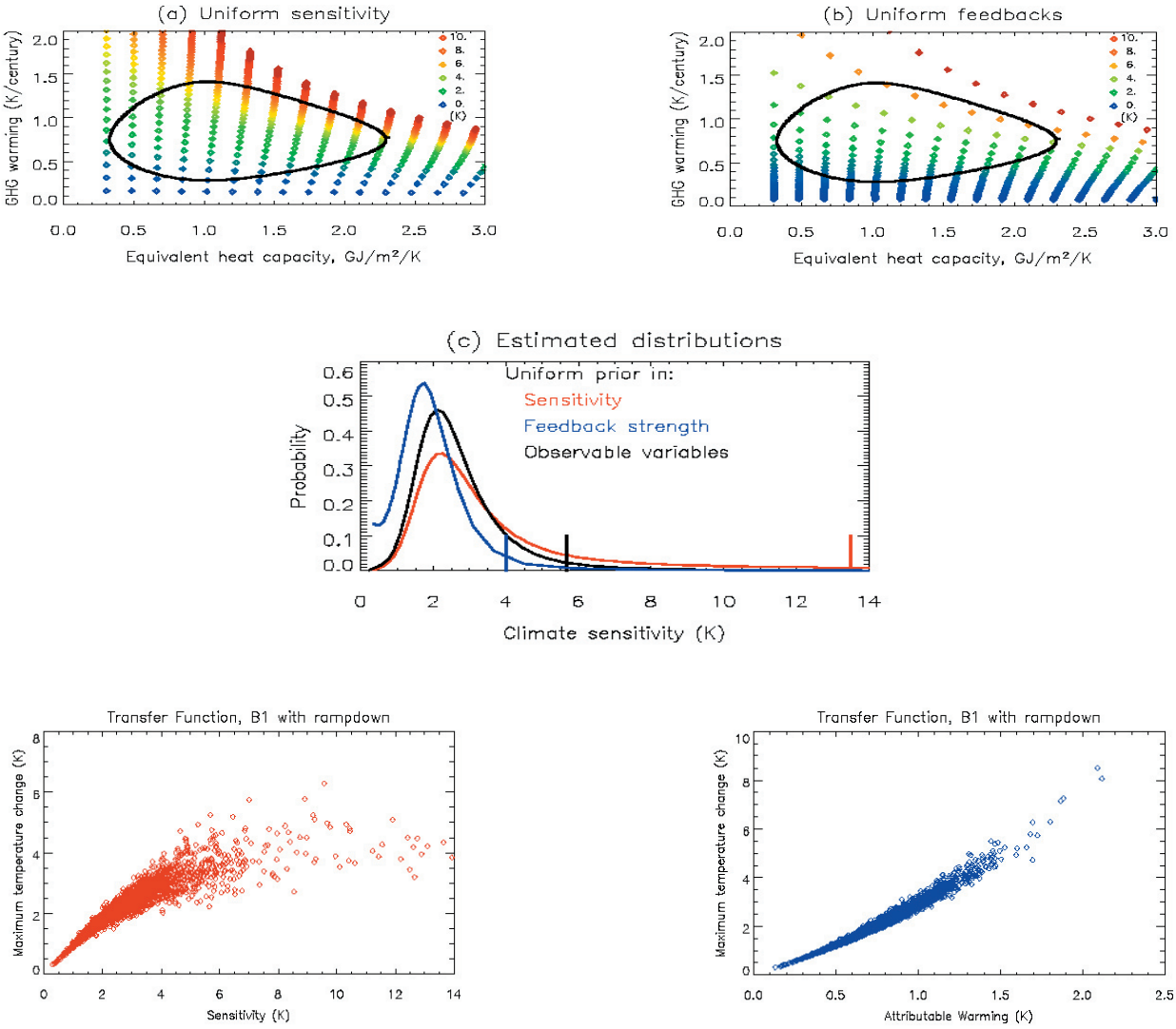


**Figure.** (a) and (b): Relationship between climate sensitivity (colours), effective ocean heat capacity and 20th century warming attributed to changes in greenhouse gases. Diamonds show energy balance model simulation results based on (a) uniform sampling of climate sensitivity, *S*, and (b) uniform sampling of feedback strength, or 1/*S*. Black contours enclose the region consistent with observations at the 5% level. Panel (c) shows distributions of climate sensitivity based on these observations, assuming a uniform prior in sensitivity (red), in feedback strength (blue) and in attributable warming and heat capacity (black), with vertical lines showing 95th percentiles. Panel (d) shows the relationship between climate sensitivity and peak warming under a B1 scenario followed by a ramp-down over the 22nd and 23rd centuries, while (e) shows the corresponding relationship between past attributable warming and peak warming under a B1-plus-rampdown scenario.

by a measure of their similarity to observed present-day climatology (as opposed to recent climate change), and infer a distribution for ECS from the weighted ensemble. They sample parameters to provide a uniform distribution of the atmospheric feedback parameter, λ, which is inversely proportional to ECS, before the constraints of the perturbed-physics ensemble and climatology are applied. We can do the same with our simple model, and the result is shown in figure (b). Because we have now sampled 1/(ECS) uniformly in place of ECS, diamonds cluster towards the horizontal axis. After applying the likelihood-weighting, the resulting posterior distribution for ECS is shown by the blue curve in figure (c), which suggest a much (factor of 3) lower 95th percentile for ECS. Which upper bound is correct?

What we are seeing is a version of "Bertrand's paradox": suppose we have a mixture of water and wine and know only that the ratio of water to wine is somewhere between 2:1 and 1:1. For each unit of wine, we have between 1 and 2 units of water, so in the absence of further information, our "best guess" is 1.5 units of water, implying a ratio of 3:2. But for each unit of

water, we have between 0.5 and 1 unit of wine, so a "best guess" of 0.75, implying a ratio of 4:3. The difference arises from the fact that assuming a uniform prior in water:wine ratio is not the same as assuming a uniform prior in wine:water ratio, just as assuming a uniform prior in ECS is not the same as a uniform prior in λ, or 1/ECS. The importance of this point depends on the level of uncertainty: the 5-95% range on ECS is still relatively large, making the impact of the prior distribution quite dramatic.

The resolution of Bertrand's paradox is to clarify the question: *why* are we interested in knowing the ratio of water to wine? If we have drunk a glass of the mixture and want to know the amount of wine we have drunk, then the answer is somewhere between 0.33 and 0.5, with a best guess of 0.42, corresponding to a ratio of 7:5. The key is to apply the principle of indifference (uniform prior) to the quantity we are interested in, not to incidental quantities that are used to derive it, like the water-to-wine ratio or the ECS.

The only circumstance in which ECS is directly relevant to policy is when we are considering the response to an indefinite stabilisation scenario and quantifying the risk of climate impacts that are linear in the long-term equilibrium warming. A strict interpretation of Article 2 of the UNFCCC suggests that this is the principal objective of policy, in which case the relevant prior to use is uniform in ECS. Unfortunately, efforts to provide a range of uncertainty in ECS beginning from this prior, whether constraining ECS through the analysis of atmospheric feedbacks, through the comparison of climate models with climatology or through analysis of the transient response all continue to yield a high upper bound. The reason is that the first two approaches tend to provide information on λ, while the third approach yields information on TCR, neither of which is linearly related to ECS, with $d(\lambda)/d(ECS)$ and $d(TCR)/d(ECS)$ (which determine their information content with respect to sensitivity) both tending to zero as ECS increases. If the 95th percentile on ECS exceeds 7K, for example, then there is a significant (>5%) risk of a warming in excess of 4K even if atmospheric concentrations are stabilised at 450ppmv. Hence, if we assume an indefinite stabilisation scenario, there is a sense in which no stabilisation target currently under discussion can be considered “safe”.

How realistic, however, is an indefinite stabilisation scenario? Because of the relationship between sensitivity and adjustment time, these high-end sensitivities only materialise if concentrations are held constant at the stabilisation target for many decades, or even centuries. It is surely more plausible that future generations, having already reduced greenhouse gas emissions by 60-80% to achieve stabilisation, will be able to continue reducing emissions sufficiently to allow atmospheric concentrations to decline. Even a modest rate of decline (less than 10% over the first 40 years of the 22nd century after following the B1 scenario to 2100) means that the peak warming ceases to scale with ECS (figure d). In this simple model, the peak warming under such a concentration path is close to linear in both TCR and past attributable warming (figure e). TCR is also a better predictor than ECS for transient warming to 2100 under both A1FI and B1 scenarios [5,6] and for the warming commitment due to past emissions (the peak warming if emissions were to cease tomorrow).

Hence we propose that studies attempting to constrain climate sensitivity objectively will be most relevant to many policy questions if they begin by applying the principle of indifference to (assuming a uniform prior in) TCR rather than ECS or λ. This is almost exactly equivalent to assuming a uniform prior in past attributable warming [9]: the posterior distribution for ECS assuming this prior is shown by the black curve in figure (c). In this simple comparison with the transient response over the 20th century, this yields a 10-90% range for climate sensitivity of 1.3-4.5K, with a median value of 2.5K, in remarkably close agreement with the "classic" IPCC range of uncertainty [10].

**References**


1. N.G. Andronova and M.E. Schlesinger. Causes of global temperature changes during the 19th and 20th centuries. *Geophysical Research Letters*, 27:2137–3140, 2000.
2. C. E. Forest, P. H. Stone, A. P. Sokolov, M. R. Allen, and M. D.Webster. Quantifying uncertainties in climate system properties with the use of recent climate observations. *Science*, 295:113–117, 2002.
3. R. Knutti, T.F. Stocker, F. Joos, and G.K. Plattner GK. Constraints on radiative forcing and future climate change from observations and climate model ensembles. *Nature*, 416:719–723, 2002.
4. S. Levitus, J. Antonov, T. Boyer & C. Stephens, Warming of the world ocean. *Science* **287,** 2225–2229, 2000.
5. J. Hansen, G. Russell, A. Lacis, I. Fung & D. Rind, Climate response times: Dependence on climate sensitivity and ocean mixing. *Science* 229, 857–859, 1985.
6. M. R. Allen, P. A. Stott, J. F. B. Mitchell, R. Schnur and T. Delworth, Uncertainty in forecasts of anthropogenic climate change, *Nature*, **41**7,617-620, 2000.

7. P. A. Stott and J. A. Kettleborough. Origins and estimates of uncertainty in predictions of twenty-first century temperature rise. *Nature*, 416:723–726, 2002.
8. J. M. Murphy, D. M. H. Sexton, D. N. Barnett, G. S. Jones, M. J. Webb, M. Collins and D. A. Stainforth, Quantification of modelling uncertainties in a large ensemble of climate change simulations, *Nature*, to appear, 2004
9. J. M. Gregory, R. Stouffer, S. Raper, N. Rayner, and P. A. Stott. An observationally-based estimate of the climate sensitivity. *Journal of Climate*, 15, 2002. 3117-3121, 2002.
10. T. Wigley & S. Raper, Interpretation of high projections for global-mean warming. *Science*, **293**, 451-454, 2001.

**IPCC Workshop on Climate Sensitivity**
Paris, France, July 26–29, 2004
*Pre-Conference Volume*

# Aerosol Forcing and pdfs of Climate Sensitivity

Natalia G. Andronova and Michael E. Schlesinger

*Climate Research group, Department of Atmospheric Sciences, University of Illinois at Urbana-Champaign, natasha@atmos.uiuc.edu and schlesin@atmos.uiuc.edu*

According to recent findings, the radiative forcing by anthropogenic tropospheric aerosol maybe an offset for the strongly positive radiative forcing due to anthropogenic greenhouse gases. This offset would result in higher climate sensitivity, as required to reproduce the recent trend in the observed near surface temperature. Uncertainties in the estimation of the magnitude of the aerosol forcing are greater than for the well-mixed greenhouse gases. This is mostly due to the different nature of aerosols and their ability to modify the radiative properties of other important climate agents such as clouds and ice and snow. Here we discuss the uncertainties of the aerosol forcing and how they influence the estimation of the sensitivity of the climate system.

### Introduction

The 2001 IPCC Report estimated the total aerosol forcing as having a mean value of –0.5 W/m$^2$ and an uncertainty range of –4.1 to 0.4 W/m$^2$, mostly due to uncertainties in the indirect sulfate aerosol forcing. These estimates, which included sulfate, mineral dust, black and organic carbon from burning fossil fuel, and organic carbon from biomass burning, were based on *direct* calculations of the forcing using comprehensive radiative transfer and chemical transport models.

Recently, the IPCC estimates have been revised in two ways. First, Boucher and Haywood (2001), using different assumptions about the distribution of aerosol forcing within the IPCC range, ran a Monte-Carlo simulation to construct probability density functions (pdfs) for the radiative forcing, and particularly for the total aerosol forcing. They obtained a mean value of –1.6 W/m$^2$ and a 5% to 95% confidence interval of –3 W/m$^2$ to –0.5 W/m$^2$, respectively. Their analysis showed that their pdfs are very sensitive to how they treated the distribution of the indirect sulfate aerosol forcing values. Second, Hansen and Sato (2001) revised their own estimates of the total aerosol forcing published in 1998 to obtain a total aerosol forcing with a mean of –0.6 W/m$^2$ and an uncertainty range of –0.6±1.1 W/m$^2$. In the latter work the uncertainty range was skewed to the right toward less negative forcing, thereby allowing for the uncertainties due to carbonaceous aerosol and, particularly, due to the black carbon. Our synthesis of the data described above is presented on Fig. 1A.

The "*inverse*" estimations of the aerosol forcing have been based on comparison of multiple simulations by a simple climate model of the temperature change due to various sets of radiative forcings in comparison with the historical observational record. Most of these estimations included constraints on the direct and/or indirect sulfate forcing. Our pdf synthesis of all "inverse" estimations of the aerosol forcings (Wigley and Raper, 2001; Andronova and Schlesinger, 2001; Gregory et al, 2002; Knutti et al, 2002, Forest et al, 2002), together with the direct IPCC estimation of the sulfate forcing, are presented in Fig.1B. From Fig. 1B it can be seen that the range of uncertainties for the inverse calculations are much smaller than for the direct calculations. Our own "inverse" calculations of the aerosol forcing (Andronova and Schlesinger (AS), 2001), based on the hemispheric version of our simple climate model, showed that adding any positive forcing, such as tropospheric ozone forcing, to the suite of radiative forcings moves the entire distribution of the sulfate radiative forcing to the left to reproduce the observed temperature change, thereby making it more severe (see Fig. 1C).

### Aerosol forcing and climate sensitivity

Our calculations of the constrained aerosol forcing, presented in AS, were made simultaneously with the estimation of the values of the climate sensitivity. We constructed the pdf for climate sensitivity using 80,000 realizations of the climate noise, defined as a difference (residual) between the simulated (forced) temperature change and the observed temperature departure. A simple atmosphere/ocean model was used to drive temperature response to 16 different radiative forcing models. The radiative forcing models, used to simulate temperature anomalies, represented multiple combinations of individual forcings from greenhouse gases (including $CO_2$, CFC-11, CFC-12, $N_2O$, $CH_4$), tropospheric ozone forcing, anthropogenic and natural sulfate aerosol forcing (direct and indirect), forcing due

to variation in the solar constant and volcanic forcing. Realizations of the climate noise were constructed by using the bootstrap re-sampling method, which was applied 5000 times to the residual obtained for each radiative forcing model. Each individual value of the climate sensitivity was estimated by minimizing the root mean square error between the simulated and observed temperatures. The results showed that in general the aerosol forcing estimations are inversely related to the estimations of the climate sensitivity -- with less negative aerosol forcing the climate sensitivity tends to be smaller. Thus, making aerosol forcing less negative (e.g., by inclusion of the carbonaceous aerosols) will reduce the climate sensitivity and will slightly reduce the uncertainties of the climate sensitivity estimations (see Fig. 1D).

### Conclusion

To reduce the uncertainty in the estimation of climate sensitivity requires reducing the uncertainty in the radiative forcing, particularly by anthropogenic tropospheric aerosols. In spite of the progress made in understanding the mechanisms of the aerosol chemical interactions and radiative transfer, the uncertainties are large. Progress is needed in the direct estimation of the indirect aerosol forcing and the magnitude of the forcing by carbonaceous aerosol.

### References


Andronova, N. G. and M. E. Schlesinger, 2001, Objective estimation of the probability density function for climate sensitivity. J. Geophys. Res., 2001. 106(D19), p. 22,605-22,612.

Boucher, O. and J. Haywood, 2001, On summing the components of radiative forcing of climate change. Climate Dynamics, 18, p.297-302.

Forest, C. E., P. H. Stone, A. P. Sokolov, M. R. Allen and M. D. Webster, 2002, Quantifying Uncertainties in Climate System Properties with the Use of Recent Climate Observations. Science, 295, p. 113-117

Gregory, J. M., R. J. Stouffer, S. C. B. Raper, P. A. Stott and N. A. Rayner, 2002, An observationally based estimate of the climate sensitivity. J. Climate. 15(22), p. 3117-3121.

Hansen, J. E., and M. Sato, 2001, Trends of measured climate forcing agents, Proc. Natl. Acad. Sci. U.S.A., 98, 14,778– 14,783.

IPCC (2001) Climate Change 2001, the scientific basis, contributions of working group I to the third assessment report of the intergovernmental panel on climate change. Houghton J. T., et al. (eds) Cambridge University Press, New York, USA.

Knutti, R., T. F. Stocker, F. Joos and G. K. Plattner, 2002,Constraints on radiative forcing and future climate change from observations and climate model ensembles. Nature, 416, p. 719-723.

Wigley,T. M. L. and S. C. B. Raper, 2001, Interpretation of High Projections for Global-Mean Warming, Science, 293, p 451-454.


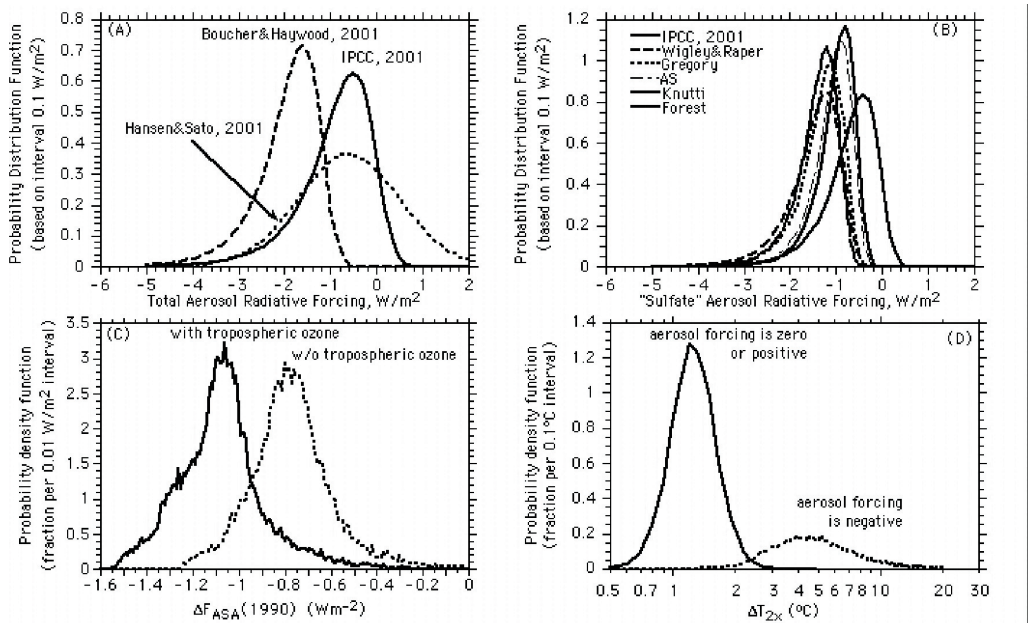


**Figure 1**. Probability distribution functions for (A) total aerosol forcing; (B) sulfate aerosol forcing; (C) the sulfate aerosol forcing for 1990 by Andronova and Schlesinger (2001) both with and without radiative forcing by tropospheric ozone; and (D) climate sensitivity for the two cases in (C) on a log scale.

**IPCC Workshop on Climate Sensitivity**
Paris, France, July 26–29, 2004
*Pre-Conference Volume*

# Geographical Aspects of Feedback/Sensitivity

G.J. Boer

*Canadian Centre for Climate Modelling and Analysis, Meteorological Service of Canada*

Changes in the vertically integrated energy budget of the climate system are expressed as

$$dh'/dt = A' + R' = A' + g + f = A' + \Lambda T' + f \rightarrow 0 \text{ at equilibrium} \quad (1)$$

where $X' = X - X_0$ is the difference between a perturbed, $X$, and control, $X_0$, climate quantity, $dh'/dt$ energy storage, $A'$ convergence of energy by transport processes and $R'$ radiative flux into the column. $R'$ is expressed as the sum of the radiative forcing $f(\lambda,\varphi,t)$ and the radiative feedback $g = \Lambda T'$, the product of the surface temperature change $T'(\lambda,\varphi,t)$ and the feedback parameter $\Lambda(\lambda,\varphi,t)$. The connection between global average forcing and temperature (indicated by angular brackets) follows as

$$\langle T' \rangle = \langle f - dh'/dt \rangle / -\hat{\Lambda} = \hat{s}\,\langle f - dh'/dt \rangle\,\hat{s} \rightarrow \hat{s}\,\langle f \rangle \text{ at equilibrium} \quad (2)$$

where the global feedback parameter $\hat{\Lambda} = \langle \Lambda T' \rangle / \langle T' \rangle = -1/\hat{s}$ is the temperature weighted average of the local feedback parameter $\Lambda(\lambda,\varphi,t)$ and is inversely proportional to the sensitivity parameter $\hat{s}$. For mixed layer ocean versions of coupled climate models, the sensitivity is found to differ by as much as a factor of two (e.g Figure 9.18 of IPCC2001).

Boer and Yu (2003) argue that the geographical expression (1) gives a more basic representation of feedback/sensitivity than does the global representation (2). Figure 1 (below) displays the normalized local feedback parameter $\Lambda_l = \Lambda T'/\langle T' \rangle$, for which $\hat{\Lambda} = \langle \Lambda_l \rangle$, obtained from a near equilibrium simulation with the CCCma CGCM2 with greenhouse gas and aerosol concentrations stabilized at year 2050 values from the IS92a scenario. The high latitude regions of positive feedback are associated with the surface ice/snow albedo feedback while those in the tropical Pacific depend on changes in the structure of moisture, temperature and cloudiness. Negative regions are associated with increased outgoing IR from the warmer surface and atmosphere and/or with or decreased solar associated with changes in cloud distribution and optical properties.

Local contribution to feedback

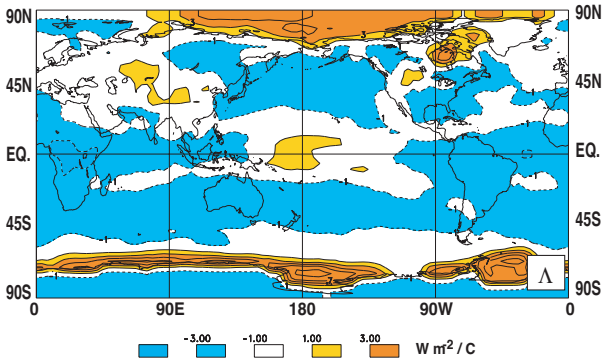


If $\Lambda(\lambda,\varphi,t)$ is a feature of the physical climate system which is independent of $f$ and $T'$, at least to first order, then (1) indicates that the temperature response pattern $T'(\lambda,\varphi,t)$ need not resemble the forcing pattern $f(\lambda,\varphi,t)$ and may be spatially remote from it as seen in Figure 2 on the next page (where subscripts $g$ and $a$ indicate GHG and aerosol forcings and temperature responses). The forcing is redistributed by the transport and local feedbacks act to "localize" the temperature response. Forcing is amplified in the regions of positive feedback (e.g. at high latitudes) and damped in regions of negative feedback. Thus temperature response patterns are determined largely by the pattern of the feedbacks and only secondarily by the pattern of the forcing. Moreover, if $A'$ is approximately linear in $T'$ then (1) implies that forcing and response patterns add linearly (e.g. Forster et al., 2000). Finally, (2) indicates that global feedback $\hat{\Lambda}$ and sensitivity $\hat{s}$ are not independent of the temperature and forcing patterns. Different forcing patterns with the same global mean $\langle f \rangle$ may give different global mean temperature responses. This is because forcing preferentially in regions of positive feedback gives a larger global mean temperature response than does forcing uniformly or forcing preferentially in regions of negative feedback. This "efficacy" of the forcing (e.g. Hansen and Nazarenko, 2004) arises from the local nature of the feedbacks as measured by $\Lambda(\lambda,\varphi,t)$.

The feedback $g$ and the feedback parameter $\Lambda$ can be decomposed into components as $g = g_S + g_L = g_A + g_C = g_{SA} + g_{SC} + g_{LA} + g_{LC}$ associated respectively with ***S***olar, ***L***ongwave,

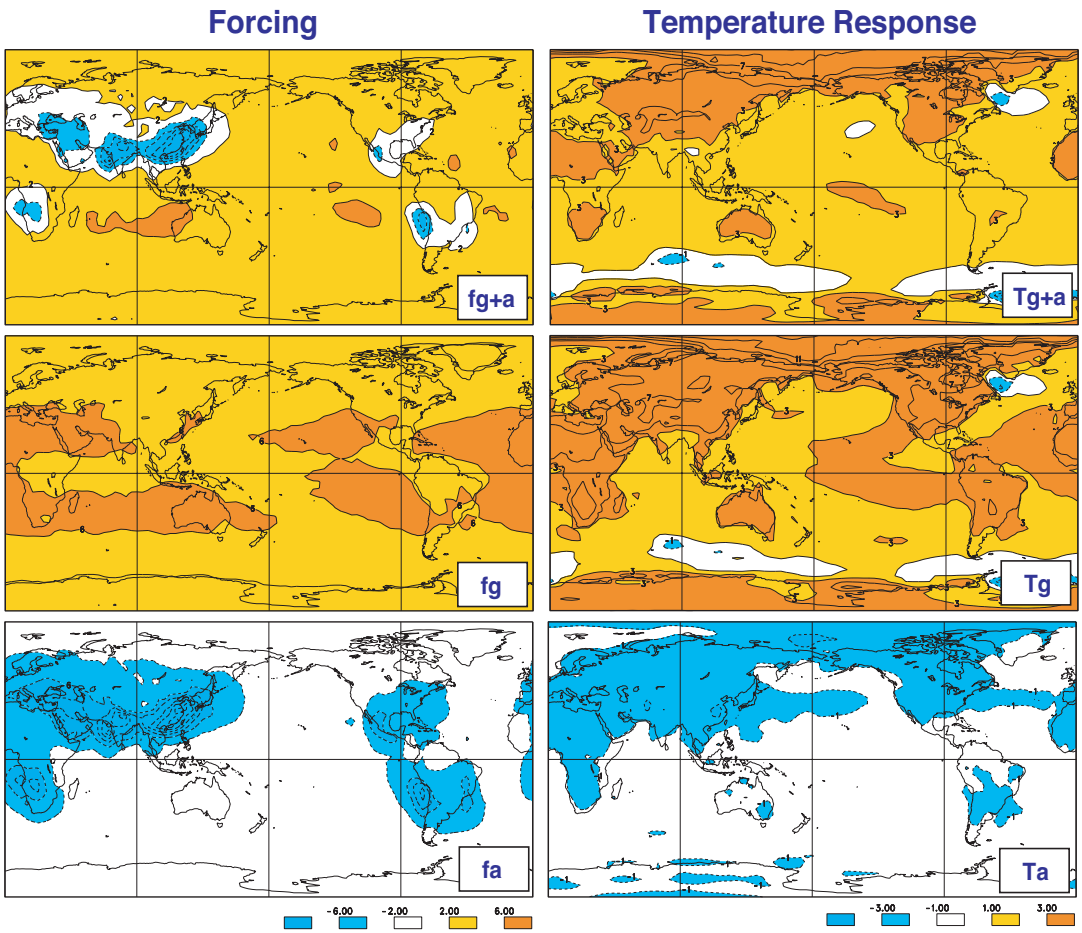


clear-sky ***A***tmosphere/surface and ***C***loud feedbacks. These components give some information on the different processes involved in the model response and may also form the basis for understanding and intercomparing the behaviour of different models as expressed by their radiative responses. A comparison of the global mean values of feedback components between two versions of the NCAR coupled model (CCSM2.0.1, and CSM1.4) and the CCCma CGCM3 model, calculated for the last 10 years of a 50 year simulation forced with a switch-on 5% solar increase ($\langle f \rangle \approx 8$ W m$^{-2}$), is shown in Table 1. The stronger negative feedback (hence lower sensitivity) of the NCAR models compared to CGCM3 is immediately apparent and the difference in solar cloud feedback $\Lambda_{SC}$ is the main reason for this. Longwave cloud feedback is weakly negative and both long and shortwave clear-sky feedbacks are similar across models. The dependence of feedback/sensitivity on cloud treatment in models is reiterated.

**Table 1.** Global averages of feedback parameter components for two versions of the NCAR CGCM and the CCCma CGCM3. Units are W m$^{-2}$ C$^{-1}$ (prepared by M. Stowasser of IPRC).

| | $\langle\Lambda\rangle$ | $\langle\Lambda_{SA}\rangle$ | $\langle\Lambda_{SC}\rangle$ | $\langle\Lambda_{LA}\rangle$ | $\langle\Lambda_{LC}\rangle$ |
|---|---|---|---|---|---|
| **CSM1.4** | -2.58 | 0.61 | -0.97 | -2.12 | -0.10 |
| **CSM2.0** | -2.30 | 0.74 | -0.84 | -2.12 | -0.08 |
| **CGCM3** | -1.29 | 0.68 | 0.33 | -2.26 | -0.04 |

In summary, the geographical distribution of feedback processes is a robust aspect of the climate system that explains a number of features of model behaviour and offers the possibility of intercomparing and better understanding model and system feedback/sensitivity.

### References

Boer, G.J. and B. Yu, 2003: Climate sensitivity and response. *Clim. Dyn.*, **20**, 415-429.

Forster, P., M. Blackburn, R. Glover and K. Shine, 2000: An examination of climate sensitivity for idealized climate change experiments in an intermediate general circulation model. *Clim. Dyn.*, **16**, 833-849.

Hansen, J. and L. Nazarenko, 2004: Soot climate forcing via snow and ice albedos. *PNAS*, **101**, 423-428.

IPCC2001: *Climate change 2001, the scientific basis*. Cambridge University Press, 881pp

**IPCC Workshop on Climate Sensitivity**
Paris, France, July 26–29, 2004
*Pre-Conference Volume*

# What Can We Learn on Climate Sensitivity from Mid-Holocene Type Simulations?

Pascale Braconnot

*IPSL/Laboratoire des Sciences du climat et de l'environnement, Orme des Merisiers, bât 701, 91191 Gif-sur-Yvette Cedex, France, email:pasb.braconnot@ cea.fr.*

## Introduction

Past climate simulations offer an unique opportunity to test our ability to represent a climate different from the modern one. Here we considerer GCM simulations of the mid-Holocene climate to assess the sensitivity of the climate system to a slightly different seasonality of the insolation forcing (incoming solar radiation at TOA). The mid-Holocene (6000 years ago; 6ka) period is one of the key periods of interest of the Paleoclimate Modeling Intercomparison Project (PMIP; (Joussaume et Taylor, 1995; PMIP, 2000) that was initiated to facilitate systematic comparisons between model simulations and between model and proxy data. PMIP also offers the opportunity to test the sensitivity of climate models, even though this aspect has not been fully developed during the first phase of the project (PMIP1) that considered only general circulation model of the atmosphere (AGCM). Coupled ocean-atmosphere models are now becoming a standard to study climate change, and several OAGCM simulations are now available for 6ka and will be considered in the following. Time periods, such as last glacial inception (about 115000 years ago, 115ka) or the Early Holocene also receive lots of attention from a wide modeling community. They will be considered in the second phase of the project (http://www-lsce.cea.fr/pmip2) during which feedbacks from ocean and vegetation as well as changes in climate variability will be analysed in more details, in order to evaluate those coupled models that are use for future climate projection (Harrison et al., 2002). Some aspects of the 115 ka climate will also be considered at the end of this short report. Evaluation of model experiments depends on the existence of spatially explicit data sets that can be compared with output from the model simulations. PMIP plays a key role in triggering data synthesis for model-data comparisons (see Harrison 2000 for a synthesis).

## Model response to mid-Holocene insolation

The major difference between mid-Holocene and present day climates comes from the Earth orbital configuration (Berger, 1978), and mainly from the position of the perihelion and from a larger obliquity. The seasonal cycle of the incoming solar radiation at the top of the atmosphere (insolation) was increased by about 5 % in the northern hemisphere and damped in the southern hemisphere. This seasonal change in insolation is the driving mechanism for the increase and the northward shift of summer precipitation over the African and Asian continents. During summer, temperature are warmer and precipitation larger over land whereas over the ocean precipitation decreases due to the larger moisture

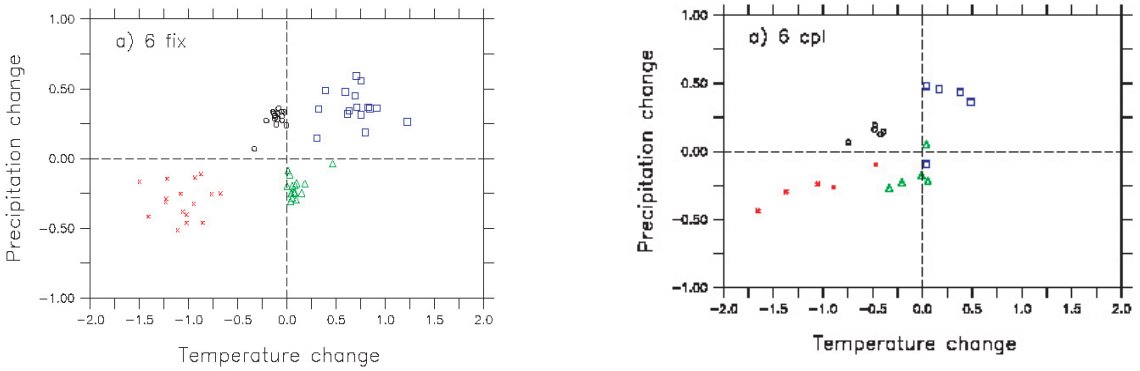


**Figure 1.** Change in 6ka tropical precipitation and temperature for a) PMIP simulations and b) coupled simulations averaged over the continent in winter (red dots), the ocean in winter (black dots), the continent in summer (blue squares) and the ocean in summer (green triangles). Each point represents a model results.

advection from the ocean to the continent (Figure 1a). In coupled experiment, SST can vary, and, in this case, some of the models produce local enhancement of precipitation over the warmer ocean waters (Figure 1b). In winter, insolation is reduced and so is the temperature over land. The winter monsoon is enhanced and precipitation increases over the ocean. These changes are thus seasonal and correspond to shift in time and space of the major climate structures. There is nearly no change in annual mean. Change in the hydrology of the tropics is a major feedback, but cannot be analysed from a global point of view. The realisms of the simulated changes can be tested against different proxy indicators and synthesis map reconstructions. This type of analysis gives rise to the key diagnostics proposed in the TAR, where, a zonal mean estimate of the amount of moisture needed to produce the observed shift in the transition between desert and steppe in Sahara has been proposed. It allows evaluating how well models reproduce this feature. During the presentation an example using new pollen data reconstruction in middle and high latitudes will be presented.

**Model differences in forcing and radiative feedbacks**

The standard definition of climate sensitivity is not well adapted for this seasonal change. However it is possible from analyses of model-model differences to extract some information about model differences. The radiative forcing can be estimated from Hewitt and Michel (1996)'s definition of shortwave forcing for mid-Holocene: $SW_{forcing}=(1 - \alpha ctrl)\ \Delta SWi$. The rational is that different climate models have different forcing because, even though we apply the same change in insolation (ΔSWi) to all of them, the effective change in absorbed short wave radiation is a function of the planetary albedo of the control simulation (αctrl). The change in net SW at TOA thus results from the sum of this forcing and of internal feedbacks that alter cloud characteristics and surface albedo, and that are also responsible for differences between models results (Bonfils *et al.*, 2001; Joussaume *et al.*, 1999). The intensity of the change in precipitation in PMIP simulations was related to two factors of the control simulation. The first one is a parameter that account for the large-scale advection of moisture in the tropics and subgrid scale parameterisation of clouds and rain. The second one is the mean temperature of the control simulation (Braconnot et al. 2002). The change in the energetic of the atmospheric column (for dry atmosphere) was analysed for PMIP simulations following the ITCZ over west Africa and the region of maximum warming further north into the Sahara (Braconnot et al. 2000). Comparison between results obtained for 6 ka and last glacial maximum revealed that, although the contribution of the different fluxes to the atmospheric budget strongly vary from a model to an other, a same model produce similar characteristics for 6ka and last glacial maximum which respond to very different forcing mechanisms (Figure 2).

**Role of ocean and vegetation feedbacks**

Ocean and vegetation feedbacks have been show to play a major role in the amplification of the climate response to the insolation forcing (i.e. Braconnot et al in press or Cane et al, 2004 for a synthesis). Only few simulations have considered simultaneously the ocean and vegetation feedback (Braconnot *et al.*, 1999). These results showed how, for the African monsoon, ocean and vegetation feedback respectively reinforce the inland advection of humidity and local recycling. These feedbacks will be illustrated for high latitudes from the analyses of Wohlfahrt et al. (2004). Changes in the land surface cover introduce an annual mean forcing on the climate resulting from changes in the surface albedo, surface roughness and roots profiles. This signal is superimposed on the seasonally varying mid-Holocene insolation forcing. In middle and high latitudes, the vegetation and ocean feedbacks respectively enhance the warming in Spring and Autumn. The synergy between the different feedbacks is for most seasons as large as the feedbacks themselves and contributes to translate the insolation seasonal forcing into a mean annual warming. As for the African monsoon the resulting climate change is larger than the sum of the individual contribution from ocean and vegetation feedbacks, stressing that their non-linear interactions play an important role and need to be considered in climate change experiments. However, even though the simulation including all the feedbacks is in better agreement with data when considering the forest extension over Europe, the match with biome data is reduced compared to AGCM or OAGCM over the mid-continental Eurasia where the drying become excessive. This point needs to be analysed from different simulations to determine if we miss a process, or a boundary condition such as lakes in the land surface scheme.

**Feedback from atmospheric moisture transport**

Coupled simulations of the mid-Holocene do not produce notable change in the annual mean overturning or thermohaline circulation. Changes in the ocean circulation have rather seasonal features (Braconnot *et al.*, 2000). The equator to pole heat transport is reduced during winter because the tropical regions are colder. In summer it helps to transfer the excess summer warming from the northern hemisphere to the southern hemisphere. The late warming of the surface ocean in

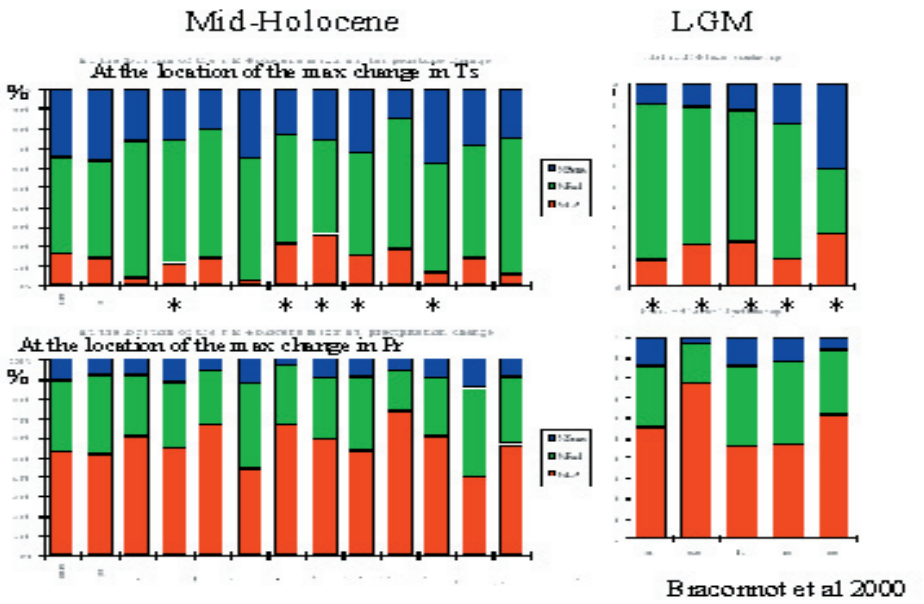


**Figure 2.** Partitioning of the latent heat release (LP), the radiative fluxes (Rad) and the sensible flux (Sens) in the energetic change of the atmospheric column (Q= LP + Rad + Sens) for mid-Holocene and last glacial maximum. Each bar represents a model result (PMIP simulations). Models that performed both 6ka and LGM simulations are marked with a star(same order from left to right). The bottom panel represents the annual mean within the ITCZ over west Africa. Values where computed for each month and then averaged. The top panel was obtained from similar calculation for the region of maximum warming located to the north of the ITCZ in the Sahara.

response to the insolation forcing has been shown to enhance the inter-hemispheric contrast in temperature, which affects both the Indian and African monsoon (zhao et al, in preparation). Interesting features are also found between simulations of 6ka and 115 ka for high latitudes when comparing the change in moisture transport and the feedback in high latitudes. Last glacial inception is a time during which high latitudes received less solar energy during summer and low latitude more energy during winter. The latitudinal pattern of insolation change as a function of latitude and month is roughly the reverse of the one found for 6ka. Using the IPSL coupled model, Khodri et al. (2001) showed that the increase in moisture transport from the equator to high latitudes was an important factor to trigger the last glacial inception. Some of the changes in the hydrological cycle of the Arctic show reverse behaviour between 115ka and 6ka. At 6ka (115ka), the sea ice cover is reduced (increased) during summer, the atmosphere transports less (more) moisture towards high latitudes, which reduces (increases) the river runoff discharge in the Arctic and prevents (favours) the building up of sea ice. In the case of 115ka these changes lead to colder summer and snow precipitation over the continents where ice sheet initiated (Khodri et al. 2001). Reconstruction of SST from proxy indicators suggests that the associated simulated change in the north-south SST gradient in the North Atlantic is consistent with reality.

### Impact of the seasonal time scale between forcing and climate response

Other important feedbacks that may alter climate sensitivity arise from the timing between the climate forcing and the timing of the climate response. Recent results show that the late response of the tropical ocean to the mid-Holocene insolation results from the fact that the maximum change in insolation occurs after the summer solstice in July (Braconnot et al. 2003). Analysis of the feedback from snow and sea-ice in high northern latitude will be discussed from simulations where the perihelion has been respectively shifted to winter or to spring from 115 ka orbital configuration. Even with a large summer insolation, if the spring melting of snow and sea-ice does not occur early enough in the season the snow-albedo feedback is not effective and the high latitude climate is cold. These seasonal changes interfere with the ocean heat transport in the north Atlantic (Khodri et al. submitted), and may be one of the reason why marine data suggest that last glacial inception was already effective 120000 years ago (Corijo et al. 1999).

### Conclusion

Even though the characteristics of climate change we present here do not represent analogue with what could happen under increased green house gas concentration, they allow us to isolate major feedbacks and to

understand the combination of scale between the change in mean climate, climate variability and extremes. Analysis of radiative changes in climates where the seasonal cycle is slightly different from the present one is also a way to better understand the present day seasonal cycle, and to test if the sensitivity of climate model is in agreement with proxy reconstruction of past environment. This work is entirely relevant to analyses for instance the climatic impact of future changes in regions of human emission of aerosols These forcing may be more effective in some seasons and contribute to changes in regional climates and climate teleconnections. Change in climate variability was not discussed here. One of the reasons is that, as for present day climate, climate models produce a wide range of possibilities and careful analyses are now required to define which part of the signal is robust and which part is model dependent. This will be one of the major challenges for PMIP2 and both the modelling and data communities in the coming years.

**References**


Berger, A., 1978: Long-term variations of caloric solar radiation resulting from the earth's orbital elements. Quaternary Research, 9, 139-167.

Bonfils, L., N. de Noblet-Ducoure, P. Braconnot, et S. Joussaume, 2001: Hot desert albedo and climate change: Mid-Holocene monsoon in North Africa. Journal of Climate, 14, 3724-3737.

Braconnot, P. et O. Marti, 2003: Impact of precession on monsoon characteristics from coupled ocean atmosphere experiments: changes in Indian monsoon and Indian ocean climatology. Marine Geology, 201, 23-34.

Braconnot, P., M. F. Loutre, B. Dong, S. Joussaume, et P. Valdes, 2002: How the simulated change in monsoon at 6 ka BP is related to the simulation of the modern climate: results from the Paleoclimate Modeling Intercomparison Project. Climate Dynamics, 19, 107-121.

Braconnot, P., O. Marti, S. Joussaume, et Y. Leclainche, 2000: Ocean feedback in response to 6 kyr BP insolation. Journal of Climate, 13, 1537-1553.

Braconnot, P., S. Harrison , J. Joussaume, C. Hewitt, A. Kitoh, J. Kutzbach, Z. Liu, B. L. Otto-Bleisner, J. Syktus, et S. L. Weber, press: Evaluation of coupled ocean-atmosphere simulations of the mid-Holocene. Kluwer.

Braconnot, P., S. Joussaume, N. de Noblet, et G. Ramstein, 2000: Mid-holocene and Last Glacial Maximum African monsoon changes as simulated within the Paleoclimate Modelling Intercomparison Project. Global and Planetary Change, 26, 51-66.

Braconnot, P., S. Joussaume, O. Marti, et N. de Noblet, 1999: Synergistic feedbacks from ocean and vegetation on the African monsoon response to mid-Holocene insolation. Geophys .Res. Lett., 26, 2481-2484.

Cane, M. , P. Braconnot, A. Clement, H. Gildor, S. Joussaume, M. Khodri, D. Paillard, S. Tett, E. Zorita, 2004 : Progress in Paleoclimate Modeling, Special issue of the CLIVAR 2004 conference, smi.

Cortijo, E. et al., 1999: Changes in meridional temperature and salinity gradients in theNorth Atlantic Ocean (308-728N) during the last interglacial period. Paleoceanography 14, 23±33).

Harrison , S., P. Braconnot, C. Hewitt, et R. J. Stouffer, 2002: Fourth international workshop of The Palaeoclimate Modelling Intercomparison Project (PMIP): launching PMIP Phase II. EOS.

Harrison , S., 2000: Palaeoenvironmental data set and model evaluation in PMIP. Vol. WCRP-111, WMO/TD-No. 1007, Paleoclimate Modeling Intercomparison Project (PMIP), proceedings of the Third PMIP workshop.

Hewitt, C. D. et J. F. B. Mitchell, 1996: GCM simulations of the climate of 6 kyr BP : Mean changes and interdecadal variability. Journal of Climate, 9, 3505-3529.

Joussaume, S. et K. E. Taylor, 1995: Status of the Paleoclimate Modeling Intercomparison Project. in Proceedings of the first international AMIP scientific conference, WCRP-92, Monterey, USA, 425-430.

Joussaume, S., et al., 1999: Monsoon changes for 6000 years ago: Results of 18 simulations from the Paleoclimate Modeling Intercomparison Project (PMIP). Geophysical Research Letters, 26, 859-862.

Khodri, M., Y. Leclainche, G. Ramstein, P. Braconnot, O. Marti, et E. Cortijo, 2001: Simulating the amplification of orbital forcing by ocean feedbacks in the last glaciation. Nature, 410, 570-574.

PMIP, 2000: Paleoclimate Modeling Intercomparison Project (PMIP), proceedings of the third PMIP Workshop. WCRP-111,WMO/TD-No. 1007, 271 pp.

Wohlfahrt, J., S. P. Harrison, et P. Braconnot, 2004: Synergistic feedbacks between ocean and vegetation on mid- and high-latitude climates during the mid-Holocene. Climate Dynamics, 22, 223-238.

**IPCC Workshop on Climate Sensitivity**
Paris, France, July 26–29, 2004
*Pre-Conference Volume*

# The 1997/98 El Niño: A Test for Climate Models

Robert D. Cess[1], Riyu Lu[2], Buwen Dong[3], and Gerald L. Potter[4]

[1] *Marine Sciences Research Center, State University of New York at Stony Brook, Stony Brook, New York, 11790, USA*
[2] *Institute of Atmospheric Physics, Chinese Academy of Sciences, Beijing 100080, China*
[3] *Hadley Centre for Climate Prediction and Research, Met Office, FitzRoy Road, Exeter EX1 3PB, UK*
[4] *Program for Climate Model Diagnosis and Intercomparison, Lawrence Livermore National Laboratory, Livermore, California, 94550, USA*

Cloud-climate interactions comprise one of the greatest uncertainties in attempting to model climate change using general circulation models (GCMs), and there is a need to devise ways of testing such interactions within models. If a GCM is to properly portray long-term climate change, it in turn must replicate cloud changes associated with events occurring on shorter time scales. Recently *Cess et al.* [2001] demonstrated that the lack of a zonal SST gradient in the tropical Pacific Ocean during the 1997/98 El Niño caused a collapse of the Walker circulation together with enhanced upward motion over the eastern Pacific. This in turn resulted, on average, in lower clouds in the western portion of the tropical Pacific and higher clouds in the eastern portion. The data used to determine these west/east cloud changes consisted of cloud profiling measurements made by the Stratospheric Aerosol and Gas Experiment (SAGE) II, together with cloud-radiative forcing (CRF) as determined for a 5-yr period (1985-1989) and for the first 4 months of 1998 by the Clouds and the Earth's Radiant Energy System (CERES) instrument on the Tropical Rainfall Measuring Mission (TRMM) Satellite. As emphasized by *Cess et al.* [2001], these cloud structure changes should serve as a useful test of a GCM, and in the present study we demonstrate this by applying this test to Version 3 of the Hadley Centre Atmospheric Model (HadAM3) [*Pope et al.*, 2000].

As in *Cess et al.* [2001], we employ zonal winds from the National Environmental Prediction Center/National Center for Atmospheric Research (NCEP/NCAR) reanalysis [*Kistler et al.* [2001]. The ERBE/CERES data are likewise the same as used by *Cess et al.* [2001] and for the same western and eastern study regions. The ERBE TOA measurements are for the first four months (JFMA) of 1985-1989 together with CERES measurements for the first four months of 1998 that represent the strongest period of the 1997/98 El Niño for which CERES data are available (CERES/TRMM data cover January through August 1998).

Two experiments have been performed with HadAM3. One consists of a control, or "normal year", experiment in which climatological sea-surface temperatures (SSTs), averaged over 30 years from 1961 to 1990 [*Smith and Reynolds,* 1998], were prescribed. The other experiment, the "El Niño" experiment, used observed SSTs from June 1, 1996 to August 31, 1998 [*Reynolds and Smith*, 1994]. These two integrations were different only in their initial conditions, which were taken from the end of spin-up integrations. For the normal-year integration, the spin-up with climatological SSTs lasted 1.5 years, after which the control experiment was run for one year beginning on December 1. For the El Niño experiment the spin-up, using observed SSTs, was from June 1, 1996 to December 31, 1996, after which the El Niño experiment was integrated from January 1, 1997 to August 31, 1998. Each experiment consists of the average of an ensemble of 10 runs.

A major change in the atmospheric circulation over the tropical Pacific, as caused by the 1997/98 El Niño, was the virtual collapse of the Walker circulation [*Bell et al.,* 1999; *Cess et al.,* 2001], and this in turn caused the west/east changes in cloud structure noted by *Cess et al.* [2001] employing both SAGE II cloud profiling and ERBE/CERES TOA radiometric measurements. This collapse of the Walker circulation is demonstrated by comparing the NCEP/NCAR zonal winds in Figure 1c (El Niño) to those in Fig. 1a (normal year). The upward branch of the Walker circulation is centered between 140°E and 160°E (Figure 1a), which corresponds to strong convection that produces high clouds in the western region. The downward branch is located to the east of 160°W, with subsidence air suppressing deep convection and producing shallow stratus and stratocumulus clouds. The Walker circulation has all but ceased in 1998 (Figure 1c), and the westerlies east of the dateline in the upper troposphere have disappeared. This collapse of the Walker circulation is directly associated with the lack of a zonal SST gradient, and further discussion of this is given in *Cess et al.* [2001]. Thus a crucial first step in using the 1997/98 El Niño as a test of a GCM is to test if the GCM produces a similar collapse

of the Walker circulation, and Figure 1 demonstrates that HadAM3 does a remarkably good job in this regard. This agreement of the model with the NCEP/NCAR horizontal winds is consistent with a related study [*Allan et al.,* 2002] who found agreement between HadAM3 and NCEP/NCAR 500-hPa vertical velocities.

This study has demonstrated, through the use of HadAM3, the utility of using the strong 1997/98 El Niño as one means of testing cloud-climate interactions within a GCM. A crucial first step is to determine if a GCM produces the observed collapse of the Walker circulation, and HadAM3 did a remarkable job of passing this test. The second phase of the test is to compare the model to ERBE/CERES TOA measurements, and the model did produce trends similar to those inferred from the satellite measurements. On average, cloud altitudes decreased over the western Pacific and increased over the eastern Pacific, both caused by the collapse of the model's Walker circulation. We feel this is a useful test to apply to other GCMs.

### References


Allan, R. P., A. Slingo, and M. A. Ringler (2002), Influence of dynamics on the changes in tropical cloud radiative forcing during the 1998 El Niño, *J. Climate, 15,* 1979-1986.

Bell, G. D., M. S. Halpert, C. F. Ropelewski, V. E. Kousky, A. V. Douglas, R. C. Schnell, and M. E. Gelman (1999), Climate assessment for 1998, *Bull. Am. Meteorol. Soc., 80,* S1-S48.

Cess, R. D., M. H. Zhang, P.-H. Wang, and B. A. Wielicki (2001), Cloud structure anomalies over the tropical Pacific during the 1997/98 El Niño (2001), *Geophys. Res. Lett., 28,* 4547-4550.

Pope, V. D., M. L. Gallani, P. R. Roundtree, and R. A. Stratton (2000), The impact of new physical parameterizations in the Hadley Centre climate model–HadAM3, *Climate Dyn., 16,* 123-126.

Kistler, R. et al (2001), The NCEP-NCAR 50-year reanalysis: Monthly means CD-ROM and documentation, *Bull. Amer. Meteor. Soc., 82*, 247-267.

Reynolds, R. W., and T. M. Smith (1994), Improved global sea surface temperature analyses using optimum interpolation, *J. Climate, 7*, 929-948.

Smith T. M., and R. W. Reynolds (1998), A high-resolution global sea surface temperature climatology for the 1961-90 base period, *J. Climate, 11*, 3320-3323.


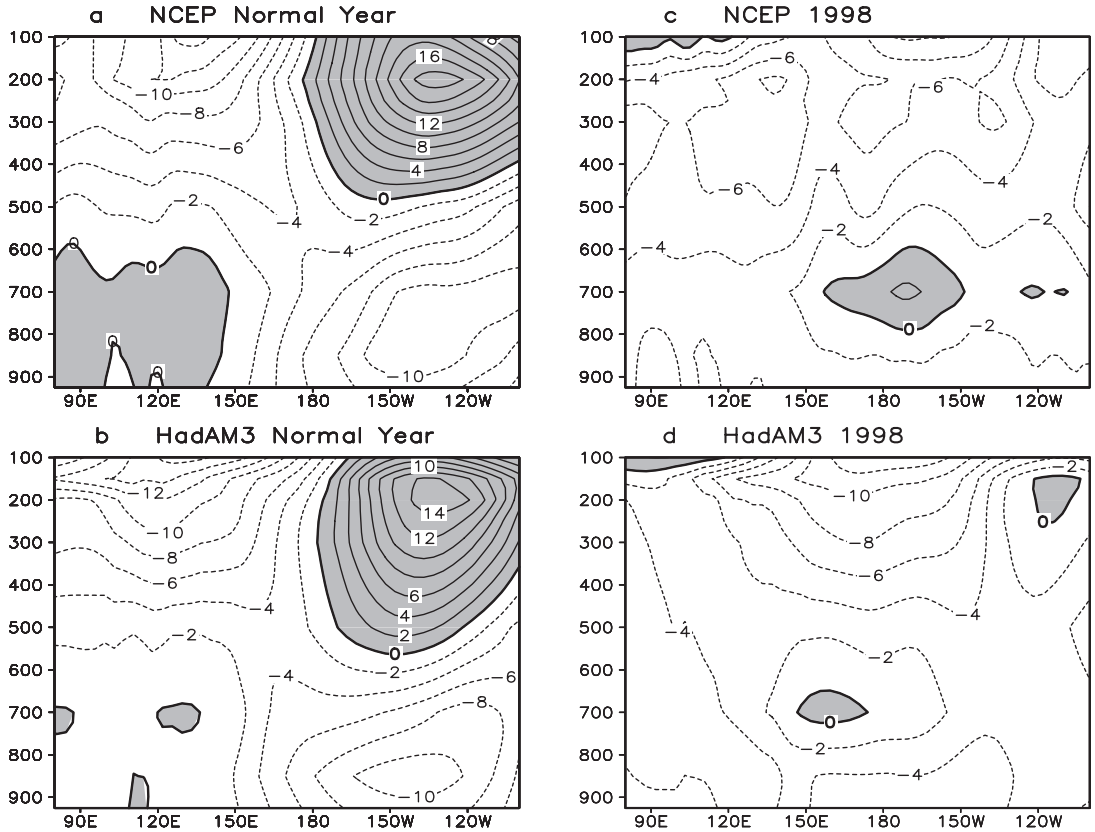


**Figure 1.** Pressure–longitude cross sections of zonal wind (m/s) averaged from 5°S to 5°N and for the first four months (JFMA) of each year. (a) NCEP normal year. (b) HadAM3 normal year. (c) NCEP 1998. (d) HadAM 1998.

**IPCC Workshop on Climate Sensitivity**
Paris, France, July 26–29, 2004
*Pre-Conference Volume*

# State of Radiation Codes in GCMs

Qiang Fu

*Department of Atmospheric Sciences, University of Washington, Seattle, WA 98195, USA*

The state of radiation codes used in current global climate models will be reviewed to highlight both main radiative transfer processes and current issues in modeling atmospheric radiation. Some basic aspects of radiative transfer processes including water vapor continuum, light scattering by nonspherical ice particles, and effects of 3D radiative transfer will be emphasized. The main challenges as well as prospective approaches to complete our understanding of these processes will be addressed in terms of fundamental theory, modeling, and observations.

**IPCC Workshop on Climate Sensitivity**
Paris, France, July 26–29, 2004
*Pre-Conference Volume*

# Controls on the Interannual Variability of Planetary Albedo and Relevance for Climate Sensitivity

Alex Hall and Xin Qu

*UCLA Dep't of Atmospheric and Oceanic Sciences*

We assess the controls on planetary albedo variability by examining the ISCCP (Rossow and Garder, 1993a and 1993b) D2 data set, covering the period 1983-2000. For both clear and all-sky cases, the ISCCP data set (D2) contains surface and top-of-the-atmosphere radiation fluxes on a 2.5° X 2.5° grid at 3 hour temporal resolution. These were generated based on observations at 3 different channels (visible, near IR, and IR) and a radiative transfer model. The current D2 data set contains improvements over previous ISCCP releases. These increase low-level cloud detection significantly and reduce biases in cloud optical thickness over snow and ice (Rossow and Schiffer, 1999).

Planetary albedo fluctuations may originate at the surface or in the atmosphere. Within the atmosphere, clouds are likely the main sources of planetary albedo fluctuations because their high reflectivities create a large albedo contrast between a clear and cloudy atmosphere. For this reason, we focus on separating contributions from surface and cloud. Seasonal-mean planetary albedo anomalies are regressed onto seasonal-mean surface albedo anomalies, seasonal-mean cloud anomalies associated with cloud cover variations and seasonal-mean cloud anomalies associated with cloud optical thickness variations.

Based on this regression analysis, the variance of planetary albedo (left hand side of the following equation) can be attributed to four terms:

$$\underset{\text{I}}{\left\langle a_p' \right\rangle^2} = \underset{\text{II}}{\left\langle a_{ps}' \right\rangle^2} + \underset{\text{III}}{\left\langle a_{pc}' \right\rangle^2} + \underset{\text{IV}}{\left\langle a_r' \right\rangle^2} + \left\langle a_{ps}', a_{pc}' \right\rangle^2 \quad (1)$$

where I. is the planetary albedo variance unambiguously related in linear fashion to surface albedo variability, II. is the variance unambiguously related in linear fashion to cloud cover and optical depth variability, III. is the residual component that cannot be linearly related to either surface or cloud variability, and the covariance term IV. is the portion linearly related to surface and cloud variability but not unambiguously attributable to either because of correlations between surface optical properties and cloud.

We divided the earth into six regions and analyzed them separately. Our choice of regions is guided by known differences in the behavior of surface albedo variability: (a) northern hemisphere snow-covered lands, (b) northern hemisphere sea ice zone, (c) southern hemisphere sea ice zone, (d) snow-free lands, (e) ice-free ocean, and (f) Antarctica. Note that the definition of the regions varies seasonally. We averaged the contributions of the four components in Eq. (1) over each region for each season after first normalizing by the total planetary albedo variability (see figure 1). We will refer to this figure to compare the contributions of surface and clouds to planetary albedo variability among regions and among seasons within the same region.

An examination of the light grey bars of Fig 1 reveals that the contribution of the residual (component III in Eq. (1)) is negligible compared to the total contribution of surface albedo, cloud cover and cloud optical thickness during most seasons in nearly all regions, implying that these are the factors contributing most to planetary albedo variability. This is also viewed as a validation of our linear regression analysis technique. The contribution of the covariance term (component IV of Eq. (1), white bars of Fig 1) is also generally small (less than 10%), though it may be non-negligible in the SH sea ice zone during MAM. A weak negative correlation between fluctuations in surface albedo and those in cloud cover and cloud optical thickness occurs in the SH sea ice zone at this time of year, possibly attributable to cloud-cryosphere interaction. There also appears to be a weak but consistently positive correlation between surface and cloud properties in the snow-free lands during all seasons, possibly due to cloud-vegetation interaction.

A comparison of the black and dark grey bars of Fig 1 shows that over the snowfree lands and ice-free oceans, the cloud contribution overwhelms the surface contribution during all seasons; however, the surface

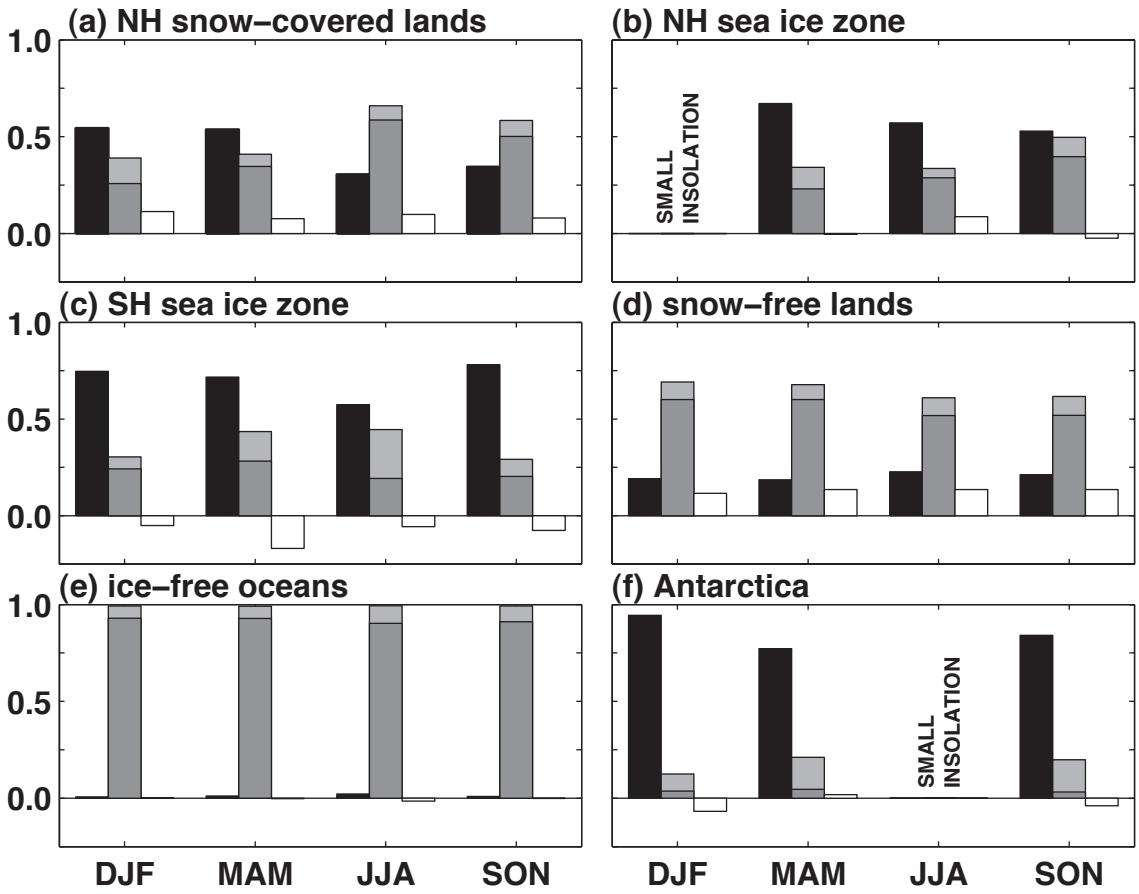


**Figure 1.** The contributions of surface albedo variations (black bar), cloud variations (dark grey bar), the covariance between surface albedo variations and cloud variations (white bar) and the residual (light grey bar) to planetary albedo variability averaged over six regions: (a) NH snow-covered lands; (b) NH sea ice zone; (c) SH sea ice zone; (d) snow-free lands; (e) ice-free oceans and (f) Antarctica. Terms I-IV of Eq. (1) were divided by the variance in planetary albedo (left side of Eq. (1)) to generate a normalized contribution to planetary albedo variability from each constituent. These were then averaged over the six regions.

makes the dominant contribution to planetary albedo variability in snow and ice regions at nearly all times of year. The surface contribution is so much larger in the snow and ice areas mainly because of the large surface albedo variability associated with snow and ice fluctuations (not shown). The surface contribution is also larger in the SH sea ice zone than its NH counterpart in all seasons. This is likely because surface albedo varies more in the SH sea ice zone at all times of year. In Antarctica, the surface contribution overwhelms the cloud contribution during all seasons with sunshine. This can largely be explained by two facts: One is that the relatively transparent SH polar atmosphere does little to attenuate the impact of surface albedo anomalies on top-of-the-atmosphere radiation; the other is that cloud-related planetary albedo variability is negligible in this region.

The dominance of the surface contribution to interannual planetary albedo variability in the cryosphere regions and the apparent inability of clouds to mask the signature of surface albedo anomalies in net incoming solar radiation in these areas supports the positive surface albedo feedback seen in many future climate simulations. Just as present-day anomalies of surface albedo owing to variations in the cryosphere result in anomalies in net incoming solar radiation, an increase in net incoming solar radiation would occur if snow and ice were to retreat in the future.

The results presented in figure 1 can also be used to evaluate surface albedo processes in current climate models. To allow for as direct a comparison with the ISCCP data as possible, we used a simulated time series with approximately the same mix of internal variability and externally-forced climate change. A recent CCSM3 scenario run was used, with data taken from the same time period as ISCCP (1983-2000). We performed analysis identical to that shown in figure 1 on this data, and present the results in figure 2. A comparison of

these two figures reveals that in all cryosphere regions, the contribution of the surface to planetary albedo variability is significantly smaller in CCSM3. It turns out this is because CCSM3 has substantially less surface albedo variability (not shown) than ISCCP in snow and ice regions. Understanding the reasons for this discrepancy may lead to ways to improve CCSM3's surface albedo parameterization, and in the process, improve its simulation of surface albedo feedback.

**References**

Rossow, W.B., and L.C. Garder, 1993a: Cloud detection using satellite measurements of infrared and visible radiances for ISCCP. *J. Climate*, 6, 2341-2369.

Rossow, W.B., and L.C. Garder, 1993b: Validation of ISCCP cloud detections. *J. Climate*, 6, 2370-2393.

Rossow, W.B., and R.A. Schiffer 1999. Advances in understanding clouds from ISCCP. *Bull. Amer. Meteor. Soc.* 80, 2261-2288.

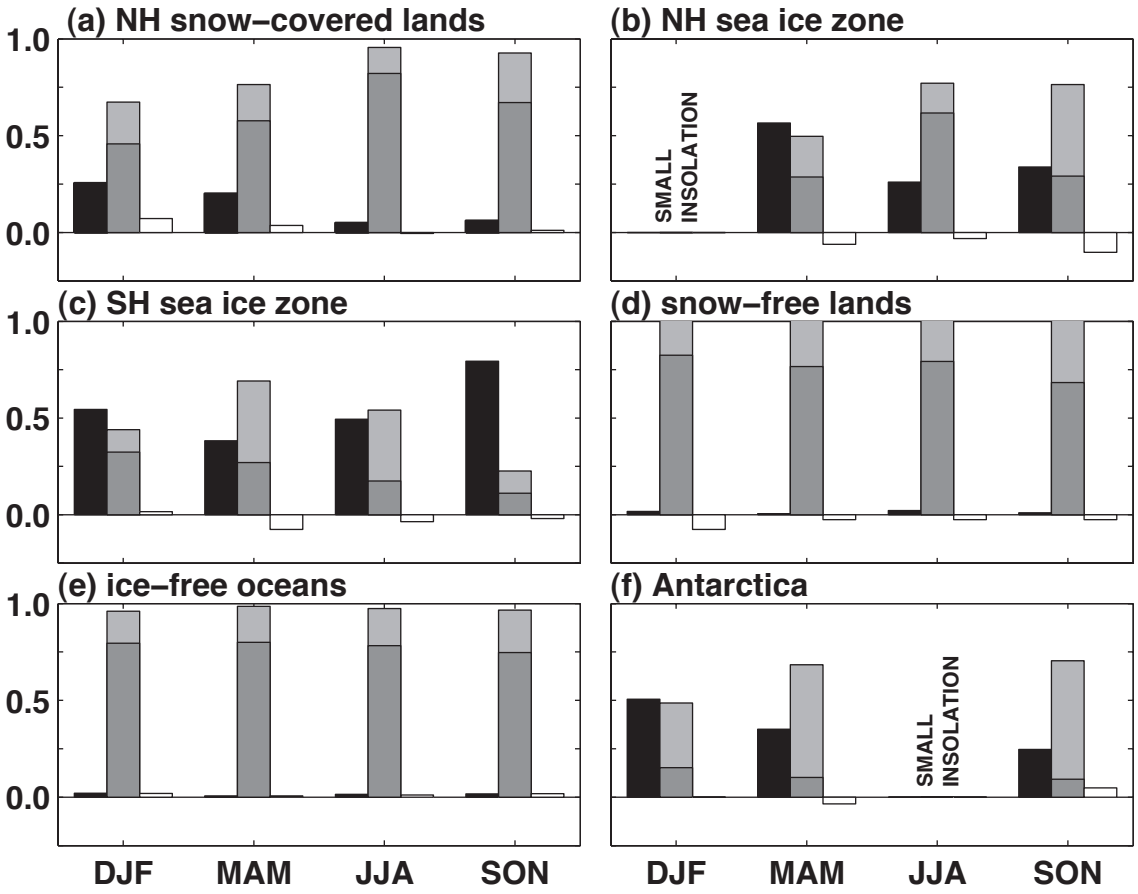


**Figure 2.** As in figure 1, except for the CCSM3 scenario run. Data was taken from years 1983-2000 of the run.

**IPCC Workshop on Climate Sensitivity**
Paris, France, July 26–29, 2004
*Pre-Conference Volume*

# Estimating Temperature Response to Radiative Forcing from Paleoclimate Records of the Last Millennium

Gabriele C. Hegerl and Thomas J. Crowley

*Division of Earth and Ocean Sciences, Nicholas School for the Environment and Earth Sciences, Duke University, Durham, NC 27708*

Paleoclimatic reconstructions of hemispheric temperature over the last few hundred to thousand years contain valuable information on climate response to external forcing such as volcanism, changes in solar radiation and increases in greenhouse gases. While the information on forcing and temperature response is less certain than during the instrumental period, the long records provide a better opportunity to separate the response to different external forcings that are spuriously correlated over the short instrumental period. Also, results based on paleoclimatic data can be used to validate our understanding of forced climate signals from the instrumental period. We have therefore used information in these reconstructions to detect temperature response to natural and anthropogenic forcings (Hegerl et al., 2003) and in an attempt to estimate climate sensitivity from paleoclimatic data (Hegerl et al., to be submitted shortly).

### Paleoclimatic data

We have used temperature reconstructions based on tree-ring data that preserve low-frequency variability from Briffa et al. (2001) and Esper et al. (2002), an updated record from Crowley (2000) and the Mann et al. (1999) reconstruction to represent the uncertainty in our knowledge of past temperature fluctuations. Two of the records, Esper et al (2002) and Crowley (2000) are standardized averages of variations in paleoclimatic indices related to temperature. We have taken care to calibrate these to hemispheric scale temperature variability in a manner that preserves the magnitude of the ratiative forcing in these records. This can be done by a regression approach that makes realistic assumptions about noise and uncertainty in both instrumental data and paleoclimatic data (see Allen and Stott, 2003). The resulting records of paleoclimatic variability show slightly more variability than in previously used calibratons. A perfect model test applying the same calibration procedure to synthetic data (using underlying climate signals from an Energy Balance Model and adding realistic amounts of noise to both, then use decadal data from 1880 to 1960 to calibrate) showed that the result yields reliable, robust calibration results.

### Radiative forcing data

Long data for CO2 forcing can be derived from ice cores. The estimate of the solar forcing time series is based on the Lean et al. (2001) solar irradiance reconstruction. It has been extended back by splicing the C14 residual record of Stuiver and Quay into it during the period of overlap. An updated version of a global volcano reconstruction (Crowley 2000) has been used to estimate past volcanic forcing (see Hegerl et al., 2003; Crowley et al., 2003). The time series utilizes only long ice core records of volcanism that extend back to A.D. 1200, namely four ice cores from Greenland and five from Antarctica produce a composite of sulphate flux for each hemisphere. A mid-line sulfate aerosol forcing is used from 1850 on. The temperature response to these external influences is simulated by a two-dimensional Energy Balance Model (EBM) with realistic geography and seasonal cycle. Care is taken to compare records with data from EBM simulations that represent the same seasonal (growing season or annual mean) and geographical (land only or land and ocean, latitude strips) representation as used in the paleoclimatic reconstruction.

We have first attempted to detect the temperature response to the different forcings by a multiple regression of the reconstructions onto the EBM fingerprints for volcanic forcing, greenhouse gas forcing (with superimposed aerosol forcing over the industrial period) and solar forcing. These fingerprints have been derived by EBM simulations forced with the individual forcing agents. Figure 1 shows the result using the Crowley reconstruction, results using the other reconstructions were comparable. The response to volcanic forcing is reliably detected in all reconstructions, and the simulated temperature response to volcanic eruptions compares favorably with observations. The response to solar forcing is detected in hemispheric mean data only over some periods in

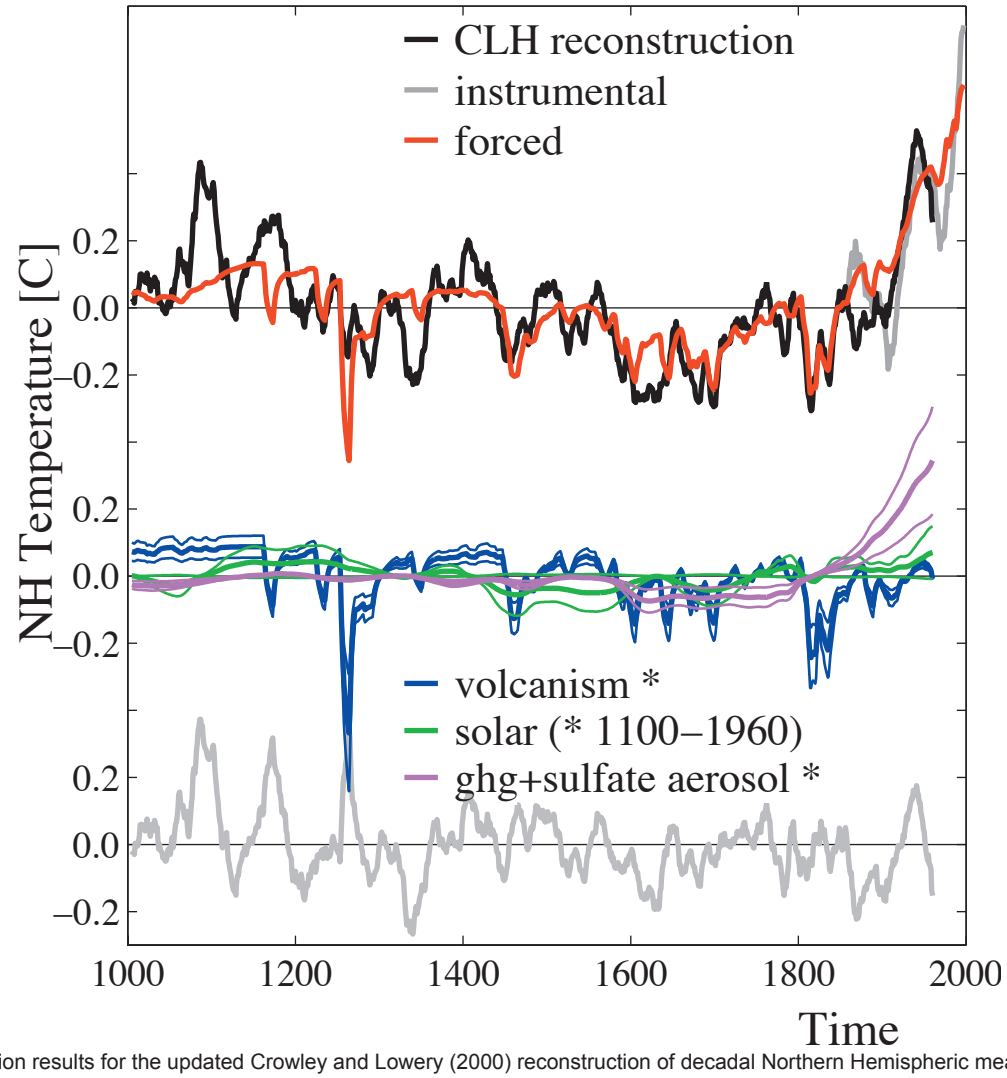


Figure 1: Detection results for the updated Crowley and Lowery (2000) reconstruction of decadal Northern Hemispheric mean temperature (north of 30N, calendar year average; from Hegerl et al., 2003). Upper panel: Paleo reconstruction (black) compared to the instrumental data (grey) and the best estimate of the combined forced response (red), middle panel: response attributed to individual forcings (thick lines) and their 5-95% uncertainty range (thin lines), lower panel: residual variability attributed to internal climate variability and errors in reconstruction and forced response. An asterisk ``*'' denotes a response that is detected at the 5% significance level. Results from other reconstructions are similar.

some records (those that represent annual rather than growing season data), and appears weak. Although most paleoclimatic records can be used only to the middle of the 20th century, the temperature response to $CO_2$ can be detected by this time in most records. Since the detection of the volcanic signal is dependent on a realistic representation of the temperature response to volcanism, it is important that particularly the response time to volcanism is realistic in the model. Figure 2 shows that this is the case.

Since the results from the detection of individual signals are encouraging, we have also used simulations forced with a combination of all relevant forcing agents in an attempt to estimate the probability density function (pdf) of climate sensitivity from paleoclimatic data. Our estimate of the pdf includes uncertainty in the paleo reconstructions, in solar and volcanic forcing, in ocean diffusivity, and in aerosol forcing. Results are quite comparable to those from instrumental data (Andronova and Schlesinger, 2000; Forest et al., 2000; Gregory et al., 2001) and will be shown at the workshop.

**References**

Allen M. R. and Stott P.A, Climate Dynamics, 21, 477-491 (2003).

Andronova, N. G. and M. E. Schlesinger, Geophys. Res. Let., 27 (14), 2137-2140 (2000).

Briffa, K. R., et al., J. Geophys. Res., 106, 2929—2941 (2001).

Crowley, T.J. Science, 289, 270-277 (2000).
Crowley, T.J., et al., Geophys. Res. Let. 30, doi:10.1029/2003GL017801 (2003).
Esper, J., E. R. Cook, F. Schweingruber, Science 295, 2250 (2002).
Forest, C.E., M.R. Allen, P.H. Stone, and A.P. Sokolov, Geophys. Res. Let. 27, 569-572 (2000).
Gregory, J. M. et al. J. Climate 15, 3117-3121 (2002).
Hegerl, G. C. et al., Geophys. Res. Let. 30(5). 1242. doi: 10.1029/2002GL016635 (2003)
M. E. Mann, R.S. Bradley, M. K. Hughes, Geophys. Res. Lett. 26, 759 (1999).

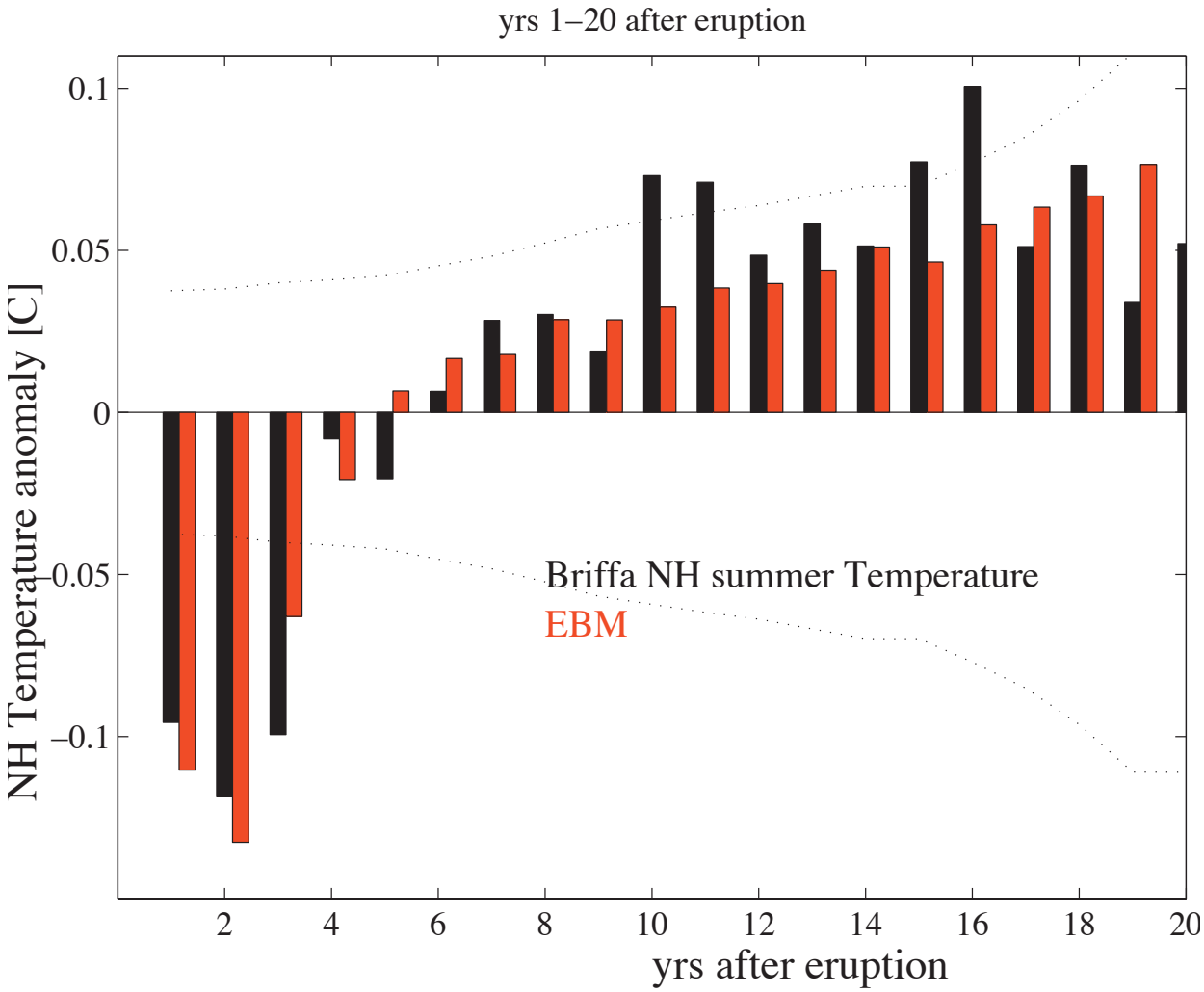


**Figure 2.** Comparison of the average response to volcanic eruptions in the energy balance model and the Briffa et al. (2001) reconstruction from the year of the eruption (year 1) to the next major eruption. 5-95% uncertainty ranges for the observed response are given by the dotted lines (note that sample size decreases with time). From Hegerl et al. (2003).

**IPCC Workshop on Climate Sensitivity**
Paris, France, July 26–29, 2004
*Pre-Conference Volume*

# What Can Be Learned from Variations in Atmospheric $CO_2$ and Temperature over the Past Millennium?

Fortunat Joos

*Climate and Environmental Physics, Physics Institute, University of Bern, Switzerland (joos@climate.unibe.ch)*

Uncertainties in climate projections arise from uncertainties in natural and anthropogenic forcings and from the feedbacks between climate change and biogeochemical cycles, in particular climate-carbon cycle feedbacks. Here, the proxy-records of variations in NH temperature and in atmospheric $CO_2$ are applied within a model framework to constrain solar forcing, the contribution of solar forcing and solar forcing amplification to the 20$^{th}$ century warming, and to constrain the response of atmospheric $CO_2$ to modest climate change (Gerber et al., 2003; Ammann et al., 2004; Joos and Prentice, 2004). A probabilistic framework offers a way to assess uncertainties in climate projections in a self-consistent way and consistent with available observations while taking into account not only uncertainties in the climate sensitivity but also uncertainties in radiative forcing, in the carbon climate-cycle, and other uncertainties (Knutti et al., 2003).

### Constraints on solar forcing and solar-induced climate change.

Understanding and quantifying natural climate variability on decadal to centennial time scales is a prerequisite to detect and attribute anthropogenic warming and to project future climate change. It is important to extend the evaluation of models used for climate projections through the pre-industrial period when natural variations were pronounced while anthropogenic influence was small.

The magnitude of low-frequency solar irradiance changes is highly uncertain. Tentative correlations with records of cosmogenic nuclei ($^{10}$Be, $^{14}$C), sunspots, aurora histories in combination with the behaviour of solar-like stars have been used to estimate past solar irradiance. The temporal evolution of different proxy series is in reasonable agreement for the past millennium. However, the scaling required to translate a proxy record into solar irradiance anomalies is highly uncertain and published estimates of multi-decadal solar irradiance changes vary by a factor of five. Apart from changes in total solar energy output, amplification of solar forcing and changes in stratospheric ozone distribution and wave dynamics or modifications of cloud properties by variations in cosmic-radiation are under discussion.

Various Northern Hemisphere (NH), and one global, surface temperature reconstructions for the past millennium have become available. These proxy-based reconstructions are affected by uncertainties and individual studies deviate notably from each other. However, taken together they suggest that natural low-frequency NH-temperature variations over the past millennium were within 0.3 to 0.9$^{o}$C. The instrumental-based temperature record shows an increase in global average surface temperature of 0.6 ± 0.2$^{o}$C over the 20$^{th}$ century.

Low-frequency solar irradiance changes were varied by a factor of 6.5 between different simulations with the NCAR coupled climate system model (Ammann et al., 2004). Simulations extended over the past 1150 years and include volcanic and anthropogenic forcing. Three key findings emerge.

First, the model is able to reproduce main features of the paleo temperature records. A clear link between the radioisotope-based solar irradiance record, NH-temperature reconstructions, and modelled temperature variations is found.

Second, large, low frequency solar irradiance variations are not compatible with the NH-temperature proxy records within the framework of the NCAR model. The range of model results encompass the range of reconstructed preindustrial NH-temperature variations. Given the low climate sensitivity of the NCAR model, smaller, possibly much smaller, than larger background trends in solar irradiance produce modelled climates in better agreement with the temperature proxy records.

Third, the cosmogenic isotope records and the NH-temperature proxy records constrain the contribution of natural climate variations to 20$^{th}$ century warming to be less than 0.2$^{o}$C. All simulations with anthropogenic

forcing included match the observed temperature increase over the industrial period and simulated global average surface temperature was higher during the most recent decades than during the previous 1100 years. On the other hand, only small warming over the industrial period is found in runs with solar and volcanic forcing only. This is the case even for the high solar scaling that yields larger than reconstructed temperature variations before the industrialization.

**Constraints on climate-carbon cycle feedbacks.**

Uncertainties in the response of the carbon cycle to future warming leads to uncertainties in projected warming of several degree Celsius. This is the same order of magnitude as uncertainties associated with the response of the physical climate system to a prescribed forcing, e.g. by greenhouse gases. Different carbon cycle – climate models have yielded different results on how future climate change affects the evolution of atmospheric $CO_2$. Projected increase in atmospheric $CO_2$ was found to be higher by a factor of 1.1 to 2 in simulations with global warming than in simulations without global warming. It is therefore imperative to consider the climate-carbon cycle feedback as well as the associated uncertainty in climate projections.

The term climate sensitivity is often defined as the response of the climate system to a unit change in radiative forcing and is expressed as the change in global average surface temperature for a nominal doubling of $CO_2$. The climate sensitivity of a model is then derived by prescribing a change in atmospheric $CO_2$ and evaluate the models temperature response. The response of the tropospheric water cycle, including changes in cloud cover, tropospheric water content, or changes in surface albedo through snow cover changes are included in most such assessments of the climate sensitivity. In contrast, the response of biogeochemical cycles and in particular the response of atmospheric $CO_2$ to climate change is not considered in this classical radiative forcing-climate sensitivity framework. In the IPCC TAR, models used to project atmospheric $CO_2$ included the climate-carbon cycle feedback. However, atmospheric $CO_2$ was prescribed in the TAR climate projections. Uncertainties associated with the climate-carbon cycle feedback have not been considered and consistency between the projected climate and the prescribed $CO_2$ is not guaranteed for a given emission scenario.

A probabilistic framework is useful to estimate the uncertainties associated with the climate-carbon cycle feedback, with forcings by various agents, and with the classical climate sensitivity. Uncertainties in natural and anthropogenic forcings both during the industrial and earlier period, combined with uncertainties in observations, and internal climate variability hamper our ability to constrain the climate sensitivity. Recent attempts to constrain the climate sensitivity from observations have shown that there exists the possibility that the change in global average surface temperature for a nominal doubling of $CO_2$ may well exceed the widely cited range of 1.5 to 4.5°C. The risk for high warming is further amplified by a potentially large positive climate-carbon cycle feedback. Higher temperature leads to higher growth rate of atmospheric $CO_2$ and, in turn, to an amplified warming.

The ice core atmospheric $CO_2$ record combined with the range of NH temperature reconstructions covering the past millennium provides an opportunity to evaluate the climate-carbon cycle feedback. While the temperature variations over the past millennium were relatively modest compared to the projected changes, the proxy records form nevertheless an important yard stick for coupled carbon cycle-climate model.

Figure 1 illustrates the relationship between the variations of decadal to multi-decadal northern-hemisphere surface temperature, atmospheric $CO_2$

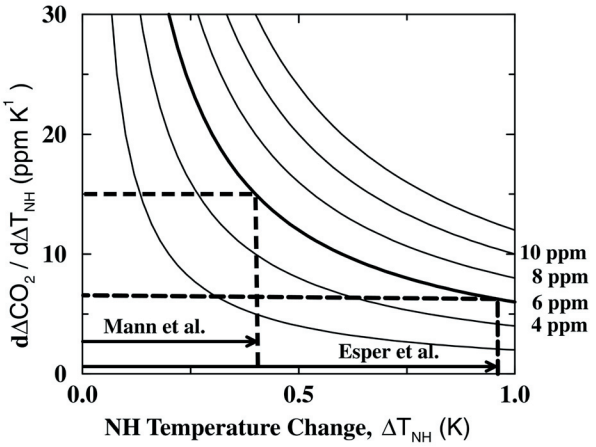


**Figure 1**. This diagram illustrates the relationship between northern-hemisphere (NH) surface temperature change, climate-carbon cycle feedbacks, and variations in atmospheric $CO_2$. Isolines depict different ranges for $CO_2$ variation during the last millennium and are plotted against changes in decadal-average NH-temperature (horizontal axis) and the climate-carbon cycle feedback expressed as change in atmospheric $CO_2$ concentration per degree change in decadal-average NH surface temperature (vertical axis). The range of NH-temperature variations reconstructed by Mann et al. (1999) and Esper et al. (2002) are shown by solid arrows. Combining the estimates for low-frequency NH-temperature variations and CO2 variations yields a climate-carbon cycle feedback range of 6 to 16 ppm $K^{-1}$ (dashed).

concentration, and the strength of the climate-carbon cycle feedback (as ppm $CO_2$ released per K temperature increase in the Northern Hemisphere). The strength of the feedback depends on several factors including the change in solubility of $CO_2$ in seawater and the responses of productivity and heterotrophic respiration to temperature and soil water. We assume that the pattern of climate change (temperature, precipitation, cloud cover), as far as relevant for atmospheric $CO_2$, remained approximately constant. The current best estimate of the actual $CO_2$ range during the past millennium (prior to the Industrial Revolution) is 6 ppm, based on emerging high-quality measurements (Siegenthaler and Monnin, pers. comm.). If we accept the ranges of temperature variations reconstructed by Mann et al. (1999) and by Esper et al. (2002) as equally possible, then the $CO_2$ concentration range of 6 ppm constrains the climate-carbon cycle feedback to between 6 and 16 ppm $K^{-1}$ (for global mean surface temperature changes of less than ~1ºC). This implies that the feedback of 12 ppm $K^{-1}$ found with the IPCC TAR version of the Bern carbon cycle-climate model in transient simulations over the past millennium is compatible with the proxy records. On the other hand, models with a very strong climate-carbon cycle feedback (for modest climate change) are not compatible with the $CO_2$ and NH-temperature proxy records.

**Selected References**

(pdf-files on http://www.climate.unibe.ch/~joos/publications.html)

Ammann C.M., F. Joos, D. S. Schimel, B. L. Otto-Bliesner, R. A. Thomas, Constraining the range of solar irradiance changes during the last millennium, in preparation.

Esper, J., E. R. Cook, and F. H. Schweingruber. Low-frequency signals in long tree-ring chronologies for reconstructing past temperature variability. Science, 295: 2250-2253, 2002.

Gerber S., F. Joos, P. P. Brügger, T. F. Stocker, M. E. Mann, S. Sitch, and M. Scholze. Constraining temperature variations over the last millennium by comparing simulated and observed atmospheric CO2. *Climate Dynamics,* 20, 281-299, doi: 10.1007/s00382-002-0270-8, 2003.

Joos F. and I. C. Prentice. A paleo-perspective on changes in atmospheric CO2 and climate. In *The Global Carbon Cycle: Integrating Humans, Climate and the Natural World,* C. Field and M. Raupach (Eds.), SCOPE series 62, Island Press, Washington DC, USA, 165-186, 2004.

R. Knutti, T. F. Stocker, F. Joos, and G.-K. Plattner. Probabilistic climate change projections using neural networks. *Climate Dynamics,* 21, 257-272, 2003.

Mann, M. E., R. S. Bradley, and M. K. Hughes. Northern Hemisphere temperatures during the past millennium: Inferences, uncertainties, and limitations. *Geophysical Research Letters*, 26: 759-762.1999.

**IPCC Workshop on Climate Sensitivity**
Paris, France, July 26–29, 2004
*Pre-Conference Volume*

# Climate Sensitivity Inferred from Paleoclimatic Records

Jean Jouzel

*Institut Pierre Simon Laplace / Laboratoire des Sciences du Climat et de l'Environnement CEA/CNRS CE Saclay 91191 Gif/ Yvette France*

"Our most precise knowledge of climate sensitivity comes from data on ancient and recent climate change". This sentence was not written by a paleoclimatologist but by J. Hansen and coworkers (1993) in an excellent review article "How sensitive is the world's climate" published more than 10 years ago. These authors added that "the best empirical information on equilibrium climate sensitivity is provided by climate variations of the past 200 000 years", the time span over which $CO_2$ and $CH_4$ data were then available from the Vostok Antarctic ice core, and derived a climate sensitivity $\Delta T_{2*CO2}$ of 3 ± 1°C for doubled $CO_2$.

As a paleoclimatogist, I was very pleased by this review article, but I am not so convinced that all climate modellers share Jim Hansen's enthusiasm for paleoclimate estimates of climate sensitity. Probably (e.g., Crowley, 1993), more has to be done to convince both paleoclimatologists and climatologists of the potentialities of paleodata in this respect, keeping them aware of the limitations inherent to this approach. This will hopefully be an outcome of our IPCC workshop which leaves ample room to this topic. Before these various presentations, it might be useful to briefly review published literature in this domain and this will be the main purpose of my talk. Very schematically, existing approaches fall in three categories with estimates respectively based on pre-quaternary data (the distant past with both relatively badly known climate forcings and responses), on quaternary data (indeed limited to the last few hundred thousands of years for which greenhouse gas data are available from ice cores), and on more recent data (the last millenia which is potentially interesting, even though the climate signal is weak). Among other examples, I will briefly examine the following with a focus on pre-quaternary and quaternary timescales.

Hoffert and Covey (1992) combined data from two paleoclimates, one colder (the Last Glacial Maximum, LGM, 20 000 years ago) and one warmer (the Mid-Cretaceous Maximum, MCM, about one hundred million years ago), to infer a $\Delta T_{2*CO2}$ of 2.1 ± 0.4°C; see also criticism by R. Lindzen (1992) and Covey et al. (1996). However, it is clear that we have to be cautious going further back in time as recently exemplified by a paper by Shaviv and Veizer (2003). Starting from a reconstruction of cosmic ray fluxes and of its apparent high correlation with temperature over the last 520 million years, these authors inferred that $CO_2$ has a smaller effect than previoulsy thought with a $\Delta T_{2*CO2}$ as low as 0.75°C. Indeed, in Rahmstorf et al. (2004), we clearly point out that the claimed correlation between cosmic ray flux and temperature appears to not hold up under scrutiny and that in any case the author's estimate of the effect of a $CO_2$ doubling is highly questionable.

The late quaternary is probably more appropriate to provide estimates of $\Delta T_{2*CO2}$ although there are, here again, limitations. The advantadges are that glacial-interglacial temperature changes are large (mean value of about 5°C) and that greenhouse gas changes are well documented as well as, albeit indirectly, other potential forcings such as the one linked with change in aerosol loadings. Although, the initial instigator of ice ages is the variation of insolation due to periodic changes of the Earth's orbit, the contribution of greenhouse gases can be investigated. Prior to the above mentioned Hansen et al. estimate, we inferred from Vostok and other data (Lorius et al., 1990) climate sensitivity over the last 150 000 years (last climatic cycle). Over this time period the contribution of greenhouse gases was estimated to be between 40 and 65%—a figure however higher than inferred from climate model experiments as performed by Berger and colleagues (1993)—leading to the conclusion that a $\Delta T_{2*CO2}$ of 3 to 4°C may be a realistic value.

Extending this calculation to four climatic cycles (Vostok data), which has not yet been done, should not drastically change this estimate as the correlation between greenhouse gases and Antarctic climate does not vary significantly from one glacial cycle to the next. The situation might differ, and indeed appears quite promising, with the recent extension of the ice core record to 800 000 years (EPICA Dome C ice core). There is a change of pacing prior the last four climatic cycles with less warmer interglacial periods. This

should offer, once greenhouse data will be available, the possibility to test situations (interglacials) with relatively similar boundary conditions and, hopefully, different greenhouse levels (see presentations of P. Braconnot and J. Overpeck dealing with interglacials). In addition one weakness of this approach, i.e. the fact that it deals with transient climate changes, should be, at least partly, overcome by the use of models of intermediate complexity which allow to depict such transient climatic changes.

Obviously, the steady state approach followed by Hansen et al. (1993) and by many other groups using data from the Last Glacial Maximum, has also a lot to offer (see presentations of S. Rahmstorf and B. Otto-Bliesner). However they have limitations too, which also applies for transient estimates. Such limitations come, in particular, from the uncertainties in the estimate of the mean global surface temperature change and from the fact that climate sensitivity between the ice age and today may differ from that between today and a warmer world, due for example to cloud processes (e.g., Ramstein et al., 1998).

The use of data from the last millenium which will be discussed by G. Hegerl and N. Andranova, and, dealing more specifically with the $CO_2$ cycle itself, by F. Joos, is more recent. On this timescale, I will focus on climate forcings, which are directly or indirectly estimated from ice core data, and on associated uncertainties.

**References**

Berger, A., Loutre, M. F., Tricot, C. and Gallée, H., Water vapour, CO2 and insolation over the last glacial-interglacial cycles, Phil. Trans. R. Soc. Lond. B, 341, 1993, p. 253-261.

Covey, C., Sloan, L. C. and Hoffert, M., Paleoclimate data constraints on climate sensitivity : The paleocalibration method., Climate Change, 32, 1996, p. 165-184.

Crowley, Geological assessment of the greenhouse effect, Bulletin of the American Meteorological Society, 74, 1993, p. 2363-2373.

Hansen, J., Lacis, A., Ruedy, R., Sato, M. and Wilson, H., How sensitive is the world's climate, Research and exploration, 9, 1993, p. 143 - 158.

Hoffert, M. and Covey, C., Deriving global climate sensitivity from paleoclimate reconstructions, Nature, 360, 1992, p. 573-576.

Lindzen, R., Paleoclimate sensitivity, Nature, 363, 1993, p. 25-26.

Lorius, C., Jouzel, J., Raynaud, D., Hansen, J. and Le Treut, H., Greenhouse warming, climate sensitivity and ice core data, Nature, 347, 1990, p. 139-145.

Rahmstorf, S., Archer, D., Ebel, D. S., Eugster, O., Jouzel, J., Maraun, D., Neu, U., Schmidt, G., Severinghaus, J., Weaver, A. J. and Zachos, J., Cosmic Rays, Carbon dioxide and Climate, E.O.S, 85, 2003, p. 38, 41.

Ramstein, G., Serafini-Le Treut, Y., Le Treut, H., Forichon, M. and Joussaume, S., Cloud processes associated with past and future climate changes, Clim. Dyn., 14, 1998, p. 233-247.

Shaviv, N. and Veizer, J., Celestial driver of Phanerozoic climate, GSA Today, 13, 2003, p. 4-10.

**IPCC Workshop on Climate Sensitivity**
Paris, France, July 26–29, 2004
*Pre-Conference Volume*

# Climate Sensitivity - The Role of Aerosol Effects

Stefan Kinne

*Max-Planck-Institute for Meteorology, Hamburg, Germany*

## INTRODUCTION

### *AEROSOL and CLIMATE*

Industrialization and land-use changes have increased the aerosol load in the Earth's atmosphere. However, in what way this aerosol increase has influenced the available radiative energy to the Earth-Atmosphere-System (in particular the distribution of solar and terrestrial radiation) remains unclear. Uncertainties are related to the complexity in distribution and properties of aerosol and to interactions with other atmospheric particles (in particular clouds). In an effort to better address the different nature of these aerosol-climate complexities, it is commonly distinguished between the impact from the aerosol presence (***direct effect***) and the impact of aerosol induced modifications to other atmospheric properties (***indirect effects***).

### *FORCING*

The climate impact for any change to the atmospheric composition is commonly quantified by the change of the radiative energy escaping to space. Increases to the energy loss stand for ***cooling***. Reductions to the energy loss stand for ***warming***. This so-called 'radiative forcing' at the top of the atmosphere (ToA) is (for more detail) often further separated by spectral region (solar and terrestrial) and by location (atmosphere and surface). To provide just one number, regional and seasonal forcing is commonly summarized by a globally and annual averaged forcing value. For anthropogenic aerosol such ToA forcing is believed to be a cooling. However, there is a strong modulation of this impact (even in sign) by region and season. One of the explanations is that aerosol forcing does not only depend on the various aerosol properties but also on environmental properties. Some of the critical parameters for aerosol forcing are introduced next.

## DIRECT EFFECT

### *PARAMETERS*

The direct ToA aerosol forcing is mainly modulated by aerosol properties (of concentration, size, absorption and altitude), by surface properties, by the presence of clouds and available sun-light.

***Aerosol size*** determines spectral regions of importance. Aerosol covers several orders of magnitude in size - from a few nanometers to at least ten micrometer. However, from a radiative transfer perspective only the larger aerosol sizes (>0.1 μm) are important. With a natural concentration minimum at 1.0 μm sizes (due to growth and removal processes) the larger aerosol particles are usually separated in two size modes. Aerosols of the smaller accumulation mode (0.1 -1.0 μm) are largely 'anthropogenic', while aerosols of the larger coarse mode (>1.0 μm) are mainly of 'natural origin'. The smaller aerosol particles of the accumulation mode mainly influence the energy distribution in (the visible region of) the solar spectrum. The larger aerosol particles of the coarse mode affect the entire solar spectrum as well as part of the terrestrial spectrum.

***Aerosol absorption*** at ***solar*** wavelengths has an important influence on the distribution of aerosol forcing within the atmosphere. Aerosol solar absorption (self-) heats its atmospheric layers. As this atmospheric forcing allows less solar (scattered) radiation to escape from the atmospheric aerosol layers, the forcing at the surface will be more negative, while at the same time aerosol (reflection associated) solar energy losses at the ToA are reduced (less cooling). In fact, ToA warming is expected from strongly absorbing aerosol.

***Aerosol absorption*** at ***infrared*** wavelengths can trap terrestrial radiation that is otherwise lost to space. Such aerosol greenhouse ToA warming, however, will only be significant for the combination of elevated aerosol and larger particles of the coarse mode (e.g. dust). Many studies ignore the infrared component to the ToA aerosol forcing, because the altitude / large size combination is rare, and because even for those cases the solar (albedo) effect usually dominates the (infrared) greenhouse effect (on the basis of daily averages).

***Solar surface albedo*** below the aerosol layer has a strong effect on strength and sign of (clear-sky) aerosol solar ToA forcing. Over dark surfaces (e.g. ocean) aerosol associated solar energy losses to space are maximized: ToA cooling can be expected – unless aerosol is strongly absorbing. Over bright surfaces

(e.g. deserts and especially snow) aerosol additions to already high solar energy losses to space are small: ToA warming can be expected, because already weak aerosol absorption will lead to ToA warming.

***Cloud presence*** complicates aerosol ToA forcing to the point that the relative altitude between aerosol and clouds must be known. If located below clouds the aerosol impact becomes small, because the solar energy available for interactions with aerosol is strongly reduced. However, when aerosol is located above clouds, then these clouds act similar to bright surfaces with an overall tendency towards ToA warming. Aerosol associated ToA cooling under clear-sky conditions will represent an overestimate (on the order of 50%) with respect to all-sky conditions.

### *MEASUREMENTS?*

Radiative forcing by nature is a difference to an aerosol (component) free or less loaded (e.g. pre-industrial) reference state. Thus, a measurement of the aerosol direct radiative forcing is basically impossible. At best, a combination of different satellite sensors may provide clear-sky forcing estimates (e.g. EOS Terra: MODIS/MISR → aerosol optical depth in cloud free regions; CERES → associated ToA fluxes). However, those estimates will be limited to few regions and seasons where the ToA solar aerosol signal exceeds statistical noise. In addition, measurements cannot distinguish between natural and anthropogenic contributions (although new efforts involving size information [assuming sub-micron sized aerosol to be of anthropogenic origin] may provide rough estimates). Thus, when interested in the impact on anthropogenic aerosol on climate (globally and under realistic all-sky conditions) we need to turn to modeling. And our current understanding on the influence of aerosol on climate is almost entirely based on model simulations.

### *MODELING*

Coarse gridded (ca. 200*200km, 20 vertical levels) global circulation models (GCM) or chemical transport models (CTM) are applied to provide estimates for the aerosol impact on climate. In recent years almost all models added more detail to their aerosol modules to improve aerosol representation (concentration, size, hygroscopicity, absorption and altitude) and to improve aerosol processing (e.g. subscale variability, cloud schemes). In recognition, that aerosol has a lifetime of a few days and originates from a multitude of different sources, most aerosol modules in these global models now distinguish among at least five different aerosol components:

***BC*** (‘Black Carbon’ or ***EC*** ‘elementary carbon’) originates from wildfires and consumption of bio-fuel and fossil-fuel. Black carbon is a strongly absorbing aerosol of accumulation mode. An initially hydrophobic behavior is moderated with time as mixtures with other components occur.

***OC*** (‘Organic Carbon’ or ***POM*** [⇔1.4*OC] ‘Particulate Organic Matter’), originates (as BC but more abundant) from wildfires and the consumption of bio-fuel and fossil-fuel. A minor fraction also enters via the gas phase. Organic carbon is a weak to moderately absorbing aerosol of the accumulation mode. Organic carbon is moderately hydrophilic (which means this aerosol type will increase in size as the ambient relative humidity increases).

***SU*** (‘sulfate’) predominantly enters the atmosphere via the gas-phase from fossil fuel consumption, volcanic exhaust and oceanic phytoplankton (DMS – dependent on solar surface flux). Sulfate is a non-absorbing aerosol of the accumulation mode. Sulfate is hydrophilic.

***DU*** (mineral ‘dust’) originates from mainly from dry lake beds. Critical parameters are near-surface winds, soil moisture, vegetation and snow cover. Dust is (excluding strong UV absorption) a weak absorbing aerosol of the coarse mode and usually considered hydrophobic.

***SS*** (‘sea-salt’) aerosol originates from sea-spray. The most critical parameter is the near- surface wind. Sea-salt aerosol is a non-absorbing aerosol of the coarse mode. Sea-salt is highly hydrophilic and at high ambient humidity aerosol size is comparable to cloud droplet sizes.

Aerosol at any particular location and time is always a mixture of aerosol components. While some of the aerosol components are externally mixed, internal mixtures of components occur as well. Since optical or hygroscopic properties of internal mixtures usually differ from volume weight averages of individual components, some of the more advanced aerosol modules in global modeling now even consider internal mixing. Aerosol component modeling is usually done in three consecutive steps:

***STEP 1:*** Based on (particle and gas) emission inventories for each aerosol type, global models process aerosol (e.g. gas-to-particle conversion, growth, removal, redistribution be clouds) to yield mass concentration.

***STEP 2***: Mass is converted into (the optical property of) aerosol optical depth (as a function of wavelength), where assumptions for aerosol size (-distribution) and water uptake (humidification and ambient relative humidity) are critical.

***STEP 3***: Aerosol optical depth spectral data along with spectral data on aerosol absorption (based on absorption assumption of contributing aerosol types) are processed in radiative transfer schemes to yield an aerosol forcing.

Each of these steps introduces uncertainties. Unclear in particular are uncertainties introduced in *STEP 1*, where in contrast to *STEP 2* (measurements supply data) or *STEP 3* (accurate methods exists) reference data are lacking. In addition, with the increased complexity of aerosol modules many new assumptions were introduced, which have not been completely tested. Thus, at least at this stage the uncertainty in modeling actually may have increased. Even worse, our current understanding of uncertainty may be biased.

*UNCERTAINTY*

Uncertainty is often not what is appears to be. Differences for the simulated end-products (ToA radiative forcing) are not necessarily a good estimate for forcing uncertainty, if aerosol processing (e.g. emission strength, transport, removal, chemistry in *STEP 1)* is not completely understood and/or poorly evaluated. Currently most models to some degree 'tune' aerosol processing at a subsequent step to readily available data on aerosol optical depth (e.g. global fields from satellite remote sensing or data from local AERONET statistics). To emphasize this point, simulated global annual averages for the mid-visible aerosol optical depths among 15 global models agree within a factor of 2. More importantly however 10 models fall in the 0.126-0.145 range. For these 10 models maximum-minimum factors are displayed in Figure 1 on a component basis for optical depth, dry mass and mass extinction efficiency (the ratio of the former two properties). These large differences raise many questions. Here are some:

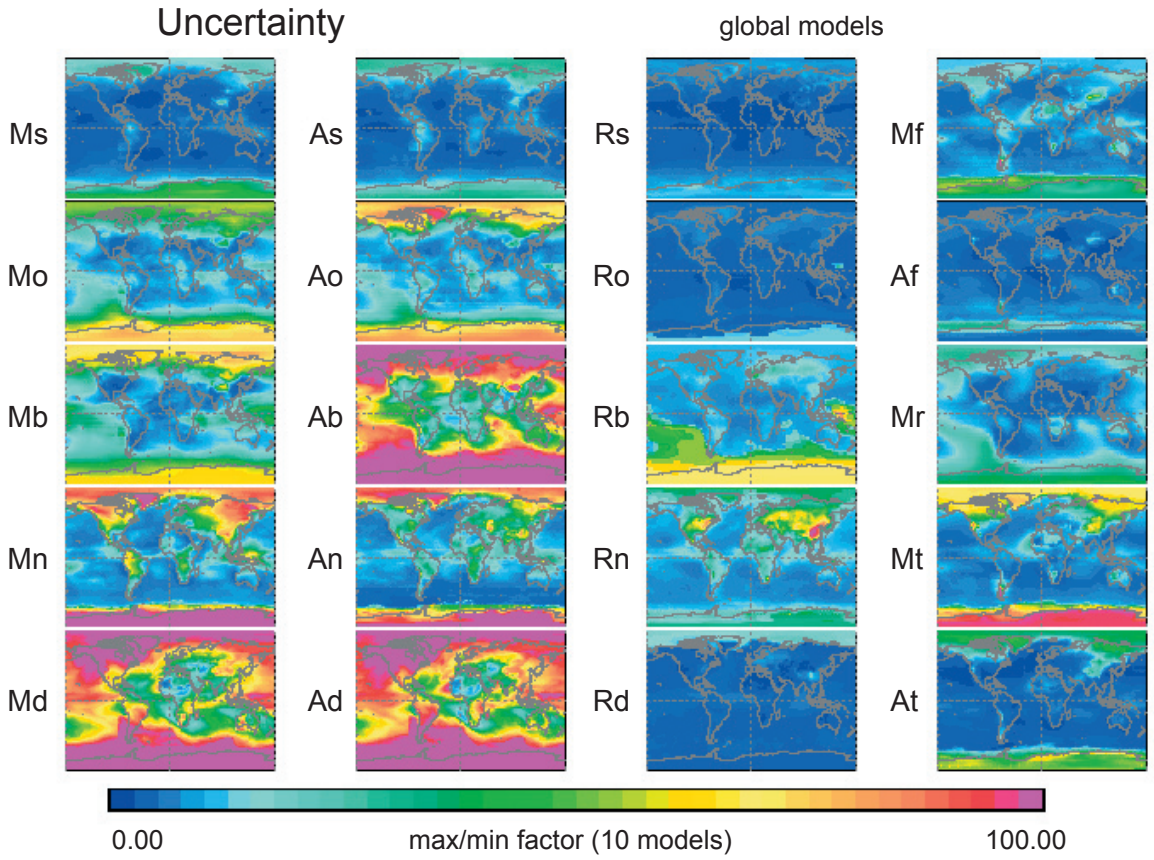


**Figure 1.** Uncertainty factors in global modeling based on local (1*1 degree) maximum / minimum ratios of (yearly averaged) monthly means of 10 global models (CTM or GCM). Aerosol properties for mass (M), mid-visible optical depth (A) and mass extinction efficiency (R) are addressed by component (s – sulfate, o – organic carbon, b – black carbon, n – seasalt, d – dust). The right row of panels presents totals (t) of all components, fractions (f) attributed to small sizes (<1μm) and the bc/oc mass ratio (r). Note, that all 10 global models agree to better than 20% for the annual, globally averaged mid-visible aerosol optical depth.

**QUESTIONS**

- Are aerosol forcing simulations (via emission data) accurate enough to be useful?
- Is modeling still missing important processes and interactions (e.g chemistry, scale)?
- Are individual models sufficiently explored in terms of strength and weaknesses?
- How to place resources in modeling (detail overkill vs. detail need)?

**INDIRECT EFFECTS**

Aerosol indirect effects summarize the climatic impact of all aerosol related modifications to other atmospheric properties. Particular important are aerosol induced changes to clouds, because clouds are the main modulators to the distribution of radiative energy in the atmosphere. Aerosol can influence clouds in many ways. Some of these effects support ToA cooling (e.g. smaller droplets, extended lifetime) while others support ToA warming (e.g. suppressed convection). Thus, even the sign of the overall indirect effect is not assured. Process studies (e.g. shiptracks) often provide only a distorted picture, because many indirect effects are often temporally delayed and locally detached (e.g. changes in precipitation patterns). Asides from properties of clouds and environment properties (e.g. background aerosol) also the aerosol properties are essential. In light of the large uncertainties regarding the aerosol direct effect several questions come to mind:

*QUESTIONS*

- Can we learn more by looking at observational data than relying on modeling?
- Are we aware of all aerosol indirect effect (and associated feedbacks)?
- Are cloud schemes in global model sufficiently accurate for aerosol - cloud interactions?

**ACTIONS**

*DIRECT EFFECT*

Different approaches are taken to improve uncertainties of the direct aerosol forcing. Two of those are outlined below. The first approach is a measurement-based diagnostic for aerosol modules. Its goal is to identify and eliminate weak modeling components, to quantify uncertainties at each modeling step and translate these uncertainties into a forcing uncertainty. The second approach seeks to apply data (and data uncertainty) directly into forcing, circumventing many model uncertainties associated with aerosol processing. Yet, even these more data oriented approaches require still significant model support.

1. To better quantify the skill of aerosol component modules in global modeling and to restrict modeling freedom, measurements are the key. This is recognized the AeroCom activity. Its goals are to diagnose (weaknesses in) aerosol modules and to quantify uncertainties at each modeling *STEP* and for each aerosol component (e.g. *SU, BC, OC, SS, DU*). Any proper assessment of differences between models with data requires an understanding for data quality (which is often worse than promised) and data representation. Evaluations are mainly based on available statistics of ground based in-situ sampling (e.g. IMPROVE network), of ground-based remote sensing (e.g. AERONET or EARLINET networks) and remote sensing from space (e.g. MODIS and MISR sensor data). AeroCom has initiated consistency tests for aerosol processing by requesting model-output for prescribed (yr 2000) harmonized input on emission and meteorology. Special attention will be given to outliers, as outliers indicate a deficiency, either by one or by all other models. Also, consistency among models is not necessary a measure of uncertainty (e.g. models agree best for organic carbon aerosol, one of the least understood aerosol components). AeroCom's goal is to quantify 'real' uncertainty at sub-steps in forcing simulations and to translate these into overall forcing.

2. With new and more capable sensors from remote sensing and better statistics from ground data, there are now efforts to tie direct aerosol forcing estimates stronger to observational data. For instance, detailed data on aerosol properties from ground statistics (e.g. AERONET inversions provide data on concentrations, absorption and size). These data can be merged with satellite remote sensing of aerosol, clouds and surface (solar albedo). Aerosol direct forcing estimates from such data are presented in Figure 2. Other ideas involve better estimates based on the merging of data-streams from measurements and global modeling. For instance, (global) modeling can be applied to extend sparse sampling in space and time or models can provide needed information not available from measurements (e.g. forcing efficiency). Still, the fact that these methods are under considerations reflects the overall large uncertainty associated with aerosol direct forcing, especially on a regional basis.

*INDIRECT EFFECTS*

Also several approaches are taken improve uncertainties for the aerosol indirect forcing, by recognizing and eliminating poor assumptions. Two of those approaches are outlined below. The first approach is based on the exploration of correlations among retrieved aerosol and clouds from space observations. The second approach

focuses on sensitivities to particular assumptions in aerosol-cloud interactions among models.

1. Correlations between 'quasi-simultaneous' retrievals of clouds and aerosol can be used to locate hot-spots for aerosol cloud interactions. Correlation maps serve are incentive to studies on important and dominant processes and as a footprint that needs to be matched by models (to demonstrate modeling skill). Under the AeroCom exercise correlations of aerosol and cloud properties are explored, based on daily retrievals with the MODIS sensor for the year 2000. Modelers are asked to simulate with (prescribed) year 2000 aerosol emissions and year 2000 meteorology to assure similar background conditions.

2. Under auspices of the US lead Climate Change Science program (CCSP) (and in close collaboration with AeroCom) a model-intercomparison of aerosol-cloud interactions in global modeling has been proposed. For several control experiments, with different degrees of freedom, the output of several models (including the associated forcing) is compared. Goal of this exercise is to identify and remove estimates of models with poor processing from uncertainty estimates.

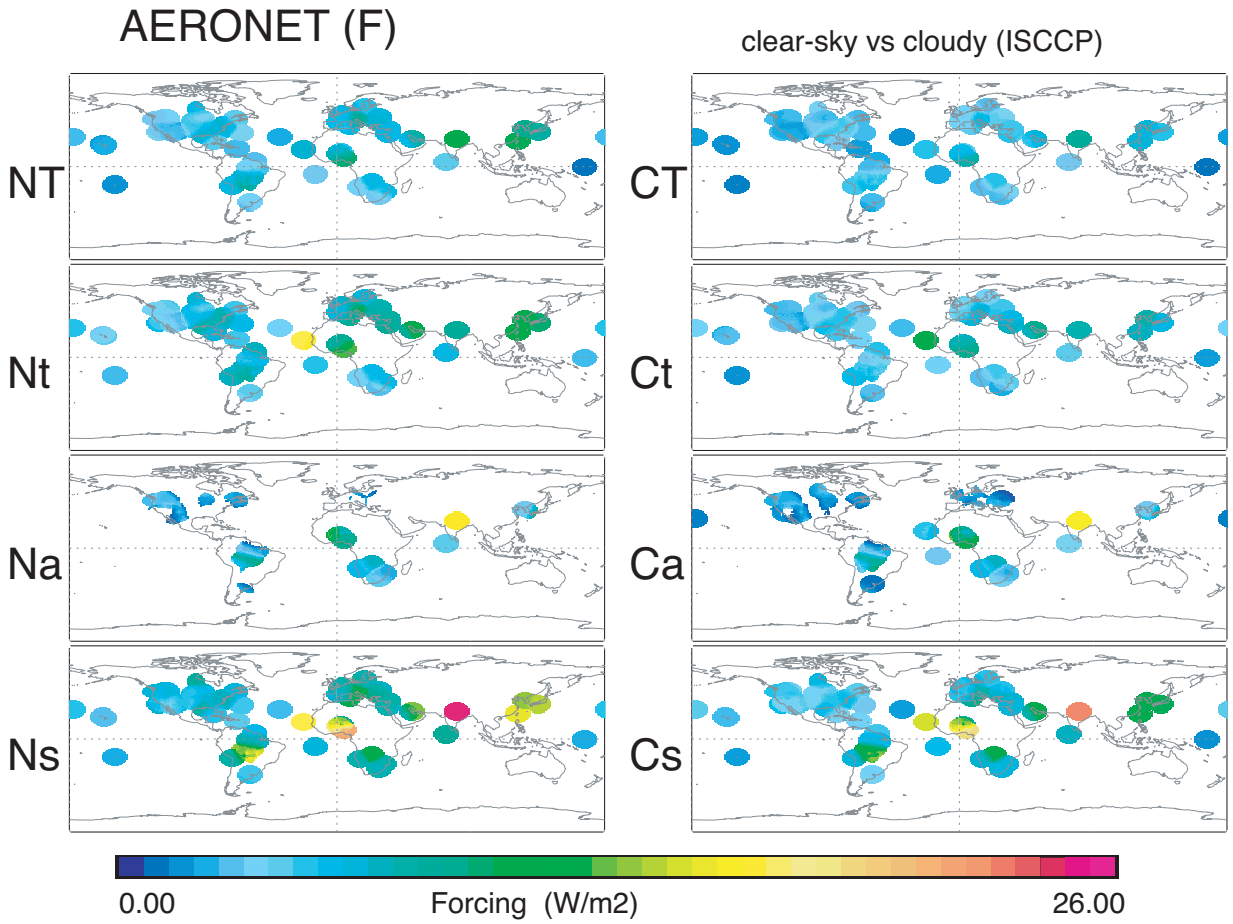


**Figure 2.** Aerosol Forcing based on 1998-2001 AERONET data. The presented yearly means are based on monthly statistics. Separate results are shown for forcings at the top of the atmosphere (t), in the atmosphere (a) and at the surface (s). The left column of panels shows the forcing under clear-sky condition (N), the right column of panels shows the forcing under cloudy conditions (using ISCCP cloud data). Also shown in the first row are forcings at the top of the atmosphere solely due to aerosol sizes of the accumulation mode (T, as anthropogenic estimate).

**IPCC Workshop on Climate Sensitivity**
Paris, France, July 26–29, 2004
*Pre-Conference Volume*

# A Comparison of Climate Sensitivity Among the Japanese Models

**Akio Kitoh[1], Akira Noda[1], Seiji Yukimoto[1], Seita Emori[2], Toru Nozawa[2], Tomoo Ogura[2], Masahide Kimoto[3], Ayako Abe-Ouchi[3], and Akimasa Sumi[3]**

[1] *Meteorological Research Institute, Tsukuba, Japan*
[2] *National Institute for Environmental Studies, Tsukuba, Japan*
[3] *Center for Climate System Research, University of Tokyo, Tokyo, Japan*

## 1. Introduction

Two Japanese models (MRI and CCSR/NIES models) showed the smallest and the largest climate sensitivity at the time of the IPCC TAR in 2001. Here we report recent changes in their models' climate sensitivity.

## 2. MRI model

The MRI-CGCM2 (Yukimoto et al. 2001; Yukimoto and Noda 2002) has several versions depending on cloud-radiation tuning. In its radiation scheme, $CO_2$, $H_2O$, $O_3$, $CH_4$ and $N_2O$ are treated as the greenhouse effect gases directly, and the direct effect of sulfate aerosol is explicitly treated, but the indirect effect is not included. For the AR4 scenario experiments, atmospheric concentration of sulfate aerosols has been calculated for all SRES emission scenarios of sulfur dioxide by a chemical transport model MASINGER developed at MRI (Tanaka et al. 2003). The global mean surface air temperature rises about 2.4K, 2.7K and 2.0K at the end of the 21st century compared to the 1961-1990 value in A1B, A2 and B2 scenarios, respectively (Uchiyama et al. 2004).

The global and annual mean surface air temperature change at 2x$CO_2$ of the MRI-CGCM2.0 in the IPCC TAR was very small, that is, 1.1K, with effective climate sensitivity of 1.4K. In this simulation, the energy budget was not balanced between the top and the bottom of atmosphere, and the global mean and meridional distribution of radiative flux at the top of atmosphere had a large difference from the observation. The revised MRI-CGCM2.3 is improved in reproducing mean climate of global-mean and meridional distribution of energy budget by mainly adjusting clouds representation. With the improved version of the model, the effective climate sensitivity increased more than 1K. The decrease of negative feedback due to cloud forcing can explain most of the changes in climate sensitivity. The major difference of cloud feedback can be explained by the change in tropical low-level clouds for shortwave forcing and in tropical middle level clouds for longwave forcing. Associated with the tropical low-level clouds, the stratus and stratocumulus clouds over the eastern part of the oceans (especially over the eastern Pacific) have large impact on shortwave forcing. The change in the tropical middle level clouds is associated with the change in deep convective clouds.

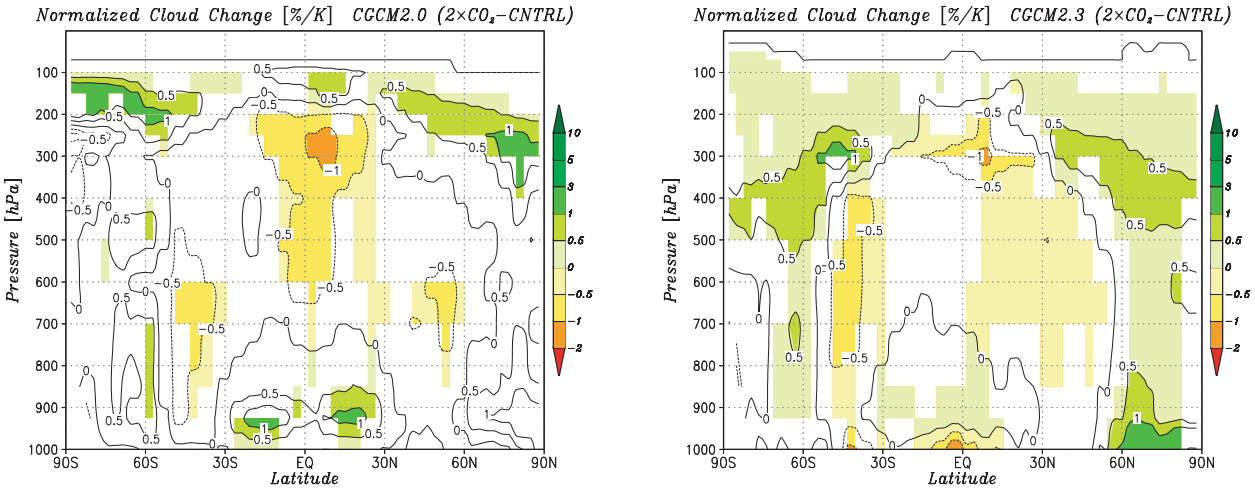


**Figure 1.** Zonally averaged annual mean cloud amount change normalized by global-mean surface air temperature change for (left) MRI-CGCM2.0 and (right) MRI-CGCM2.3.

Table 1. Climate sensitivity of the MRI-CGCM2.3 and two CCSR/NIES2 versions.

| | MRI-CGCM2.3 | CCSR/NIES-L | CCSR/NIES-H |
|---|---|---|---|
| Equilibrium sensitivity | 3.20 K | 3.95 K | 6.30 K |
| Transient (yr61-80) climate response | 2.18 K | 2.11 K | not measured |
| Equilibrium precipitation change | 7.33% | 8.75% | 13.95% |
| Transient precipitation change | 4.49% | 3.52% | not measured |

In summary, the low climate sensitivity in the TAR SRES simulation with the MRI-CGCM2.0 is mostly attributable to an insufficient tuning of the cloud-radiation process. Simulations with a revised version of the MRI-CGCM2.3 show a good agreement in the global mean surface temperature observed in the 20th century.

### 3. CCSR/NIES/FRSGC model

The CCSR/NIES/FRSGC model (CCSR/NIES1: Emori et al. 1999) has been updated by including RIAM/CCSR aerosol transport-radiation model (SPRINTARS; Takemura et al. 2000), which can handle major tropospheric aerosols (carbonaceous, sulfate, sea salt and soil dust), and also has a parameterization of both the 1st and 2nd kind indirect effects of aerosols on cloud (albedo and lifetime). This updated model (CCSR/NIES2) is described by Nozawa et al. (2003).

The global mean surface air temperature rises about 4.5K, 3.3K, 5.3K and 3.9K at the end of the 21st century compared to the 1961-1990 value in A1B, B1, A2 and B2 scenarios, respectively. These values are higher than those in the CCSR/NIES1 due to a use of a different set of absorption parameters for various gases in the radiation code and due to the difference in cloud feedback (positive in CCSR/NIES2 and negative in CCSR/NIES1). About two-thirds of the difference is explained by the former (Nozawa et al. 2003).

The CCSR/NIES2 in the TAR shows the climate sensitivity of 5.1K. The reason of generally high sensitivity is that the model shows a decrease in low-level cloud cover by warming, thus having a positive shortwave cloud feedback. Retuning of the model can generate a higher-sensitivity version (6.30K) and a lower-sensitivity version (3.95K). Difference between the two versions comes from (1) a choice of empirical function for cloud water phase diagnosis and (2) a treatment of melted cloud ice. In the former, a function similar to Mitchell et al. (1989) results in lower sensitivity while a function similar to Del Genio et al. (1996) results in higher sensitivity. In mid-to-high latitudes, there is a northward shift of cloud water distribution by warming with increase of cloud water in high latitudes. This increase in cloud water is shifted equatorward in lower sensitivity case, compared to that in higher sensitivity case, due to differences in temperature range of empirical function. For the treatment of melted cloud ice, melted cloud ice is diagnosed as cloud water (higher-sensitivity) or as rain (lower-sensitivity). In the latter case, there is less lower-level cloud water in the model climate, which may be the reason for low sensitivity.

The model is used for the 20th century simulation with 'complete' forcing both with the lower-sensitivity and higher-sensitivity versions. It is revealed that time-series of annual global mean surface air temperature with lower-sensitivity model fits better to the observed

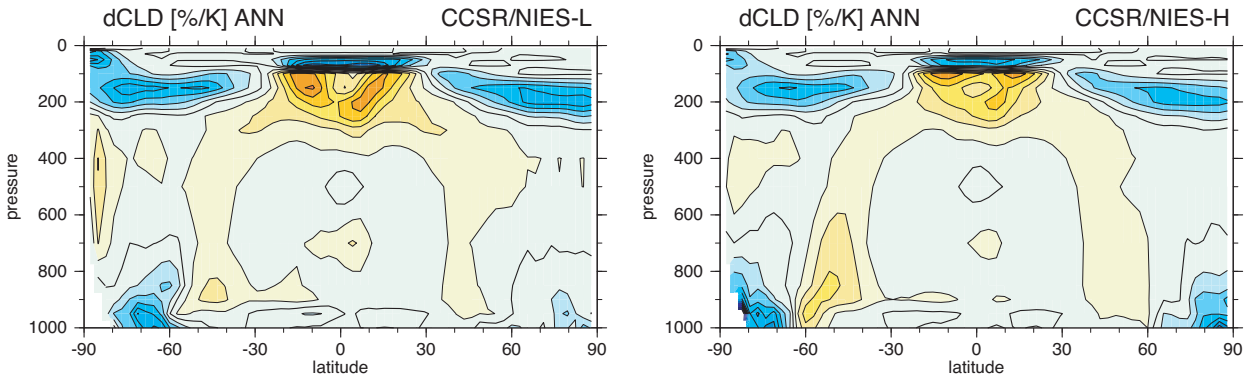


**Figure 2.** Zonally averaged annual mean cloud amount change normalized by global-mean surface air temperature change for two versions of CCSR/NIES/FRSGC model. (left) lower-sensitivity, (right) higher-sensitivity. Contour interval is 0.5. Blue color denotes increase, while yellow color denotes decrease.

data than that with higher-sensitivity model. Counter-intuitively, the higher-sensitivity model underestimates, rather than overestimates, the historical warming in the 20th century. The higher-sensitivity version seems to be too sensitive to the volcanic forcing. With the simulation of the Last Glacial Maximum, on the other hand, both versions are within the uncertainty of the sensitivity of low latitude (30°S–30°N) obtained by proxy data.

### References

Del Genio, A.D., M.-S. Yao, W. Kovari and K.K.-W. Lo, 1996: A prognostic cloud water parameterization for global climate models. J. Climate, 9, 270-304.

Emori, S., T. Nozawa, A. Abe-Ouchi, A. Numaguti, M. Kimoto and T. Nakajima, 1999: Coupled ocean-atmosphere model experiments of future climate change with an explicit representation of sulfate aerosol scattering. J. Meteor. Soc. Japan, 77, 1299-1307.

Mitchell, J.F.B., C.A. Senior and W.J. Ingram, 1989: CO2 and climate: A missing feedback? Nature, 341, 132-134.

Nozawa, T., S. Emori, A. Numaguti, Y. Tsushima, T. Takemura, T. Nakajima, A. Abe-Ouchi and M. Kimoto, 2003: Transient climate change simulations in the 21st century with the CCSR/NIES CGCM under a new set of IPCC scenarios. CGER's Supercomputer Monograph Report, Vol.8, 44pp.

Takemura, T., H. Okamoto, Y. Maruyama, A. Numaguti, A. Higurashi and T. Nakajima, 2000: Global simulation of aerosol optical thickness distribution of various origins with a three-dimensional model. J. Geophys. Res., 105, 17853-17873.

Tanaka, T.Y., K. Orito, T. Sekiyama, K. Shibata, M. Chiba and H. Tanaka, 2003: MASINGER, a global tropospheric aerosol chemical transport model coupled with MRI/JMA98 GCM: Model description. Pap. Meteor. Geophys., 53, 119-138.

Uchiyama, T., A. Noda, S. Yukimoto and M. Chiba, 2004: Study of the estimate of new climate change scenarios based on new emission scenarios. CGER's Supercomputer Activity Report, Vol.11, 41-46.

Yukimoto, S. and A. Noda, 2002: Improvements of the Meteorological Research Institute global ocean-atmosphere coupled GCM (MRI-CGCM2) and its climate sensitivity. CGER's Supercomputer Activity Report, Vol.10, 37-44.

Yukimoto, S., A. Noda, A. Kitoh, M. Sugi, Y. Kitamura, M. Hosaka, K. Shibata, S. Maeda and T. Uchiyama, 2001: The new Meteorological Research Institute coupled GCM (MRI-CGCM2) –Model climate and variability. Pap. Meteor. Geophys., 51, 47-88.

**IPCC Workshop on Climate Sensitivity**
Paris, France, July 26–29, 2004
*Pre-Conference Volume*

# Twentieth Century Climate and Probabilistic Estimates of Climate Sensitivity

Reto Knutti

*Climate and Environmental Physics, University of Bern, Switzerland*

It has recently been suggested that the largely uncertain climate sensitivity can be constrained by relating the reconstructed radiative forcing over the industrial period to the observed surface air warming and the observed ocean heat uptake. The requirement that the modelled warming matches the observed warming should thus place a strong constraint on anthropogenically forced climate models, and the ocean heat uptake should impose an even tighter restriction than the atmospheric warming because of the ocean's large heat capacity [*Barnett et al.*, 2001]. However, these conclusions are hampered by the incompleteness of climate models, by the uncertainty in the surface and ocean temperature records and the uncertainty of the reconstructed radiative forcing over the last 250 years. In particular, it is a problem that reliable data of ocean temperature with sufficient resolution are only available for the last few decades [*Levitus et al.*, 2000]. The variations in the ocean heat content on decadal time scales are large compared to the trend, and current climate models are unable to reproduce the large variability in the observed ocean heat uptake. Further, many radiative forcing components, in particular the aerosol forcing, are still very uncertain.

Figure 1 shows that when climate sensitivity is varied in a simplified climate model [*Knutti et al.*, 2002], the modelled ocean heat uptake and surface warming are consistent with the observed global ocean heat uptake for the period 1955-1995 and the global mean surface warming over the last century for a wide range of climate sensitivities. Even if the radiative forcing is assumed to be known perfectly (Fig. 1a/b), large values for climate sensitivity of more than 6°C cannot be ruled out, since the modelled warming still falls within the observational uncertainty range. The uncertainty in the model ocean mixing parameterisation further widens the possible range of climate sensitivities. If the uncertainties in the radiative forcing are taken into account (Fig. 1c/d), both very low (around 1°C) and very high values cannot be excluded. The main reason is that there is a non-zero probability for the total radiative forcing over the industrial period being zero or even negative [*Boucher and Haywood*, 2001]. If the total forcing tends to zero, climate sensitivity must be very large to still produce a warming in a climate model. A significant reduction in the uncertainties of the observational datasets as well as better constraints on the reconstructed radiative forcing are required to considerably reduce the uncertainty in climate sensitivity using this method.

Probabilistic estimates of climate sensitivity can be obtained by large ensembles of simulations with simplified climate models. In this case, climate sensitivity, ocean model parameters and the radiative forcing are varied within their uncertainty ranges, and observations over the last century are used to constrain the ensemble. All recent studies have found that if uncertainties in the observed warming, radiative forcing and the climate models are taken into account properly, the twentieth century warming is insufficient to put a reasonable upper limit on climate sensitivities or to narrow down the probable range assumed so far by IPCC. The derived probability density functions are largely consistent with the IPCC range of 1.5 to 4.5°C [*IPCC*, 2001], but as long as no expert information is included, a significant probability for climate sensitivity exceeding 4.5°C remains [*Andronova and Schlesinger*, 2001; *Forest et al.*, 2002; *Gregory et al.*, 2002; *Knutti et al.*, 2002; *Knutti et al.*, 2003].

### References

Andronova, N., and M.E. Schlesinger, Objective estimation of the probability distribution for climate sensitivity, *J. Geophys. Res.*, *106*, 22,605-22-612, 2001.

Barnett, T.R., D.W. Pierce, and R. Schnur, Detection of anthropogenic climate changes in the World's oceans, *Science*, *292*, 270-274, 2001.

Boucher, O., and J. Haywood, On summing the components of radiative forcing of climate change, *Clim. Dyn.*, *18*, 297-302, 2001.

Forest, C.E., P.H. Stone, A.P. Sokolov, M.R. Allen, and M.D. Webster, Quantifying uncertainties in climate system properties with the use of recent climate observations, *Science*, *295*, 113-117, 2002.

Gregory, J.M., R.J. Stouffer, S.C.B. Raper, P.A. Stott, and N.A. Rayner, An observationally based estimate of the climate sensitivity, *J. Clim.*, *15*, 3117-3121, 2002.

IPCC, Climate Change 2001: The scientific basis. Contribution of working group I to the Third Assessment Report of the Intergovernmental Panel on Climate Change, edited by J.T. Houghton, Y. Ding, D.J. Griggs, M. Noguer, B.J. van der Linden, X. Dai, K. Maskell, and C.A. Johnson, pp. 881, Cambridge University Press, Cambridge, United Kingdom and New York, NY, USA, 2001.

Jones, P.D., M. New, D.E. Parker, S. Martin, and I.G. Rigor, Surface air temperature and its changes over the past 150 years, *Rev. Geophys.*, *37*, 173-199, 1999.

Knutti, R., T.F. Stocker, F. Joos, and G.-K. Plattner, Constraints on radiative forcing and future climate change from observations and climate model ensembles, *Nature*, *416*, 719-723, 2002.

Knutti, R., T.F. Stocker, F. Joos, and G.-K. Plattner, Probabilistic climate change projections using neural networks, *Clim. Dyn.*, 257-272, DOI 10.1007/s00382-003-0345-1, 2003.

Levitus, S., J.I. Antonov, T.P. Boyer, and C. Stephens, Warming of the world ocean, *Science*, *287*, 2225-2229, 2000.

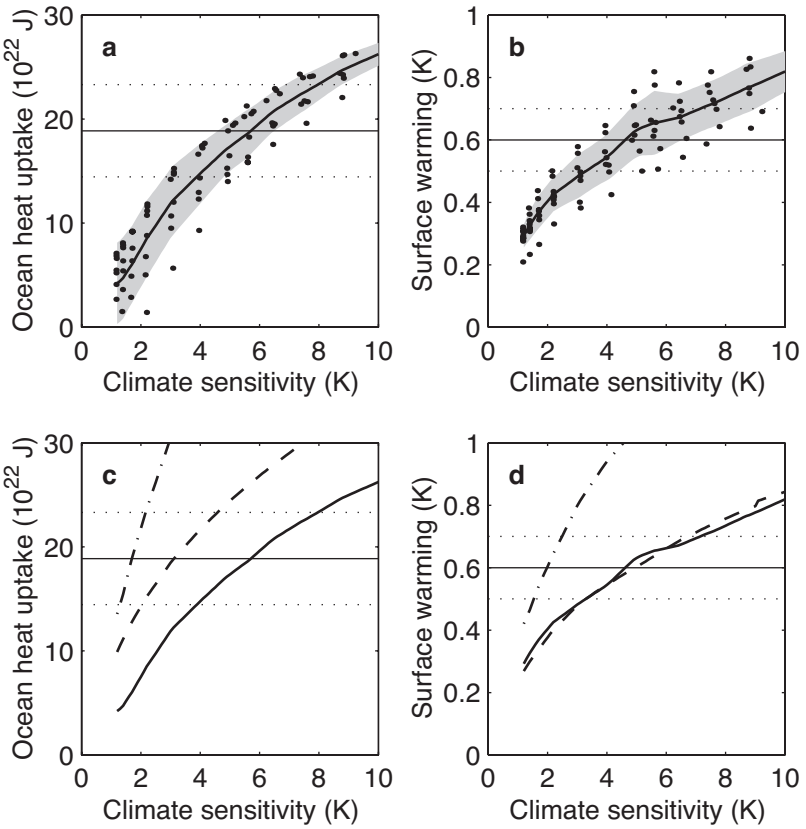


**Figure 1**(taken from *Knutti et al.* [2002]): Relation between radiative forcing, climate sensitivity and modelled atmospheric/oceanic warming. (a/b) Global ocean heat uptake 1955 - 1995 (to a depth of 3000 m) and global mean surface air temperature increase 1900 - 2000 versus climate sensitivity (expressed as global mean equilibrium surface temperature increase for a doubling of preindustrial atmospheric $CO_2$) for eight model setups (different subgrid-scale mixing parameterisations and different vertical diffusivities), using standard reconstructed anthropogenic and natural radiative forcing. Each dot indicates one model simulation. The bold solid curve and shaded band denote the mean and uncertainty (one standard deviation) arising from different ocean mixing properties. Horizontal solid and dotted lines mark the mean and uncertainty (one standard deviation) of the observed ocean heat uptake [*Levitus et al.*, 2000] and observed surface temperature increase [*Jones et al.*, 1999]. (c/d) Model mean values as in (a/b), but when neglecting natural, i. e. solar and volcanic forcings (dashed) or when neglecting the indirect aerosol forcing (dash-dotted). Constraining the climate sensitivity from the observed warming is mainly hampered by uncertainties in the radiative forcing components and temperature data rather than by the range covered by various setups of the climate model used.

**IPCC Workshop on Climate Sensitivity**
Paris, France, July 26–29, 2004
*Pre-Conference Volume*

# Radiative Damping of Annual Temperature Variation: A Proposal for Testing Feedback

S. Manabe[1] and Y. Tsushima[2]

[1] *Princeton University, Princeton, New Jersey*
[2] *Frontier Research System for Global Change, Yokohama, Japan*

The equilibrium response of global mean surface temperature to radiative forcing is essentially determined by the so-called feedback parameter, which is the rate of radiative damping of the unit anomaly of the global mean surface temperature due to the outgoing radiation from the top of the atmosphere (TOA). By dividing the radiative forcing of climate by the feedback parameter, one gets the radiatively forced, equilibrium response of global surface temperature. This implies that the stronger is the rate of radiative damping of surface temperature, the smaller is its equilibrium response to a given radiative forcing.

According to the third IPCC (2001) report, the previously estimated range of the equilibrium response of the global mean surface temperature to the doubling of atmospheric carbon dioxide has not reduced substantially over the last decade and remains between 1.5 and 4.5°C. Clearly, the large range in the estimated sensitivity of surface temperature is attributable in no small part to our inability to reliably determine the influence of feedback upon the radiative damping of surface temperature anomaly.

The present study proposes a method for testing global-scale feedback in a climate model. Using the data from the Earth Radiation Budget Experiment (ERBE), we estimate the gain factor of the feedback, which operates upon the annually varying anomaly of the global mean surface temperature. (Here, gain factor represents the influence of feedback upon the radiative damping of the global surface temperature anomaly.) To evaluate the performance of a model for simulating feedback process, the gain factor thus estimated is then compared with the gain factor of the feedback simulated by a model.

The annual variation of the global mean surface temperature is attributable mainly to the difference in effective thermal inertia between continent and ocean rather than to the small annual variation of global mean, incoming solar radiation. Because the seasonal variation of surface temperature is much larger over continents than over oceans, the annual variation of the global mean surface temperature is dominated by the contribution from the continents in Northern Hemisphere. Its annual range is about 3.3°C with highest temperature in July and the lowest in January. The range is comparable in magnitude to a current estimate of the equilibrium response of global mean surface temperature to the doubling of $CO_2$ concentration in the atmosphere.

Since the pattern of the annual variation of surface temperature (see, for example, Figure 1b of Tsushima and Manabe, 2001) differs greatly from that of global warming simulated by a model, it is quite likely that the rate of the radiative damping of theglobal mean surface temperature anomaly is significantly different between the two. Nevertheless, we decided to use the annual variation for the quantitative evaluation of simulated feedback in a climate model, because the annual variation of climate is the largest observable climatic change. The availability of data from the ERBE is another decisive factor for conducting the analysis presented here.

It is well-known, however, that the annual variation of surface temperature is highly transient response to annually varying insolation that is out of phase between the two hemispheres. Thus, it is not our intension to determine the magnitude of feedback, incorrectly assuming that surface temperature were continuously in equilibrium with the annually varying, incoming solar radiation. Instead, we estimate here the magnitude of feedback effect that operates upon the annually varying anomaly of the global mean surface temperature using the outgoing fluxes of terrestrial and reflected solar radiation from the top of the atmosphere.

In the absence of feedback effect, the outgoing radiation at the top of the atmosphere is approximately equal to the fourth-power of the effective planetary emission temperature, following the Stefan-Boltzmann's law of blackbody radiation. In the actual atmosphere, however, it deviates significantly from the blackbody radiation. When the temperature of the atmosphere increases, for example, its absolute humidity usually increases, thereby

enhancing the infrared opacity of the troposphere. Thus, the radiative damping of surface temperature anomaly is weakened. This explains why the water vapor feedback is positive.

The changes in the temperatures of the atmosphere and the Earth's surface affect not only the outgoing terrestrial radiation but also the reflected solar radiation at the top of the atmosphere. For example, an increase in surface temperature is likely to reduce the area covered by snow and sea ice, thereby reducing the heat loss due to the reflection of incoming solar radiation. Thus, the effective radiative damping of surface temperature anomaly is reduced, thereby enhancing the sensitivity (enlarging the equilibrium response) of surface temperature to given radiative forcing.

In the present study, we estimated the rate of radiative damping of annually varying anomaly of the global mean surface temperature, using the TOA-fluxes of terrestrial radiation and reflected solar radiation obtained from ERBE. Because of feedback, the intensity of radiative damping is 70% less than and is only 30% of what is expected for the black body with the planetary emission temperature. In short, the gain factor of feedback we obtained is 0.7.

Similar feedback analysis is conducted for three general circulation models of the atmosphere, in which the microphysical properties of cloud are explicitly predicted. Figure 1 illustrates the gain factors which are obtained from both GCMs and ERBE observation. It shows that the gain factors of feedback obtained from the three GCMs are similar to the value obtained from ERBE observation. However, when it is subdivided into solar and terrestrial components, they are quite different from the observation. While solar and terrestrial gain factors obtained from ERBE observation are similar in magnitude to each other, solar gain factors of all three models are smaller than terrestrial gain factors. It turned out that the difference in solar and terrestrial components of gain factor is mainly attributable to the failure of the models to simulate individually the two components of the cloud feedback.

Earlier, Tsushima and Manabe (2001) estimated cloud gain factors, using ERBE data of solar and long wave components of cloud forcings over the domain between 60ºN and 60ºS. In the present study, we have repeated this computation, extending the domain to the entire globe. Despite the expansion of the analysis domain, the cloud gain factors computed from the ERBE remain to be small, and are hardly different between the two studies. On the other hand, solar and terrestrial components of the gain factor of the cloud feedback obtained from the models are not necessarily small. Because they tend to compensate each other, the gain factor of the cloud feedback as a whole is small in agreement with observation.

*Although the geographical distribution of the annually varying, surface temperature anomaly is quite different from the pattern of global warming simulated by a model, the test presented here may be used for the identification of the systematic bias of feedbacks simulated by a model. For example, it may be applied to the other feedbacks involving water vapor and snow/sea ice.*

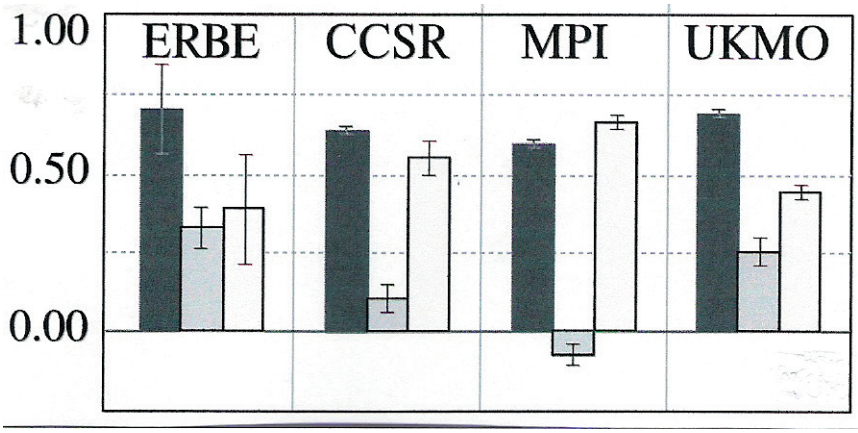


**Figure 1.** Gain factors from the ERBE observation and old versions of the three models, which were constructed at the Center for Climate System Research/National Institute for Environment Study (CCSR/NIES), the Max-Planck Institute for Meteorology (MPI), and the United Kingdom Meteorological Office (UKMO) and were submitted to AMIP-I model intercomparison project (Gates, 1992). Black bar represents the gain factor of all feedbacks combined. Dark and light grey bars represent solar and terrestrial components of the gain factor, respectively. Here, gain factor is defined as the factor that represents the reduction from the radiation from the blackbody with the planetary emission temperature (Hansen et al., 1984; Wetherald and Manabe, 1988). Positive and negative gain factors indicate positive and negative feedbacks, respectively.

**References**

Gates, W. L., 1992, AMIP: The Atmospheric Model Intercomparison Project. *Bulletin of American Meteorological Society*, 73, 1962-1970.

Hansen, J. et al., 1984, Climate sensitivity: Analysis of feedback mechanisms. In *Climate Process and Climate Sensitivity*, edited by J. Hansen and T. Takahashi, *Geophysical Monograph Series*, vol. **29**, 130-163, American Geophysical Union, Washington, D. C.

Tsushima, Y., and S. Manabe, 2001, Influence of cloud feedback on annual variation of global mean surface temperature, *Journal of Geophysical Research (Atmosphere)* **106(D19)**, **22**, 635-22,646, (October 16, 2001).

Tsushima, Y., A. Abe-Ouchi, and S. Manabe, 2003, Radiative damping of annual temperature variation: A proposal for testing simulated feedback. submitted to *Climate Dynamics*.

Wetherald, R. T., and S. Manabe, 1988: Cloud feedback process in a general circulation model, *Journal of Atmospheric Sciences,* **45,** 1397-1415.

**IPCC Workshop on Climate Sensitivity**
Paris, France, July 26–29, 2004
*Pre-Conference Volume*

# Ocean Heat Uptake and Climate Sensitivity in Five Coupled Models

Gerald A. Meehl

*National Center for Atmospheric Research*

Five global coupled climate models are compared for their climate sensitivity characteristics related to ocean heat uptake. To a greater degree than the other components, the atmospheric model "manages" the relevant global feedbacks including ice/albedo, water vapor and clouds (Meehl et al., 2004). The atmospheric model also affects the meridional overturning circulation in the ocean, as well as the ocean heat uptake characteristics. This is due to changes in surface fluxes of heat and fresh water that affect surface density in the ocean. For global sensitivity measures, the ocean, sea ice and land surface play secondary roles, even though differences in these components can be important for regional climate changes. Two models with the same atmosphere and sea ice components but different ocean (PCM and PCTM) have the most similar response to increasing $CO_2$, followed closely by CSM with the same atmosphere and different ocean and sea ice from either PCM or PCTM. The CCSM has a different response from either of the other three, and in particular is different from PCTM in spite of the same ocean and sea ice but different atmospheric model components. CCSM3 differs mainly from CCSM in regards to physics in the atmosphere, and consequently has a different response yet again, consistent with the idea that changes in the atmosphere have the greatest effect on overall climate sensitivity, including ocean response (Fig. 1).

Ocean heat uptake efficiency is shown to depend on the specific characteristics of the atmosphere in particular, with a change in the atmospheric model (from PCTM to CCSM) reducing not only the strength of the MOC in the control run, but also affecting the heat uptake efficiency with increased $CO_2$ (Fig. 2). The change from CCSM to CCSM3 has the opposite effect. That is, the CCSM, with the lowest climate sensitivity, has a somewhat greater percent reduction of MOC compared to the PCTM. However, the CSM has a slight strengthening of MOC, greater high latitude warming, but less heat uptake efficiency. The CCSM3 has greater sensitivity than CCSM, with almost twice the percent change (weakening) of the THC (Fig. 3).

Therefore, the nature of the climate system response to an input of increased energy to the system from increased $CO_2$ can be partitioned in various ways between atmosphere and ocean, with the nature of that partitioning related to the specific characteristics of the feedbacks in the system mainly having to do with the atmospheric model.

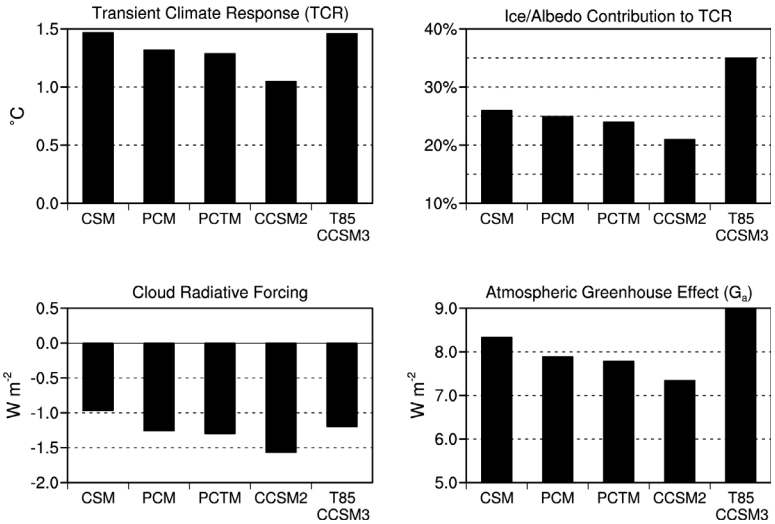


**Figure 1.** a) Globally averaged surface air temperature difference (C) around the time of CO2 doubling for years 61-80 minus control (transient climate response or TCR); b) ice-albedo feedback contribution (%) to TCR from the five models; c) as in (a) except for cloud radiative forcing ($Wm^{-2}$); d) as in (a) except for atmospheric greenhouse effect ($Wm^{-2}$).

**Reference**

Meehl, G.A., W.M. Washington, J.M. Arblaster, and A. Hu, 2004: Factors affecting climate sensitivity in global coupled models. J. Climate, 17, 1584–1596.

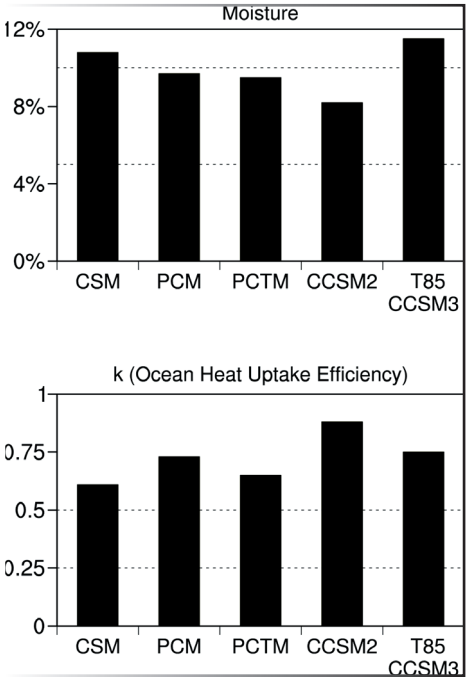


**Figure 2.** a) Same as Fig. 1a except for percent change in total column moisture, b) same as (a) except for ocean heat uptake efficiency.

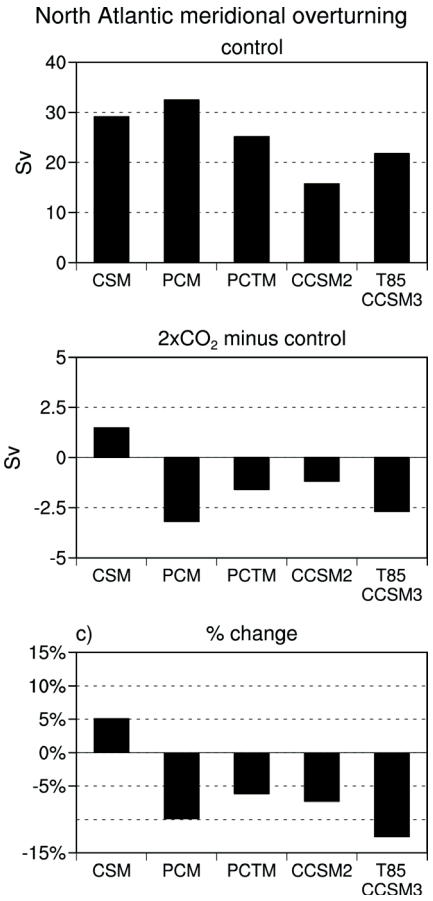


**Figure 3.** North Atlantic Ocean meridional overturning circulation (MOC) a) maximum values from the control run for the five models (Sv), b) differences of MOC around the time of $CO_2$ doubling, years 61-80, minus respective control run averages for the five models (Sv), and c) percent change in MOC for a doubling of $CO_2$ (values in (b) divided by values in (a)).

**IPCC Workshop on Climate Sensitivity**
Paris, France, July 26–29, 2004
*Pre-Conference Volume*

# Probabilistic Estimates of Climate Sensitivity from GCM Ensembles

James Murphy, David Sexton, Matthew Collins, Glen Harris and Mark Webb

*Hadley Centre, Met Office, FitzRoy Road, Exeter EX1 3PB, UK*

For a given scenario of external forcing GCM projections of climate change are subject to uncertainties arising from modelling errors and the effects of natural variability. In principle these uncertainties can be estimated by constructing large ensembles of simulations which sample alternative representations of Earth system processes and alternative initial states. In practice resource limitations have prevented this so we typically rely on pooling individual simulations from different GCMs to create small ensembles from which uncertainties are estimated (e.g. Cubasch et al 2001, Palmer and Räisänen 2002). These provide useful information but do not provide a credible basis for the construction of probabilistic projections because (a) the ensembles are too small, (b) they are not constructed to sample uncertainties in a systematic manner (Allen and Ingram 2002) and (c) they have not been accompanied by objective measures of reliability which can be used to weight the projections of different GCMs.

We report a first step towards addressing these issues (See Murphy et al (2004) for a fuller description). Simulations of the equilibrium response to doubled $CO_2$ were made using 53 versions of the Hadley Centre GCM coupled to a mixed layer ocean. Each ensemble member differed from the standard version (HadAM3, see Pope et al, 2000) by a perturbation to one of 29 poorly-constrained parameters influencing various surface and atmospheric physical processes. A number of parameters were found to influence climate sensitivity, however it was not possible to construct a probability distribution directly from the ensemble results because the effects of multiple parameter perturbations, representing interactions between uncertainties in different processes, were not sampled. However, the impact of such interactions can be estimated by assuming that the effects of individual parameter perturbations combine linearly. This allows us to predict the results of a much larger (multi-million member) ensemble of GCM versions containing multiple parameter perturbations sampled by assuming a uniform prior for each of the 29 parameters within limits estimated by experts.

If we assume that all model versions are equally plausible we obtain a probability density function (pdf) for climate sensitivity with a 5-95% probability range of 1.9-5.3 Deg C. However we have also developed a "Climate Prediction Index" (CPI) for the purpose of weighting model versions according to reliability. The CPI is currently determined from normalised error variances of simulated climatological patterns of 32 surface and atmospheric variables. Weighting the simulations of GCM versions according to the CPI changes the 5-95% probability range to 2.4-5.4 Deg C.

Previously pdfs of sensitivity have been estimated by exploring the range of predictions of simpler climate models consistent with observed changes in the forcing and response of climate since the industrial revolution (Andronova and Schlesinger 2001, Forest et al 2002, Gregory et al 2002, Knutti et al 2002). Our approach differs from the above studies and allows us to estimate a pdf for sensitivity determined by both the complex physical interactions built into the GCM and the fit of different model versions to a wide range of present day observations. However it is subject to a number of caveats, including the following:

(1) We consider only uncertainties in surface and atmospheric physical processes, neglecting uncertainties associated with feedbacks involving the ocean circulation, the terrestrial biosphere, atmospheric chemistry and ocean biogeochemistry.

(2) Perturbing uncertain parameters in a single GCM does not, in any case, sample the full range of possible modelling uncertainties. In particular, "structural" differences between GCMs developed at different centres (different choices of resolution, variations in the basic nature of parameterisation schemes, variations in the range of parameterisations included) are not sampled.

(3) The results depend on the assumed *a priori* distributions for parameter values, in particular on their expert-specified extremes.

(4) Errors arise from the assumption that the effects of individual parameter perturbations combine linearly.

(5) The estimated reliability of alternative model versions depends on the chosen metric of model skill, the set of verifying observations on which it is based, the relative weights attached to different observations and the assumptions required to convert values of the metric into estimates of relative likelihood.

These caveats reflect the fact that ensemble climate prediction is in its infancy. Addressing them will involve a number of substantial developments. For example (1) would require ensemble simulations carried out with full Earth System Models, while (2) would require coordinated ensemble experiments involving systematic exploration of process uncertainties in a number of different GCMs; (3) could be assessed by comparing parallel ensembles generated using alternative priors for uncertain parameters and (4) requires the production of very large ensembles which sample parameter space more comprehensively (Stainforth et al 2004). Regarding (5), further research is needed to determine the best methods of relating uncertainties in verifiable aspects of GCM simulations to uncertainties in their projections of future changes (see accompanying abstract by Senior et al).

Ultimately the assessment of climate-related risks requires provision of probabilistic projections for time-dependent changes. For example carbon cycle feedbacks may be relatively unimportant as a source of uncertainty in equilibrium climate sensitivity, yet may be a key source of uncertainty in the transient response to realistic emissions scenarios (e.g. Cox et al 2000). Furthermore, impact assessments typically require uncertainties specified at a regional level, rather than for idealised global quantities such as climate sensitivity. Our results suggest that only a comprehensive approach to sampling modelling uncertainties can provide a realistic basis for quantifying the range of possible regional changes (Murphy et al 2004, Stainforth et al 2004). It is therefore essential that the design of GCM ensembles samples uncertainties relevant to regional changes in impact-related variables such as precipitation, storm intensity and soil moisture content and that climate metrics are designed which are capable of constraining projections of regional changes.

### References


Allen, M. R. & Ingram, W. J. (2002). Constraints on future changes in climate and the hydrological cycle. *Nature* **419**,224-232.

Andronova, N. G. & Schlesinger, M. E. (2001). Objective estimation of the probability density function for climate sensitivity. *J. Geophys. Res*. **106**,22605-22612.

Cubasch, U. et al. in *Climate Change 2001, The Science of Climate Change* Ch. 9 (eds Houghton, J. T. *et al*.) 527-582 (Cambridge Univ. Press, Cambridge, 2001).

Forest, C. E., Stone, P H., Sokolov, A. P., Allen, M. R. & Webster, M. D. (2002). Quantifying uncertainties in climate system properties with the use of recent climate observations. *Science* **295**,113-117.

Knutti, R., Stocker, T. F., Joos, F. & Plattner, G. K. (2002) Constraints on radiative forcing and future climate change from observations and climate model ensembles. *Nature* **416**,719-723.

Gregory, J. M., Stouffer, R. J., Raper, S. C. B., Stott, P. A. & Rayner, N. A. (2002)
An observationally based estimate of the climate sensitivity. *J. Clim.* **15**,3117-3121.

Murphy J M. *et al.* (2004) Quantification of modelling uncertainties in a large ensemble of climate change simulations. *Nature*, to appear.

Palmer, T. N. & Räisänen, J. (2002). Quantifying the risk of extreme seasonal precipitation events in a changing climate. *Nature* **415**,514-517.

Pope, V. D., Gallani, M., Rowntree, P. R. & Stratton, R. A. (2000). The impact of new physical parameterisations in the Hadley Centre climate model – HadAM3. *Clim. Dynam*.**16**,123-146.

Senior C. A. (2004) Report on the joint WCRP CFMIP/ IPCC expert meeting on "Climate Sensitivity and Feedbacks: Summary and Recommendations", Exeter, UK, April 19-22.

Stainforth, D. A. *et. al*. (2004). Evaluating uncertainty in the climate response to changing levels of greenhouse gases. Submitted to *Nature*.

**IPCC Workshop on Climate Sensitivity**
Paris, France, July 26–29, 2004
*Pre-Conference Volume*

# Climate Sensitivity of the Last Glacial Maximum from Paleoclimate Simulations and Observations

Bette Otto-Bliesner, Esther Brady, and Zav Kothavala

*National Center for Atmospheric Research, Boulder, Colorado, US*

Global coupled climate models run for future scenarios of increasing atmospheric $CO_2$ give a range of response of the global average surface temperature. Regional responses, including the North Atlantic overturning circulation and tropical Pacific ENSO, also vary significantly among models. The second phase of the Paleoclimate Modeling Intercomparison Project (PMIP 2) is coordinating simulations and data syntheses for the Last Glacial Maximum (21,000 years before present [21 ka]) to allow an independent assessment of climate sensitivity.

Atmospheric $CO_2$ concentrations at the Last Glacial Maximum (LGM) have been estimated using measurements from ice cores to be 185 ppmv, approximately 50% of present-day values. Global, annual mean surface temperature simulated by the T42 slab ocean version of CCSM3 shows a cooling of –2.8°C for LGM $CO_2$ levels and a warming of 2.5°C for a doubling of $CO_2$. The climate sensitivity factors calculated from these two simulations are 0.8° $K/Wm^{-2}$ for LGM and 0.7 °$K/Wm^{-2}$ for $2xCO_2$. At LGM atmospheric $CH_4$ concentration is estimated to be 350 ppbv, $N_2O$ concentration to be 200 ppbv, and chlorofluorocarbons were not present. Large ice sheets covered North America and Eurasia and sea level was reduced by approximately 105 m. When these additional forcings are included in the T42 slab ocean version of CCSM3, global surface temperature cools 5.7°C compared to present. A T42 fully coupled CCSM3 simulation for LGM shows comparable, but somewhat larger, cooling of global surface temperature of 5.9°C.

Regional signatures of the climate system to changed LGM forcing are also an important measure of climate sensitivity. Understanding and comparing the response of the Atlantic meridional overturning circulation (MOC) to LGM forcing in coupled atmosphere-ocean climate models and in proxy observations is a component of PMIP-2. CCSM3 shows a weakening and shallowing of the Atlantic meridional overturning circulation at LGM compared to present. A CSM1 simulation for LGM gives a similar tendency. CCSM3, though, with a more realistic MOC for present gives maximum overturning of 13 Sv at LGM compared to 21 Sv in the CSM1 LGM simulation. Previous water-hosing experiments with CSM1 suggest that the Atlantic MOC is sensitive to the initial state. Future simulations with CCSM3 and other PMIP-2 coupled models will explore this sensitivity.

In this talk, the climate sensitivity and the response of the Atlantic MOC and tropical Pacific Ocean for the NCAR climate models, CSM1 and CCSM3, to LGM forcing will be discussed. Results of coupled ocean-atmosphere simulations from other centers and proxy observations will also be included.

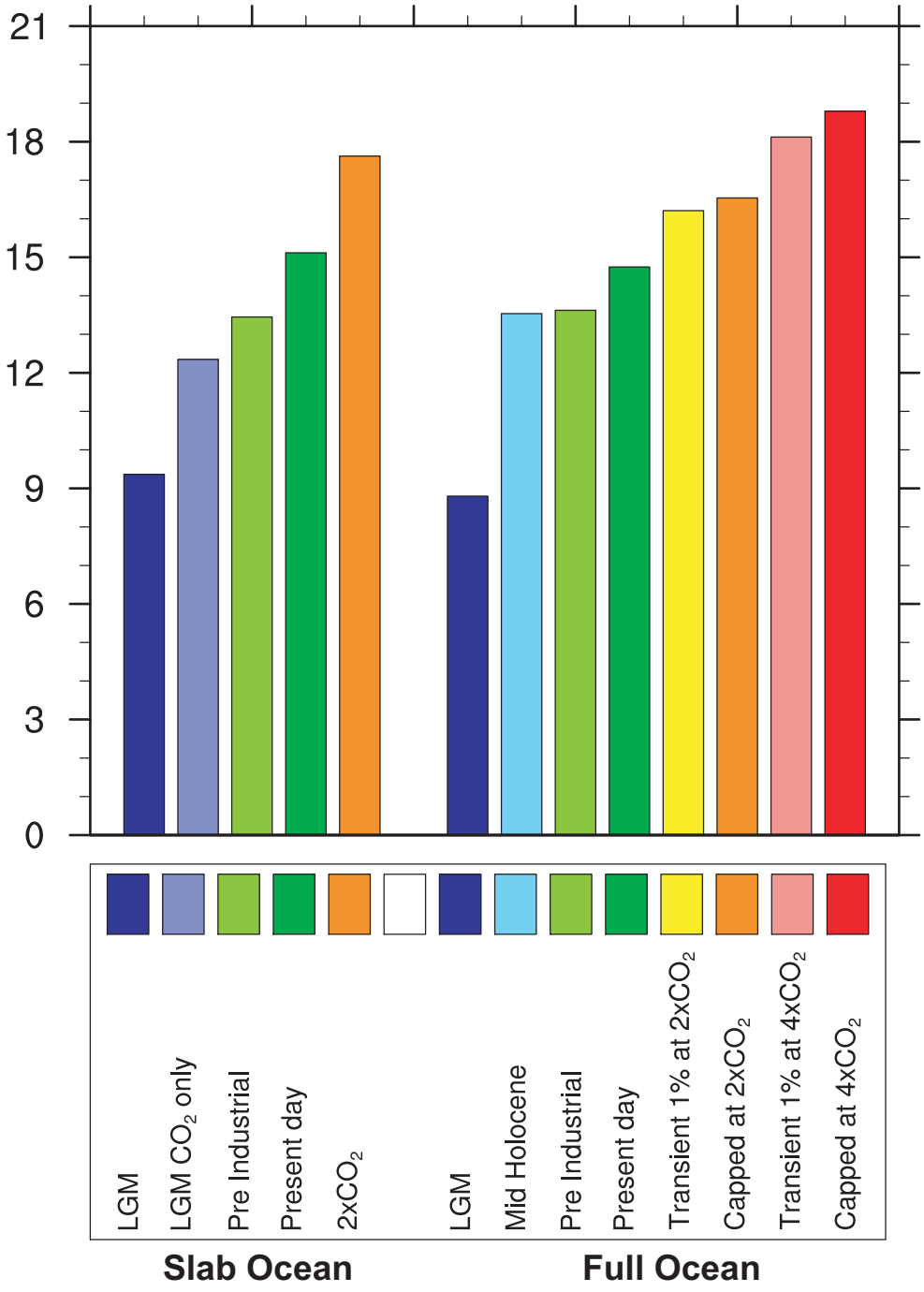


**Figure.** Global, annual surface temperature simulated by slab (left) and full (ocean) versions of CCSM3 at T42 resolution for past, present, and future climates.

**IPCC Workshop on Climate Sensitivity**
Paris, France, July 26–29, 2004
*Pre-Conference Volume*

# Paleoclimatic Evidence for Future Greenland Ice Sheet Instability and Rapid Sea Level Rise

Jonathan T. Overpeck[1], Bette L. Otto-Bleisner[2], Jeffrey T. Kiehl[3], Gifford H. Miller[4], and IGBP PAGES CAPE Project Members

[1] *Institute for the Study of Planet Earth and Department of Geosciences, University of Arizona, Tucson, AZ 88721, USA; jto@u.arizona.edu*
[2] *National Center for Atmospheric Research, P.O. Box 3000, Boulder, Colorado 80307, USA*
[3] *National Center for Atmospheric Research, P.O. Box 3000, Boulder, Colorado 80307, USA*
[4] *INSTAAR and Department of Geological Sciences, University of Colorado, Boulder, CO 80309, USA*

The peak of the last interglacial (LIG) period, starting 129,000 ± 1000 years ago, provides the most recent paleoclimatic glimpse into how the high northern latitudes respond to significant warming above present day. Changes in the Earth's orbit (e.g., the astronomical theory of climate change) resulted in significant positive warm-season insolation anomalies at this time. These anomalies were significantly larger than the peak positive anomalies associated with climate change early in the present Holocene interglacial, and for this reason it is not surprising that LIG warmth apparently had a much larger impact on the arctic than Holocene warmth. Most importantly, it appears that LIG warmth was sufficient to melt much of the Greenland Ice Sheet. Well-dated corals above present sea level provide unequivocal evidence that sea level was 3 to 6 meters above present at the peak of the LIG period (Israelson and Wohlfarth 1999; McCulloch and Esat 2000; Muhs 2002; Shackleton, Sanchez-Goni et al. 2003), and the failure to drill structurally intact ice older than this time over much of Greenland supports the contention that GIS melting was the cause of this sea water rise (Cuffey and Marshall 2000).

The goal of our work is to combine the use of paleoenvironmental data with a new modeling study to reevaluate the sensitivity of the arctic, and Greenland Ice Sheet in particular, to possible future arctic warmth comparable to that of the LIG period. We used a state-of-the-art coupled atmosphere ocean climate model to simulate the climate of 130,000 years ago, as well as the climate of the next 140 years. The model is the National Center for Atmospheric Research Community Climate System Model [CCSM], Version 2). CCSM2 includes an atmospheric model at resolution of 3.75 latitude and longitude and 26 vertical levels, an ocean model with 320x384 gridpoints and 40 levels, a sea ice model which includes both thermodynamics and elastic-viscous-plastic dynamics, and a land model that includes explicit river runoff and the physical effects of vegetation and land ice. Vegetation and land ice coverage are prescribed at their present-day distributions and are unchanged for the LIG simulations. In accordance with what is known about climate forcing at the peak of the LIG, we prescribed our experimental forcing to be the same as 1990 with the exception that seasonal insolation and atmospheric greenhouse levels ($CO_2$ = 280 ppmv, $CH_4$ = 600 ppbv) were set to be the same as 130,000 years ago. Although peak warmth of the LIG could have occurred 1-2000 years after 130,000 yr B.P., the forcing would not have been significantly different from that we prescribed. We used the same model to simulate into the future, setting atmospheric $CO_2$ to increase 1% per year from 1990 values of 355 ppmv.

Results reveal several key aspects of the LIG climate. First, we confirm that sea level rise at ca. 130,000 years ago must have been associated with Greenland Ice Sheet melting rather than melting in the Antarctic. This fact is not surprising given the large positive summertime insolation anomaly at high northern latitudes at that time (nearly 70 w/m$^2$ in early summer), and the lack of any significant warm (i.e., to above freezing) anomaly in south polar latitudes. Our simulation (Fig. 1) suggests that the summer temperatures needed to melt the GIS were on the order of 3 to 5°C above present (paleoclimate data from the Arctic support the higher end of this range), and that these temperatures were associated with a net reduction in snowfall over Greenland as well. Not surprisingly, simulated summer sea ice was greatly reduced at 130,000 yr B.P.

Comparison of the summer season warmth sufficient to have melted the GIS 130,000 years ago with simulated future climate (Fig. 1) indicates that the high northern latitudes around Greenland will be as warm as 130,000 years ago, and hence warm enough to melt the GIS, sometime before AD 2130, and when the $CO_2$ content

of the atmosphere reaches a level three to four times the pre-industrial level. As with our paleoclimate LIG simulation, it does not appear likely that increased snowfall or ocean circulation changes will retard GIS melting. Our results also suggest that the current Arctic warming, ice sheet melting and accelerating retreat of summer Arctic sea ice thickness and extent could be a harbinger of sea ice retreat similar to that associated with GIS melting around 130,000 years ago.

A closer look at past ice sheet melting *rates* yields even more startling insight into potential future sea level rise. Sea level due to ice sheet (excepting Greenland) melting averaged 11mm/year over a large part of the last deglaciation between13,800 to 7000 years ago (Bard, Hamelin et al. 1996). The penultimate deglaciation culminating with the LIG sea level high-stand 3-6m above present day, however, was driven by a significantly larger high latitude summertime insolation anomaly, and was also able to melt much of Greenland. The most realistic sea level rise scenario for this penultimate deglaciation, also based on careful dating of sea-level dependent corals, suggests that GIS melting and associated sea level rise occurred much more rapidly, with estimated rates as high as 20 mm/yr or even higher (30 to 50 mm/yr; (McCulloch and Esat 2000)). This rate of sea level rise makes sense relative to the last deglaciation and its smaller summer insolation maximum, and indicates that much of the GIS could melt in just a few centuries. It is not surprising that glaciologists have recently begun to unravel new processes by which ice sheets can collapse faster than previously thought. High levels of atmospheric pollution (i.e., soot) may also hasten ice sheet melting even more than in the past (Hansen and Nazarenko 2004), and any sea level rise related to the collapse of the GIS will be on top of sea level rise due to ocean warming and melting of other land ice.

### References

Bard, E., B. Hamelin, et al. (1996). "Deglacial sea-level record from Tahiti corals and the timing of global meltwater discharge." Nature **382**(6588): 241-244.

Cuffey, K. and S. Marshall (2000). "Substantial contribution to sea-level rise during the last interglacial from the Breenland ice sheet." Nature **404**: 591-552.

Hansen, J. and L. Nazarenko (2004). "Soot climate forcing via snow and ice albedos." Proceedings of the National Academy of Sciences of the United States of America **101**(2): 423-428.

Israelson, C. and B. Wohlfarth (1999). "Timing of the last-interglacial high sea level on the Seychelles Islands, Indian ocean." Quaternary Research **51**(3): 306-316.

McCulloch, M. T. and T. Esat (2000). "The coral record of last interglacial sea levels and sea surface temperatures." Chemical Geology **169**(1-2): 107-129.

Muhs, D. R. (2002). "Evidence for the timing and duration of the last interglacial period from high-precision uranium-series ages of corals on tectonically stable coastlines." Quaternary Research **58**(1): 36-40.

Shackleton, N. J., M. F. Sanchez-Goni, et al. (2003). "Marine Isotope Substage 5e and the Eemian interglacial." Global and Planetary Change **36**(3): 151-155.

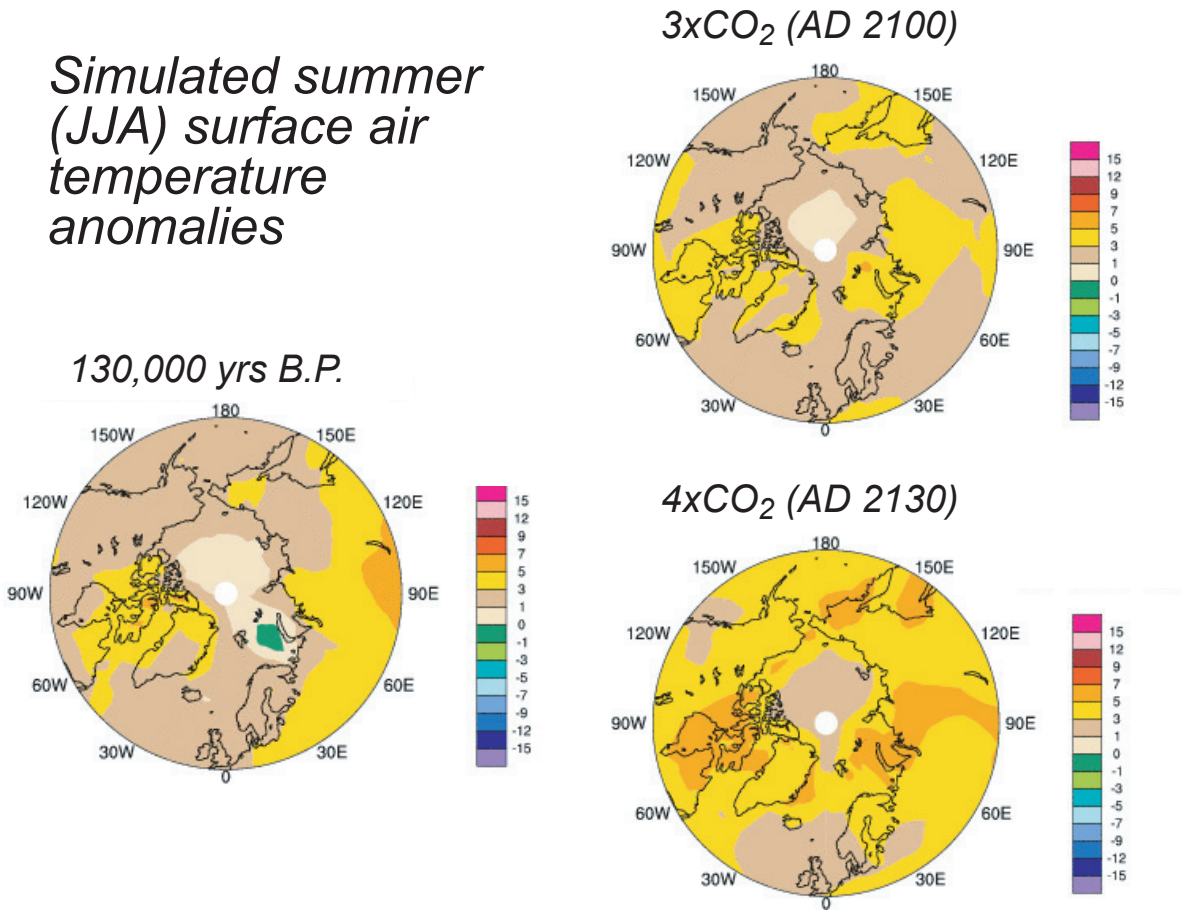


**Figure 1.** Simulated summer (JJA) surface air temperature anomalies for 130,000 years ago, 2100 AD and 2130 AD (assuming a 1% per year increase in $CO_2$ starting from a 1990 value of 355 ppmv). Results indicate that future warming comparable to 130,000 years ago be warm enough to melt the Greenland Ice Sheet at a rates comparable to those that characterized the peneultimate deglaciation (i.e., >2 meters of sea-level equivalent per century).

**IPCC Workshop on Climate Sensitivity**
Paris, France, July 26–29, 2004
*Pre-Conference Volume*

# Climate Sensitivity Range Derived from Large Ensemble Simulations of Glacial Climate Constrained by Proxy Data

T. Schneider von Deimling, H. Held, A. Ganopolski, and S. Rahmstorf

Recent studies suggest that the uncertainty range of climate sensitivity ($\Delta T_{2x}$) is only weakly constrained by the anthropogenic warming signal[1-3]. In our work we constrain $\Delta T_{2x}$ by focusing on the large radiative forcing change between the preindustrial and the glacial climate, by requiring consistency of modelled glacial cooling with paleo-data. We performed a large ensemble of glacial simulations and accounted for a complete set of the main radiative forcings. Our approach yields effective constraints on $\Delta T_{2x}$, resulting in a maximum range (5 to 95%) of 1.5 to 4.7°C – with a best guess between 2.1 and 3.6°C.

The signal of anthropogenic warming is too weak to effectively constrain $\Delta T_{2x}$, in that uncertainty in the radiative forcing over the industrial period, in the observational data and in the rate of ocean heat uptake is comparatively large. As an alternative, we use paleo-data from the Last Glacial Maximum (LGM, 21kyrs B.P.) to constrain $\Delta T_{2x}$. This period represents the largest deviation from present climate in recent geologic history, manifested in a pronounced global cooling. The LGM climate state is of high interest not only because of the large temperature signal, but also because the main forcings are well known[4], well-dated paleo data are available, and the cold climate state lasted long enough to be in near-equilibrium. Hence, it is promising to combine model simulations and paleo-data for the LGM to derive constraints on climate sensitivity.

We performed ensemble simulations using a climate model of intermediate complexity (CLIMBER-2)[5,6], consisting of a statistical-dynamical 2.5-dimensional atmosphere coupled to a multi-basin, zonaly averaged ocean model without need for flux adjustments. In our ensemble runs we consider uncertainties in eleven model parameters that strongly affect the main model feedbacks determining $\Delta T_{2x}$, namely cloud-, water vapour- and lapse rate feedback.

Using pre-industrial boundary conditions we performed 1,000 CLIMBER-2 runs in which we varied the eleven parameters simultaneously. The climate sensitivity for each of the 1,000 model versions is calculated by running the model for 3,500 years into an equilibrium climate state of 280 ppm $CO_2$, and subsequently into a new equilibrium of 560 ppm for another 3,000 years. With the chosen parameter ensemble, climate sensitivity $\Delta T_{2x}$ ranged from 1.3 to 5.5°C. Most parameter combinations result in large discrepancies of simulated pre-industrial climate and observational data. Hence, we constrained the ensemble to models consistent with global pre-industrial climate characteristics. The consistency criteria lead to a reduction of the original ensemble size by about 90%, which demonstrates that the parameter choices not only strongly affect the temperature response to $CO_2$ but also the pre-industrial climate. However, the preindustrial data constraints hardly reduced the range of climate sensitivity (in the subset of 111 models with realistic pre-industrial climate, $\Delta T_{2x}$ ranged from 1.4 to 4.9°C).

To test whether paleo-data can be used to reduce the uncertainty in the range of $\Delta T_{2x}$, we then ran the full ensemble of models for LGM boundary conditions. The main forcing changes between pre-industrial and LGM climate are accounted for in the simulation by lowered GHG concentrations ($CO_2$, $CH_4$, $N_2O$), existence of northern hemisphere ice sheets, increased atmospheric dust concentration, vegetation and insolation changes. It should be understood that we determine the climate sensitivity directly from the simulated temperature increase due to $CO_2$ doubling in each model version, and not from the temperature change between the LGM and pre-industrial period. Our results thus automatically account for differences in feedbacks and climate response between colder and warmer climates; we do not assume that the sensitivity to $CO_2$ changes is the same when going to LGM conditions as it is for $CO_2$ doubling.

Figure 1 shows the relation between the simulated warming due to a doubling of $CO_2$ and the magnitude of LGM cooling for tropical and high latitude regions. The strong correlation between climate sensitivity and LGM cooling is striking. This close link is the basis for our approach to constraining $\Delta T_{2x}$.

As estimates of global mean LGM cooling are uncertain due to the lack of global paleodata coverage,

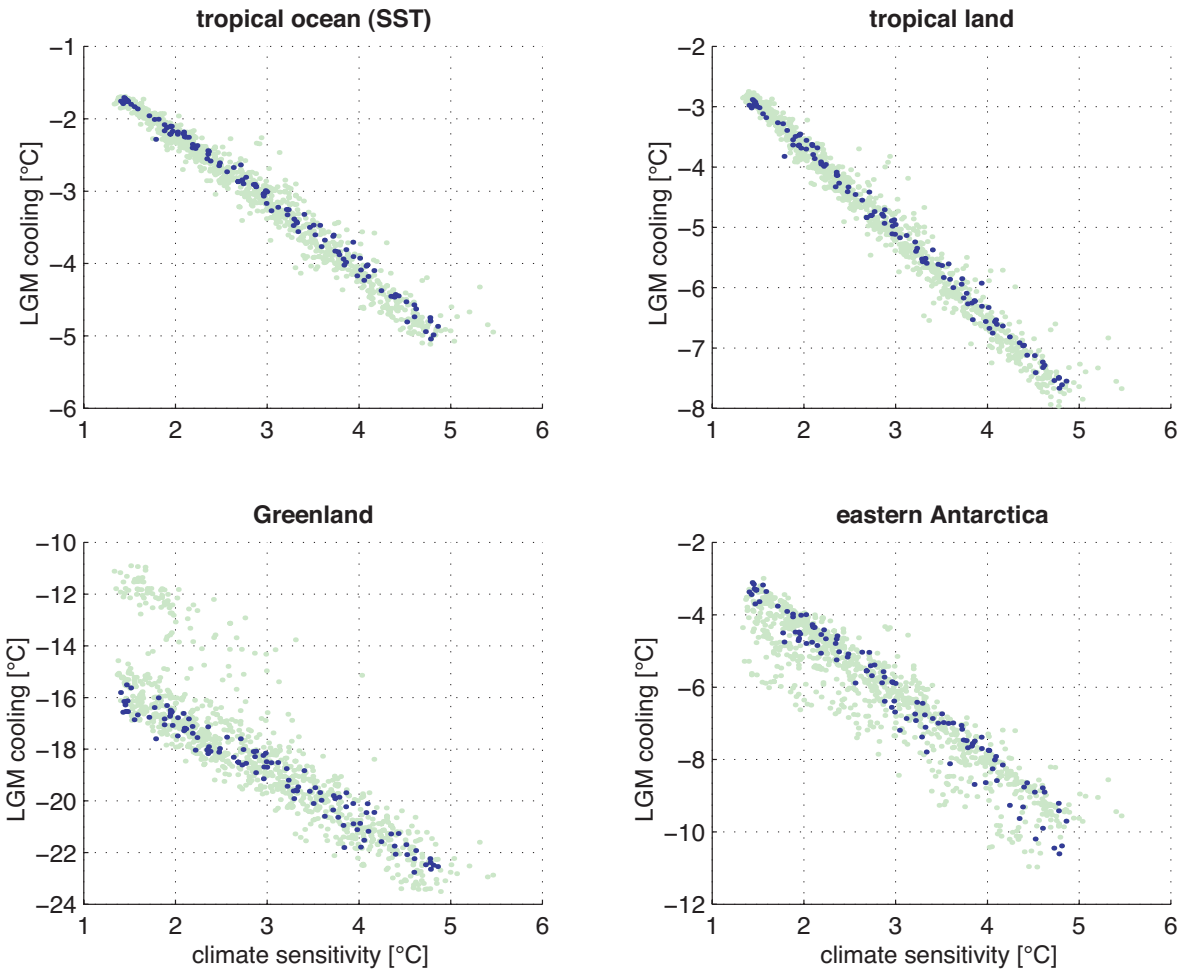


**Figure 1.** Dependence of LGM cooling (relative to the pre-industrial climate) on climate sensitivity for different regions. a, tropical (30°S-30°N) ocean, b, tropical land, c, Greenland, d, eastern Antarctica. Green points represent the entire ensemble (1,000 runs), blue points only runs consistent with pre-industrial data constraints (111 runs).

we focus on specific regions for our model-data comparison. Particularly suited are the tropical ocean regions, where data from sediment cores are abundant. Reconstructed SSTs from paleo-data have been discussed controversially over the past decades, particularly the magnitude of tropical temperature response. Yet in recent years the inter-comparison of different reconstruction techniques has led to reject very low (smaller than -1.5°C) and high (larger than -4°C) tropical SST cooling estimates[7]. We represent the uncertainty of reconstructed ΔSST by considering three assumptions of tropical SST cooling as plausible: a) low (2-3°C), b) high (3-4°C) and c) best-guess (2.5-3°C)[7,8].

The climate sensitivity ranges (5 to 95 percentile), which are consistent with a specific tropical SST cooling (a-c), are illustrated in Fig. 2 (blue intervals). When considering a specific tropical SST cooling as most likely, the corresponding climate sensitivity range is notably smaller than that given in the IPCC TAR. Uncertainty in dust forcing is accounted for by performing a second LGM ensemble where the magnitude of dust forcing is reduced by 50%. This leads to a slight shift (by about 0.5°C) of the climate sensitivity intervals to larger values (light blue intervals). Our largest climate sensitivity range, covering all uncertainty in tropical cooling (cases a-c), dust forcing, and in model parameter choices, suggests a very high probability for the climate sensitivity to lie within the range of 1.5 to 4.7°C.

Similar estimates of $\Delta T_{2x}$ can be derived using tropical land data, which are subject to larger data uncertainty. Paleo-data constraints from high latitude regions (Greenland, Antarctica) also give results consistent with those shown in Fig. 2. We thus conclude that very low (<1.5ºC) and very high (>4.7ºC) values of $\Delta T_{2x}$ are inconsistent with current understanding of LGM

climate. The cooling during the LGM as mapped by paleo-climatic proxy data gives independent and strong support for midrange estimates of climate sensitivity. Reducing the uncertainty range in LGM data will automatically reduce the uncertainty range in climate sensitivity; e.g., if the current "best guess" value for LGM tropical cooling of 2.5-3°C is confirmed, our study implies that climate sensitivity lies in the range 2.1-3.6°C.

### References


1. Forest, C. E., Stone, P. H., Sokolov, A. P., Allen, M. R. & Webster, M. D. Quantifying uncertainties in climate system properties with the use of recent climate observations. *Science* 295, 113-117 (2002).
2. Knutti, R., Stocker, T. F., Joos, F. & Plattner, G.-K. Constraints on radiative forcing and future climate change from observations and climate model ensembles. *Nature* 416, 719-723 (2002).
3. Andronova, N. & Schlesinger, M. E. Objective estimation of the probability distribution for climate sensitivity. *J. Geophys. Res.* 106, 22605-22612 (2001).
4. Hewitt, C. D., Stouffer, R. J., Broccoli, A. J., Mitchell, J. F. B. & Valdes, P. J. The effect of ocean dynamics in a coupled GCM simulation of the Last Glacial Maximum. *Climate Dynamics* 20, 203- 218 (2003).
5. Petoukhov, V. et al. CLIMBER-2: a climate system model of intermediate complexity. Part I: model description and performance for present climate. *Climate Dynamics* 16, 1 (2000).
6. Ganopolski, A. et al. CLIMBER-2: a climate system model of intermediate complexity. Part II: model sensitivity. *Climate Dynamics* 17, 735 (2001).
7. Crowley, T. J. CLIMAP SSTs re-revisited. *Climate Dynamics* 16, 241-255 (2000).
8. Lea, D. W., Pak, D. K., Peterson, L. C. & Hughen, K. A. Synchroneity of tropical and high-latitude Atlantic temperatures over the last glacial termination. *Science* 301, 1361-1364 (2003).


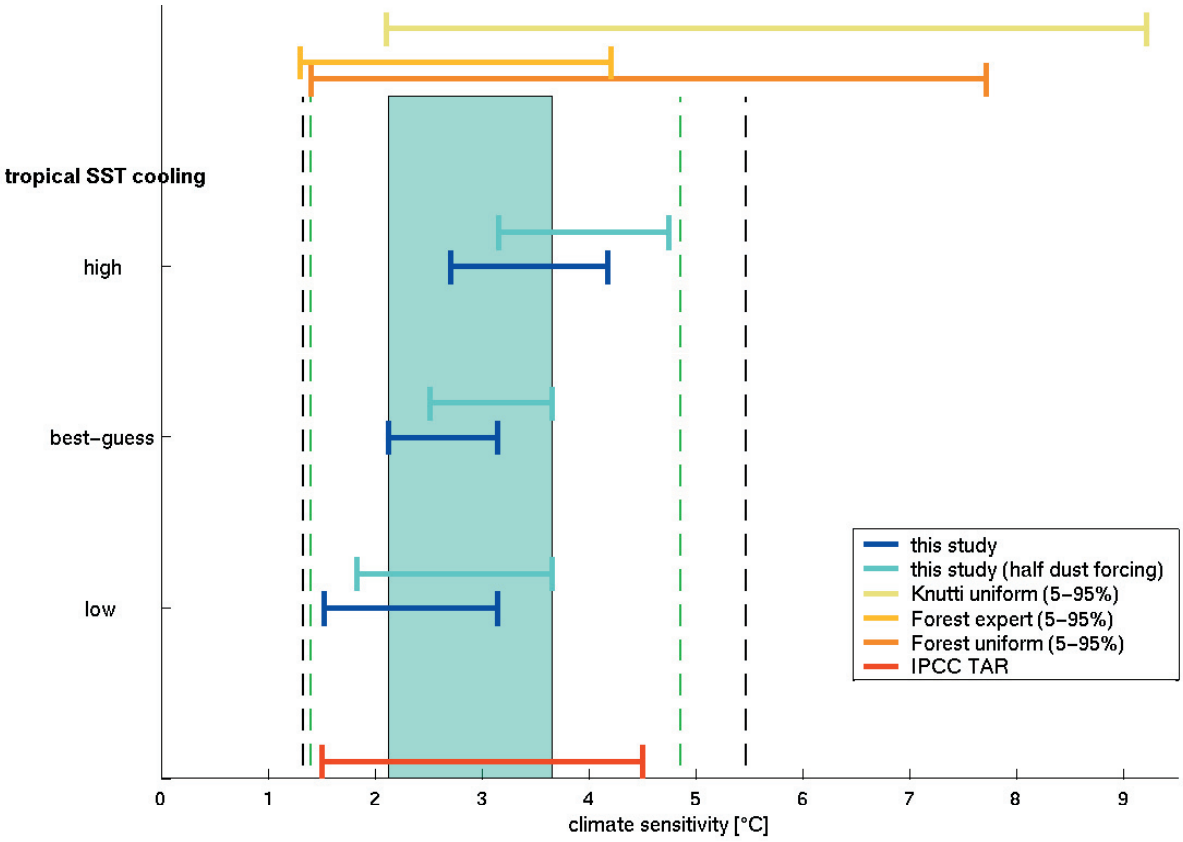


**Figure 2.** Climate sensitivity estimates. Dark blue intervals represent the ranges (5-95%) of $\Delta T_{2x}$ that are consistent with a low (2-3°C), best-guess (2.5-3°C), and high (3-4°C) tropical SST cooling. Light blue intervals show analogous ranges, which result from simulations where dust forcing is reduced by 50%. Vertical black (green) dashed lines represent the realised climate sensitivity range resulting from the complete (preindustrial data consistent) parameter ensemble. Yellow- and red coloured intervals show recent climate sensitivity estimates (see legend). The light blue box illustrates the range of $\Delta T_{2x}$ for our best-guess of tropical SST cooling when accounting for uncertainty in dust forcing.

**IPCC Workshop on Climate Sensitivity**
Paris, France, July 26–29, 2004
*Pre-Conference Volume*

# Probability Distributions of $CO_2$-Induced Global Warming as Inferred Directly from Multi-Model Ensemble Simulations

Jouni Räisänen

*Department of Physical Sciences, Division of Atmospheric Sciences, P.O.B 64, FIN-00014 University of Helsinki, Finland (Email: jouni.raisanen@helsinki.fi)*

The most straightforward way to estimate the probability distribution of $CO_2$-induced global warming is to directly use results of different climate models. This approach has an obvious (and big) caveat: climate changes in the real world may not necessarily follow model results (e.g., Allen and Ingram 2002). However, this simple method of estimating probability distributions provides a natural benchmark against which to compare the results of more rigorous methods.

Two strategic numbers associated with the global mean temperature are studied: (i) the transient climate response (TCR) defined as the warming that occurs at the time of doubling of $CO_2$ when $CO_2$ doubles in 70 years, and (ii) the equilibrium warming resulting from the doubling of $CO_2$, widely known as climate sensitivity (CS). The TCR is evaluated for 20 models participating in the CMIP2 intercomparison (Meehl et al. 2000). For CS, the 15 model results given in Table 9.1 of Cubasch et al. (2001) are used. TCR is evaluated for full atmosphere-ocean GCMs, CS for atmospheric GCMs coupled to a mixed-layer ocean.

The 20 values for TCR are in ascending order 1.0, 1.1, 1.3, 3×1.4, 6×1.6, 1.8, 2×1.9, 3×2.0, 2.1 and 3.1°C, and the 15 values for CS 2.0, 2.1, 2.2, 3.1, 3.2, 3.3, 3.4, 3.5, 2×3.6, 3.7, 4.1, 4.3, 4.8 and 5.1°C. Let us assume that these values are a random sample of some underlying probability distribution, neglecting for the moment the fact that the different models are not necessarily independent from each other. What can we infer of the properties of this hypothetical underlying distribution?

First, one needs to guess the form of the probability distribution. I only consider two candidates: a normal and a log-normal distribution. Visual comparison of the fitted distributions with the original data (Fig. 1) suggests that the TCR data are not well described by a normal distribution. This is confirmed by statistical tests, which show that the original TCR distribution is both positively skewed and leptocurtic at 98% (two-sided) significance level. The log-normal distribution provides a better fit, with no statistically significant deviations from the original data. In the case of CS both the two distributions fit the data within the uncertainty caused by the limited sample size.

Thus, if TCR and CS are to be described by the same form of an analytical distribution, the log-normal distribution appears to be a better candidate than the

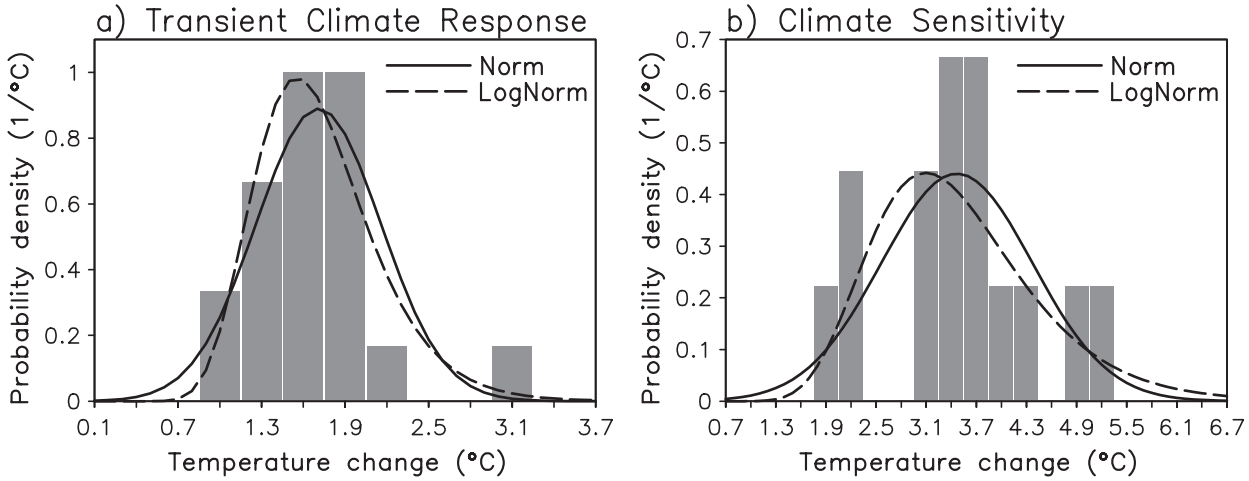


**Figure 1.** Normal (solid line) and log-normal (dashed line) probability distributions fitted to (a) TCR in 20 models and (b) CS in 15 models. The bars show the original data with a bind width of 0.3°C.

normal one. However, there is no way to rule out the possibility that the actual underlying distributions are of some other, unknown form. It may also be noted that the significant skewness and curtosis in the TCR distribution both result from one model (CCSR/NIES2; Nozawa et al. 2000) that simulates substantially larger warming than any of the others.

The 5th, 50th and 95th percentiles of the derived probability distributions are given in Table 1. The best-estimate 5-95% uncertainty range for TCR is 1.1-2.5°C, and that for CS 2.1-5.3°C, when using the log-normal distribution. For the normal distribution, both the 5th and 95th percentiles are slightly lower. The median for CS (about 3.4°C) is twice the value for TCR (1.7°C), even though it should be noted that the two distributions have been derived using slightly different sets of models. The widely cited range (1.5-4.5°C) and best estimate (commonly given as 2.5°C) for CS are somewhat on the lower side of the model results.

Because the derived analytical probability distributions are based on a limited number of model results, they suffer from sampling uncertainty. This source of uncertainty was estimated by first generating a large number of artificial 15- and 20-model random samples by using the parameters of the best-fit normal or log-normal distributions, and by then repeating the distribution fitting for each of these samples. At least for the cases considered in Table 1, the sampling uncertainty is larger than the differences between the normal and the log-normal distributions. The best-estimate 5%, 50% and 95% quantiles for the normal distribution are always within the 5-95% sampling range for the log-normal distribution, and vice versa. In the case of the log-normal fit, the sampling uncertainty is largest in the upper end of the distribution; note in particular the large (4.39-6.35°C) uncertainty in the 95th percentile of CS. For the normal distribution fit, both the lower and upper ends suffer from larger sampling uncertainty than the middle of the distribution.

**Table 1.** Quantiles of TCR and CS, as derived from the fitted analytical probability distributions. In each table entry, the first value gives the best estimate and the next two (in parentheses) the 5-95% sampling uncertainty inferred from Monte Carlo simulations.

| | Quantile | Normal Distribution | Log-Normal Distr. |
|---|---|---|---|
| TCR | 5% | 0.97 (0.72-1.23) | 1.09 (0.95-1.27) |
| | Median | 1.71 (1.55-1.87) | 1.66 (1.51-1.82) |
| | 95% | 2.45 (2.18-2.69) | 2.51 (2.17-2.89) |
| CS | 5% | 1.98 (1.39-2.59) | 2.11 (1.76-2.55) |
| | Median | 3.47 (3.08-3.85) | 3.35 (2.97-3.76) |
| | 95% | 4.96 (4.34-5.54) | 5.31 (4.39-6.35) |

### References

Allen MR, Ingram WJ (2002) Constraints on future changes of climate and the hydrologic cycle. Nature 419: 224-231

Cubasch U, Meehl GA, Boer GJ, Stouffer RJ, Dix M, Noda A, Senior CA, Raper S, Yap KS (2001) Projections of future climate change. In: Houghton JT et al (eds) Climate Change 2001. Cambridge University Press, pp 525-582

Meehl GA, Boer GJ, Covey C, Latif M, Stouffer RJ (2000): The Coupled Model Intercomparison Project (CMIP). Bull Am Meteorol Soc 81: 313-318

Nozawa T, Emori S, Takemura T, Nakajima T, Numaguti A, Abe-Ouchi A, Kimoto M (2000) Coupled ocean-atmosphere model experiments of future climate change based on IPCC SRES scenarios. Preprints, 11th Symposium on Global Change Studies, 9-14 January 2000, Long Beach, USA, 352-355

**IPCC Workshop on Climate Sensitivity**
Paris, France, July 26–29, 2004
*Pre-Conference Volume*

# Interpretation of Model Results that Show Changes in the Effective Climate Sensitivity with Time

S. C. B. Raper

*Alfred Wegener Institute, Germany*

The climate sensitivity is defined as the equilibrium warming for a doubling of the concentration of $CO_2$, expressed as

$$\Delta T_{2x} = \Delta Q_{2x} / \lambda,$$

where $\Delta Q_{2x}$ is the doubled $CO_2$ forcing ($Wm^{-2}$) and $\lambda$ is the feedback parameter ($Wm^{-2}/K$). The climate sensitivity was a very useful concept in comparison of General Circulation Models for the classic experiment with doubled $CO_2$ forcing and a mixed layer ocean. But these mixed layer ocean models are not the ones used for transient simulations and the feedbacks/sensitivity may be different (see Boer and Yu 2003a). The concept of climate sensitivity was extended to transient simulations with time-varying forcing using coupled Atmosphere Ocean General Circulation Models (AOGCMs) by Murphy (1995). Murphy defined the 'effective climate sensitivity', denoted $\Delta T_{2x}^{eff}$, as the equilibrium response to a doubling of $CO_2$ which would occur if the AOGCM was run to equilibrium with feedback strengths, realised at a particular time, held fixed. The equation for the feedback parameter then includes a heat flux below the atmosphere denoted $\Delta F$,

$$\lambda = (\Delta Q - \Delta F) / \Delta T$$

and the effective climate sensitivity can be expressed as

$$\Delta T_{2x}^{eff} = \Delta Q_{2x} \, . \, \Delta T / (\Delta Q - \Delta F).$$

The effective climate sensitivity is thus a hypothetical concept even within the realm of climate modelling. However, changes in the strengths of the climate feedbacks that accompany changes in climate and the rate of climate forcing are of great interest and importance for climate prediction and the effective climate sensitivity may be a useful way to quantify them. Following Murphy, several publications have shown that the effective climate sensitivity in transient runs with AOGCMs can vary with time but their interpretation is obscure (Murphy 1995, Watterson 2000, Senior and Mitchell, 2000, Raper et al. 2001).

The interpretation of varying effective climate sensitivity is not straightforward. This is in part due to the fact that it is a global derivative of feedbacks that occur on a local scale (see the detailed studies of Boer and Yu 2003b, 2003c). As a result, the effective climate sensitivity generally varies even in simulations with a simple model such as MAGICC (Figure1). In the case of the MAGICC model tuned to the AOGCM PCM and used in the TAR, for a step forcing of 3.6 $Wm^{-2}$, $\Delta T_{2x}^{eff}$ decreases with time (Figure 1d, X 0.5 $Wm^{-2}/K$). It is only in the special case where the land/ocean exchange coefficient X ≈ 16 $Wm^{-2}/K$ that the effective climate sensitivity is constant. In this case, a linear fit to a plot of global temperature versus flux into the surface crosses the zero temperature line at 3.6 $Wm^{-1}$, the value of the forcing (see Figure 1c, after Gregory et al. 2004), in the other two cases shown it does not. When X = 16 $Wm^{-2}/K$ the ratio of the land/ocean temperature change is a constant and the differing feedbacks of land and ocean ($\lambda_L$-4.9, $\lambda_O$ 6.6 $Wm^{-2}/K$) are given equal weight with time. When X < 16 $Wm^{-2}/K$ the land/ocean temperature change ratio decreases with time (see Figure 1b), when X > 16 $Wm^{-2}/K$ the land/ocean temperature change ratio increases with time, resulting in the changes in $\Delta T_{2x}^{eff}$ shown in Figure 1d. The former appears to be similar to the behaviour of the CCCma model in Boer and Yu, 2003c, whereas the latter is similar to the behaviour of the HadCM2 2x$CO_2$ experiment (Raper et al. 2001),

Figure 2 is analogous to Figure 1 but shows AOGCM results for the HadCM2 2x$CO_2$ experiment mentioned above. Notice the change in the relationship between the four surfaces box temperatures and the global mean temperature (Figure 2b) before and after forcing stabilization (black vertical line at 1.6 K). To train the eye, Figure 2c after Gregory et al (2004), includes the expected slope of the results after stabilization if the climate sensitivity were a constant of 2.6 K. Clearly the slope is much less than this and indicates an intercept for zero temperature change well below the forcing value of 3.471 $Wm^{-2}$. This is similar to the situation in Figure 1c for X = 100. Consistent with the findings of Figures 2b and c, the effective climate sensitivity for the HadCM2

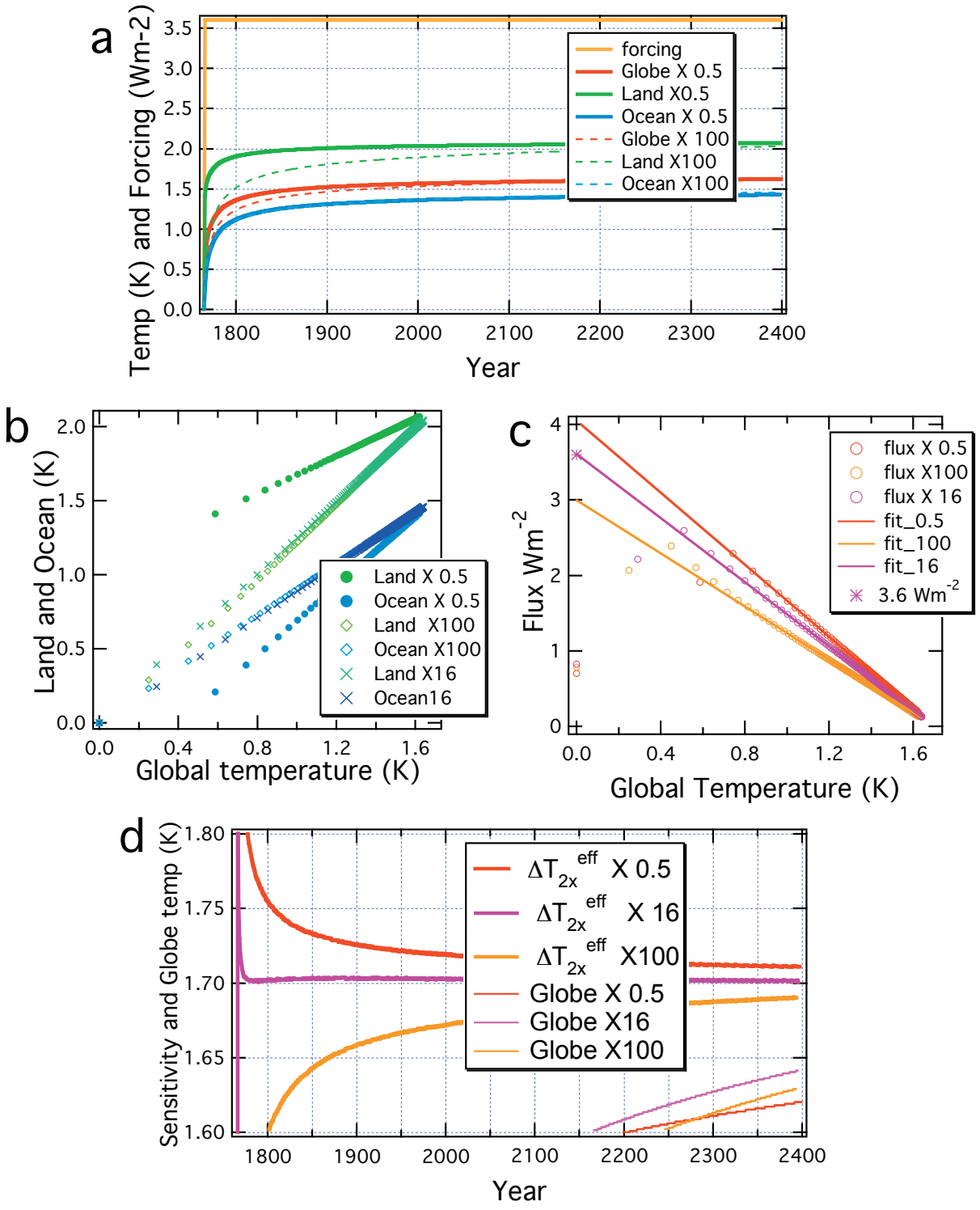


**Figure 1.** Illustration of the effect of the land/ocean heat exchange coefficient (X, $Wm^{-2}/K$) on the effective climate sensitivity using MAGICC tuned to PCM.

$2xCO_2$ experiment shows an increase in time (similar to that for X =100 in Figure 1d). (See Raper et al. 2001 for other forcings.)

Finally, as an illustration (not to be confused with a diagnosis), Figure 2d demonstrates that an increase in the effective climate sensitivity can be compatible with constant but different feedback parameters over the land and ocean, given the land and ocean temperature changes from the HadCM2 $2xCO_2$ experiment.

*How, then, to define the climate sensitivity for a coupled AOGCM?* Given that it is problematic to define and calculate the climate sensitivity for an AOGCM and the confusion that this quantity so often engenders in the non-scientist anyway – mistaking it for the projected range of changes for 2100 for example – it maybe that it is time to stop reporting about it in the Summary for Policymakers. A more transparent and relevant quantity for model comparison was introduced in the TAR: namely the Transient Climate Response (Cubasch et al., 2001).

**References:**

Boer, G.J. and B. Yu, 2003a: Dynamical aspects of climate sensitivity. Geophys. Res. Lett. 30, 1135 (doi:10.1029/2002GL016549).

Boer, G.J. and B. Yu, 2003b: Climate sensitivity and response. Clim. Dyn., 20, 415-429.

Boer, G.J. and B. Yu, 2003c: Climate sensitivity and climate state. Clim. Dyn, 21, 167-176.

Cubasch, and co-authors, 2001: Projections for future climate change. *Climate Change 2001: The Scientific Basis*, J. T. Houghton, et al., Eds., Cambridge University Press, 525–582.

Gregory, J.M., W.J. Ingram, M.A. Palmer, G.S. Jones, P.A. Stott, R.B. Thorpe, J.A. Lowe, T.C. Johns, and K.D. Williams, 2004: A new method for diagnosing radiative forcing and climate sensitivity. *Geophys. Res. Lett.* 31, L03205, (doi: 10.1029/2003GL018747)

Raper, S.C.B., J.M. Gregory and T.J. Osborn, 2001a:Use of an upwelling diffusion energy balance climate model to simulate and diagnose AOGCM results. *Clim. Dyn.*, **17**, 601-613.

Senior, C.A. and J.F.B. Mitchell, 2000: The time-dependence of climate sensitivity. *Geophys. Res. Lett*., **27**, 2685-2688.

Watterson, I. G. 2000:Interpretation of simulated global warming using a simple model. *J. Climate*,**13**, 202-215.

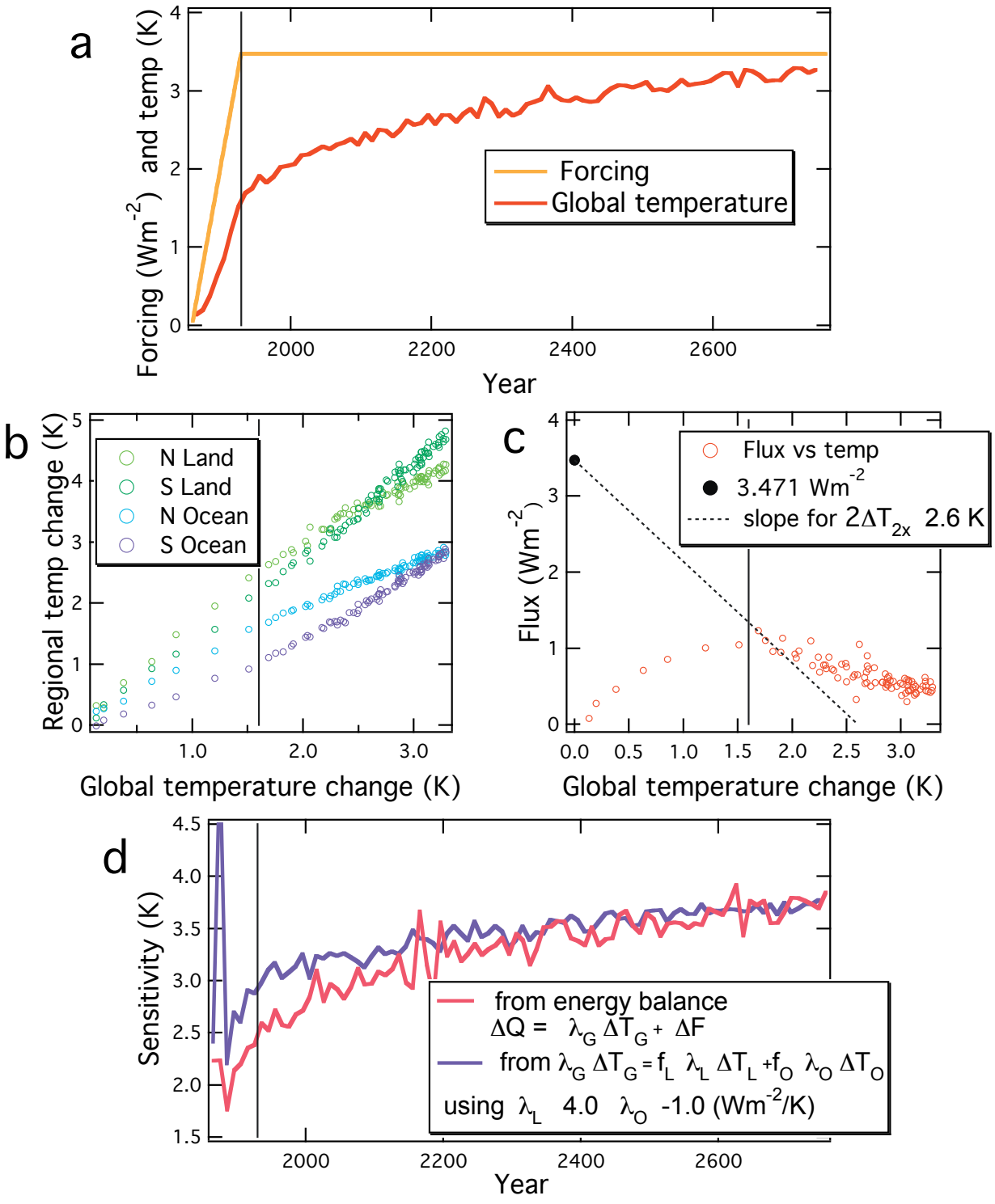


**Figure 2.** Illustration of how changing land/ocean heat flux could result in the time varying effective climate sensitivity found in a long HadCM2 integration.

**IPCC Workshop on Climate Sensitivity**
Paris, France, July 26–29, 2004
*Pre-Conference Volume*

# Use of Observations from the Mt Pinatubo Eruption to Estimate Climate Sensitivity

Alan Robock[1] and Piers Forster[2]

[1] *Department of Environmental Sciences, Rutgers University, New Brunswick, New Jersey, USA*
[2] *NOAA Aeronomy Laboratory, Boulder, Colorado, USA and also at Department of Meteorology, University of Reading, Reading, UK*

The June 15, 1991 Mount Pinatubo eruption was a large but relatively short-lived shock to the Earth's atmosphere. It thus provided an excellent opportunity to study the workings of the climate system and to test climate models, including the dynamical response to volcanically-produced temperature gradients in the lower stratosphere from aerosol heating and volcanic ozone depletion, as well as aspects of the carbon cycle and the impacts of climate change. Here we focus on using this natural experiment to test the sensitivity of the climate system to external radiative forcing. A comprehensive survey of the effects of volcanic eruptions on climate was presented by *Robock* [2000], updated by *Robock* [2002a, 2002b, 2003a, 2003b, 2004].

Most causes of climate change are gradual shifts in atmospheric composition or land surface characteristics. Volcanic eruptions, however, can produce a very large, but short-lived, perturbation to the Earth's radiative balance. While we cannot use these perturbations to test long-term processes, such as changes in the thermohaline circulation, we can take advantage of them to examine some short time-scale feedback processes and impacts. Here we discuss two such aspects, the water vapor feedback as investigated in global climate models by *Soden et al.* [2002] and *Forster and Collins* [2004], and the global temperature response and recovery from individual volcanic eruptions, as discussed by *Wigley et al.* [2004].

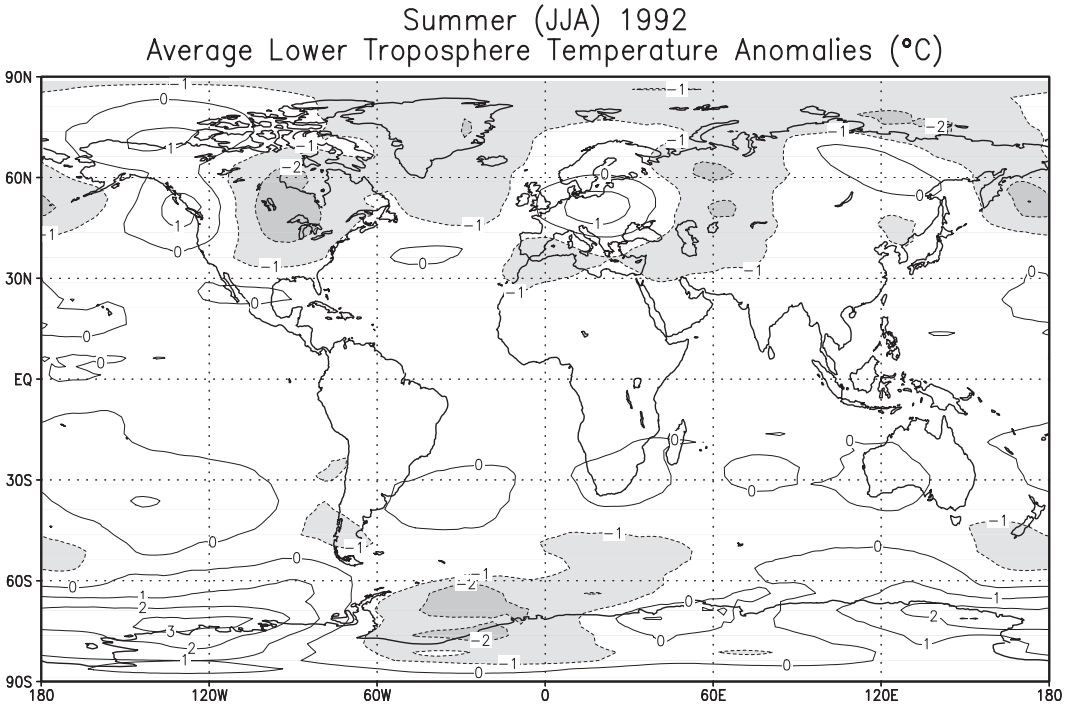


**Figure 1.** Summer (JJA) 1992 lower tropospheric temperature anomalies (with the non-volcanic period of 1984-1990 used to calculate the mean) following the 1991 Mt. Pinatubo eruption. Data from Microwave Sounding Unit Channel 2R [Spencer et al., 1990], updated courtesy of J. Christy and now called Channel 2LT. Anomalies less than -1°C are shaded. (Figure 4 of Robock [2003b].)

Figure 1 shows the lower troposphere temperature anomalies for the Northern Hemisphere summer of 1992, one year after the Pinatubo eruption. Virtually the entire planet was cooler than normal, as expected. But the amount of cooling depended on the sensitivity of the climate system to radiative perturbations, and the strength of the most important positive feedback in the climate system, the water vapor-greenhouse feedback [*Schneider and Dickinson*, 1974]. As the planet cools, the amount of water vapor in the atmosphere goes down, reducing the greenhouse effect, and amplifying the cooling. (Of course, this positive feedback also works for warming.) The timing and amplitude of future global warming depend on this sensitivity of the climate system.

*Soden et al.* [2002] used the global cooling and drying of the atmosphere that was observed after the eruption of Mount Pinatubo to test model predictions of the climate feedback from water vapor, using the Geophysical Fluid Dynamics Laboratory R30 climate model. By comparing model simulations with and without water vapor feedback, they demonstrated the importance of atmospheric drying in amplifying the temperature change and showed that, without the strong positive feedback from water vapor, their atmospheric general circulation model was unable to reproduce the observed cooling (Figure 2). These results provide quantitative evidence of the reliability of water vapor feedback in current climate models, which is crucial to their use for global warming projections.

The *Soden et al.* [2002] simulations were done with fixed cloudiness. The R30 model with interactive cloudiness has a $\Delta T_{2x}$ sensitivity of 3.4 K, and the sensitivity of the fixed cloudiness model would be less than this, but it has not been determined. To reproduce the observed temperature record after the eruption of Mount Pinatubo, the model requires a strong positive feedback, equivalent in magnitude to that predicted for water vapor. Although it is possible that other processes, such as clouds, could act in place of water vapor to provide the strong positive feedback necessary to amplify the cooling, the observational evidence clearly indicates a reduction in water vapor that is consistent with the model predictions.

*Forster and Collins* [2004] repeated parts of the *Soden et al.* [2002] study with the Hadley Centre coupled climate model (HADCM3). They analyzed 13 ensemble integrations of the climate response to the Mt. Pinatubo eruption and again compared these data to observations. They extended the comparison into the upper troposphere and also examined latitude-height patterns of the water vapor feedback. A water vapor feedback parameter of -1.6 $Wm^{-2}K^{-1}$ was found in the observations, which agreed with that found for the model ensembles. Uncertainty, principally from natural climate variations that contaminated the volcanic cooling, placed the feedback parameter between -0.9 and -2.5 $Wm^{-2}K^{-1}$. However, the study sounded a note of caution, as the latitude-height pattern of observed water vapor response following the eruption of Mt Pinatubo differed from that found in any ensemble integration of the model.

The experiments described above examine an important climate feedback mechanism using the best known large volcanic eruption. However, there have been several large eruptions in the recent past, and the sensitivity of the climate response to these eruptions, including the maximum cooling and the time taken for recovery

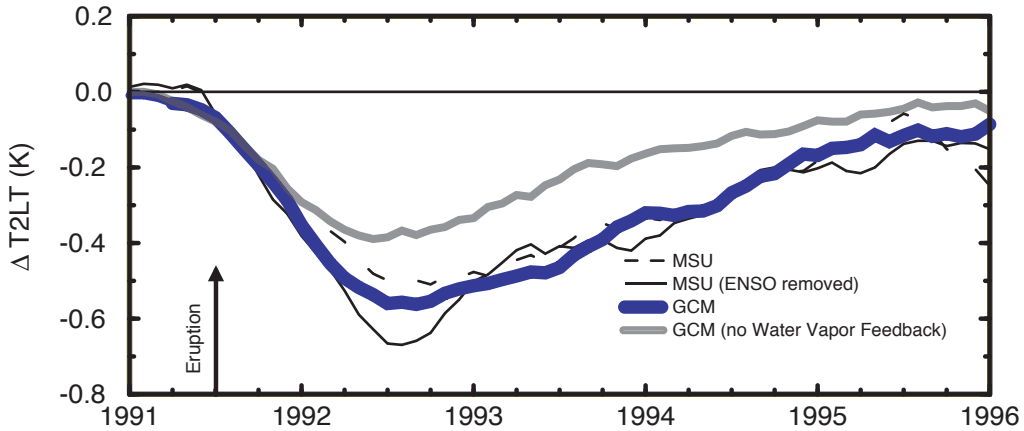


Figure 2. Observations (MSU – Microwave Sounding Unit [*Spencer et al.*, 1990] and MSU (ENSO removed) – with the effects of sea surface temperatures removed) and climate model simulations (GCM – general circulation model). The simulation was only successful with the positive water vapor feedback. (Figure 5 of *Robock* [2003b], from Figure 4 from *Soden et al*. [2002].)

can be used to determine the sensitivity of the climate system. *Wigley et al.* [2004] recently used the NCAR PCM climate model runs to evaluate an upwelling-diffusion energy balance model, and then examined the energy balance model response to the five largest eruptions of the past century, Santa Maria (1902), Novarupta (Katmai) (1912), Agung (1963), El Chichón (1982), and Pinatubo (1991). The maximum cooling for any given eruption was shown to depend approximately on the climate sensitivity raised to power 0.37. After the maximum cooling, for low-latitude eruptions, the temperature relaxed back towards the initial state with an e-folding time of 29-43 months for $\Delta T_{2x}$ sensitivities of 1-4 K. The cooling associated with Pinatubo appear required a sensitivity above the IPCC lower bound of 1.5°C, and none of the observed eruption responses ruled out a sensitivity above 4.5 K. They also showed that the lower sensitivity estimates of *Lindzen and Giannitis* [1998], using a similar technique, were flawed because their climate model was inaccurate, and could not reproduce the behavior of more sophisticated general circulation models.

These results all support the current estimates of the sensitivity of the climate system to doubling $CO_2$. However, because the forcing from volcanic eruptions is not precisely known, because the climate response cannot be uniquely associated with volcanic forcing because of El Niño and stochastic variations, and because volcanic eruptions do not provide a perfect proxy for global warming, because the nature of the external radiative forcing obviously differs between the two, there are limitations to how precisely volcanic eruptions can be used to determine the climate sensitivity.

### References


Forster, Piers M. de F., and Matthew Collins, Quantifying the water vapour feedback associated with post-Pinatubo global cooling, *Climate Dyn.*, DOI: 10.1007/s00382-004-0431-z, 2004.

Lindzen, R. S. and C. Giannitsis, On the climatic implications of volcanic cooling. *J. Geophys. Res.*, *103*, 5929-5941, 1998.

Robock, A., Volcanic eruptions and climate, *Rev. Geophys.*, *38*, 191-219, 2000.

Robock, A., Pinatubo eruption: The climatic aftermath, *Science*, *295*, 1242-1244, 2002a.

Robock, A., Blowin' in the wind: Research priorities for climate effects of volcanic eruptions. *EOS*, *83*, 472, 2002b.

Robock, A., Volcanoes: Role in climate, in *Encyclopedia of Atmospheric Sciences*, J. Holton, J. A. Curry, and J. Pyle, Eds., (Academic Press, London), 10.1006/rwas.2002.0169, 2494-2500, 2003a.

Robock, Alan, Introduction: Mount Pinatubo as a test of climate feedback mechanisms, In *Volcanism and the Earth's Atmosphere*, Alan Robock and Clive Oppenheimer, Eds., Geophysical Monograph 139 (American Geophysical Union, Washington, DC), 1-8, 2003b.

Robock, Alan, Climatic impact of volcanic emissions, *State of the Planet*, Steve Sparks and Chris Hawkesworth, Eds., Geophysical Monograph, (American Geophysical Union, Washington, DC), in press, 2004.

Schneider, S. H., and R. E. Dickinson, Climate modeling, Rev. Geophys. Space Phys., 12, 447-493, 1974.

Soden, B. J., R. T. Wetherald, G. L. Stenchikov, and A. Robock, Global cooling following the eruption of Mt. Pinatubo: A test of climate feedback by water vapor, *Science*, *296*, 727-730, 2002.

Spencer, R. W., J. R. Christy, and N. C. Grody, Global atmospheric temperature monitoring with satellite microwave measurements: Method and results 1979-1984, *J. Climate*, *3*, 1111-1128, 1990.

Wigley, T. M. L., C. M. Ammann, B. D. Santer, and S. C. B. Raper, The effect of climate sensitivity on the response to volcanic forcing, submitted to *J. Climate*, 2004.

**IPCC Workshop on Climate Sensitivity**
Paris, France, July 26–29, 2004
*Pre-Conference Volume*

# METRIC: A Comparison of Climate Sensitivity from Different Forcings

Robert Sausen

*DLR-Institut für Physik der Atmosphäre, Oberpfaffenhofen, Germany*

When comparing radiative forcings (RF) from different perturbations (e.g., from $CO_2$, $CH_4$ and $O_3$) or when using $CO_2$ equivalents in the Kyoto Protocol we implicitly assume that the climate sensitivity parameter $\lambda$ is constant. Under this assumption we can calculate the expected equilibrium response of the global mean near surface temperature $\Delta T_s$ to a given radiative forcing *RF* by a simple linear equation:

$$\Delta T_s = \lambda \, RF \, .$$

For many perturbations of the climate system like perturbations of well-mixed greenhouse gases or changes of the solar constant, the assumption is correct within one single climate model. However, the climate sensitivity parameter $\lambda$ is sensitive to the model selected, ranging from 0.5 K/Wm$^{-2}$ to 1.3 K/Wm$^{-2}$ for a wide range of climate models. This variation in $\lambda$ is believed to reflect differences in model parameterisations.

Many recent climate simulations show that the climate sensitivity parameter cannot be considered as constant in the case of inhomogeneously distributed climate forcing agents (e.g. aircraft-induced ozone perturbations), not even within one climate model. This finding was systematically explored in the EU project METRIC. Here, the climate impact (in terms of surface temperature change) of idealised geographically inhomogeneous perturbations of radiatively active species was studied with two comprehensive GCMs (ECHAM4 run by DLR and LMDz run by CNRS) and one intermediate GCM (run by UREAD). The following perturbations, each scaled to have the same global mean radiative forcing of 1 Wm$^{-2}$, were considered:

1. a globally homogeneous $CO_2$ increase,
2. a $CO_2$ increase confined to the tropics,
3. a $CO_2$ increase confined to the extra-tropics,
4. a $CO_2$ increase confined to the northern extra-tropics,
5. a globally homogeneous increase of the solar irradiance,
6. an increase of the solar irradiance confined to the tropics,
7. an increase of the solar irradiance confined to the extra-tropics,
8. a globally homogeneous ozone increase in the upper troposphere,
9. an upper troposphere ozone increase confined to the tropics,
10. an upper troposphere ozone increase confined to the extra-tropics,
11. an upper troposphere ozone increase confined to the northern extra-tropics,
12. a globally homogeneous ozone increase in the lower stratosphere.

Despite the fact that the models have quite different climate sensitivity parameters for a homogeneous $CO_2$ perturbation, the normalised response in the global mean temperature, i.e., the temperature change normalised by the respective response for the homogeneous $CO_2$ forcing, shows apparent similarities. Thus, the following general results are robust across the models. The tropical and extra-tropical perturbations result in smaller or larger temperature changes, respectively. The response to ozone perturbations in the upper troposphere tends to be smaller than for $CO_2$, while the response to the ozone increase in the lower stratosphere is the largest for each model. In the latter case, the particular high climate sensitivity parameter appears to be a consequence of enhanced stratospheric water vapour (due to feedback processes).

Available metrics of climate change, in particular radiative forcing and global warming potential (GWP) have been reviewed. Their usefulness for "measuring" climate change was discussed and some limitations were shown. E.g. it was demonstrated that reductions in $CO_2$ emissions and equivalent $CH_4$ emissions (in terms of GWP) can result in quite different temperature responses.

The development of amendments to the Kyoto Protocol gives new opportunities for refined metrics. The existing GWP concept should not be considered as default. Many relevant alternatives are available; both from natural science and economics. A clarification of *requirements* and evaluation *criteria* for development of refined indices is needed based on a broad discussion and clarification of which aspects of climate change

we are concerned about. We need to gain insight from the alternative approaches, i.e., a multi-disciplinary approach is necessary (not only based on natural science as in IPCC/WG I). GWP has limitations and inaccuracies, but is highly politically feasible. Any refined metric has to compete with this. The adequacy of GWPs could be increased by including additional RF agents and differences in the climate sensitivity parameter $\lambda$ and by using sustained step changes in emissions instead of pulses. An enhanced GWP concept may clear the path for climate policies that cover a larger part of the man-made RF, and thus, may improve mitigation in terms of comprehensiveness and cost efficiency.

Three refined/new metrics have been developed:

- the Equivalent Radiative Forcing (ERF),
- the Global Temperature Change Potential (GTP),
- the Heterogeneous Damage Metric (HDM).

ERF better accounts for the climate impact of spatially (horizontally and vertically) inhomogeneously distributed climate change agents, it also covers variations of the climate sensitivity parameter. GTP allows a better comparison of short- and long-lived species. GTP is more relevant since it is based on a temperature change rather than integrated RF and has a well-defined meaning. HDM accounts for inhomogeneities in the response.

These metrics allow potential amendments to the Kyoto Protocol to better take into account gases outside the Kyoto basket. Even more, they allow a relative weighing of the different emissions, which is more independent of the selected time horizon.

**IPCC Workshop on Climate Sensitivity**
Paris, France, July 26–29, 2004
*Pre-Conference Volume*

## Report on the joint WCRP CFMIP/IPCC expert meeting on
# 'Climate Sensitivity and Feedbacks': Summary and Recommendations

Catherine Senior

*Hadley Centre, Met Office, U.K.*

### Background

An expert meeting on 'Climate Sensitivity and feedbacks' was held at the Met Office in Exeter, U.K from April 19-22nd, 2004. The meeting was jointly arranged by IPCC WG1 and the WCRP CFMIP (Cloud Feedback Inter-comparison project: http\\www.cfmip.net), and acted both as a first meeting of CFMIP and as an expert meeting for IPCC WG1 to develop scientific questions relevant to the intergovernmental workshop on Climate Sensitivity, July 26th -29th in Paris. The Exeter meeting had as its main focus the role of clouds and cloud feedbacks in determining climate sensitivity. The meeting had 3 major sessions on 'Feedback Methods', 'Cloud: Validation and feedbacks' and 'CFMIP results and Plans'. In addition a number of key speakers gave presentations at a Royal Meteorological Society meeting on 'Climate Sensitivity and Feedbacks' held during the meeting. On the final day of the meeting, three breakout groups were asked to discuss topics that had arisen during the meeting. These topics were chosen to be issues on which we might be able to make recommendations to IPCC WG1 as ways forward to addressing some of the key scientific questions raised in the IPCC WG1 Workshop on Climate Sensitivity 'Scope and Aims' document. Here we summarise the topics of the breakout groups and the recommendations put forward

### Breakout Groups (BOGs)

#### *1. BOG1: Climate Feedback Metrics.*

During the meeting, a number of speakers had talked about the possibility of constraining climate sensitivity using a basket of measures (or metrics) aimed at validating present day climate. BOG1 started by reviewing the utility of current experimental design (notably from the CFMIP project) for such a purpose and looked at what data would be needed to allow the necessary metric tests. The focus was particularly on clouds, although it was recognized that such an approach could be broadened as required. A number of climate model ensembles (the so-called QUMP ensemble at the Hadley Centre (Murphy et al, 2004), the climateprediction.net ensemble (Stainforth et al, 2004) and the forthcoming CFMIP ensemble are available (or will be soon) and BOG1 propose a way forward for using such ensembles that aims to relate errors in model simulations (when compared to observations) to uncertainty in climate prediction. The ultimate goal being to reduce uncertainty in climate sensitivity through application of such carefully constructed metrics to a range of models.

#### *2. BOG2: CFMIP*

Those involved in CFMIP discussed the plans for the project with particular reference to IPCC WG1, and highlighted a number of key areas. A recommendation was made that the CFMIP data be used for research into developing climate metrics, notably related to clouds (stratocumulus and the link between upper tropospheric humidity and cirrus cloud were considered most urgent). Also it was recommended that the ISCCP-simulator (a software package that can be applied to model output in order to produce quantities that can be directly compared to quantities retrieved from the International Satellite Cloud Climatology Project) be included in IPCC AR4, AMIP and CMIP runs. It will be recommended to groups involved in CFMIP to diagnose instantaneous radiative forcing (as will be available for AR4 experiments) and to use partial radiative perturbations for analyzing cloud feedbacks in addition to the more common approach of looking at changes in cloud radiative forcing. A novel area of research for CFMIP is developing methodologies (e.g compositing and clustering) to evaluate aspects of clouds in models that can be shown to be important for cloud response to climate change. It is recommended that such techniques should be applied to a wider range of models, e.g. those in AMIP,CMIP and AR4. This could be best achieved if modeling groups who submit data to AR4 can be encouraged to also participate in CFMIP.

#### *3. BOG3: Climate sensitivity and response*

The third BOG discussed the relative roles and importance of transient and equilibrium climate sensitivity particularly to policy makers.

Recommendations were that modeling groups should provide the temporal evolution of the effective (or transient) climate sensitivity to IPCC AR4 and should be encouraged to analyse the spatial and temporal structure of the feedbacks under a range of IPCC forcings. There was discussion of the relationship between climate sensitivity, ocean heat uptake and temperature response and ways of constraining climate sensitivity and temperature response using the past behaviour of the climate system. One approach is the use of climate perturbations that are comparatively well know. A recommendation was made that IPCC AR4 coupled models include the simulation of the climate perturbation associated with the Mount Pinatubo eruption, paying particular attention to the nature and timescale of the simulated response, the role of ocean heat uptake and the bounds that can be placed upon climate sensitivity. Another approach is the use of observed trends (both in the instrumental record and in palaeoclimate reconstructions) to constrain climate sensitivity. A recommendation was made that studies of past forced climate variations should be pursued but will require carefully developed datasets of forcing and response. Finally constraining temperature evolution was discussed, as for small changes this is primarily dependent on forcing and ocean heat uptake and only secondarily on climate sensitivity. This means that for the next few decades constraints on warming are more likely to be inferred from warming in the recent past than those on climate sensitivity itself. Further into the future, as warming increases, sensitivity becomes a controlling factor. Hence it was recommended that a vigorous program of extending and synthesizing the instrumental record should be undertaken.

Further details of the discussion and recommendations of the three breakout groups are given in the full report of the Exeter meeting by Senior et al (2004).

### References

Murphy J M. *et al.* (2004) Quantification of modelling uncertainties in a large ensemble of climate change simulations. *Nature*, to appear.

Senior, C.A., Wielicki, B.A., McAvaney, B. and Boer, G. J., Report on the joint WCRP CFMIP/IPCC expert meeting on 'Climate Sensitivity and Feedbacks'. Briefing material for IPCC WG1 workshop on Climate Sensitivity. See Annex 1 in this volume.

Stainforth, D. A. *et. al*. (2004). Evaluating uncertainty in the climate response to changing levels of greenhouse gases. Submitted to *Nature*.

**IPCC Workshop on Climate Sensitivity**
Paris, France, July 26–29, 2004
*Pre-Conference Volume*

# Observational Constraints on Cloud Feedback and Climate Sensitivity

Keith D. Williams

*Hadley Centre, Met Office, UK*

The radiative feedback from cloud remains one of the largest uncertainties in determining the climate sensitivity. The IPCC Third Assessment Report of Working Group I (Cubasch *et al*, 2001), states that "the sign of the net cloud feedback is still a matter of uncertainty, and the various models exhibit a large spread". Traditional methods of evaluating clouds in general circulation models (GCMs) have focused on comparing multi-annual mean maps of cloud variables (typically cloud radiative forcing or total cloud amount) with satellite observations. However, the ability to simulate the time-mean geographical distribution of present-day cloud may not offer a stringent constraint on the cloud radiative feedback under climate change. For example, a model might give a poor present-day simulation of cloud, when maps of cloud amount are compared with satellite data, because the inter-tropical convergence zone (ITCZ) is misplaced, and yet contain a physically-based cloud scheme which would provide the correct radiative feedback under climate change. Conversely, a compensation of errors might result in a model producing a realistic simulation of mean present-day cloud, but not including processes which are important for an accurate climate change simulation. A more appropriate cloud evaluation may, therefore, involve a methodology more closely related to the principal cloud processes at work.

There have been several studies which have investigated the use of compositing techniques to isolate the effect of particular processes. Bony *et al.* (1997) investigate the relationship between cloud and sea surface temperature (SST) within particular dynamical regimes, identified by 500 hPa vertical velocity over the tropical oceans; whilst Ringer and Allan (2004) composite model and observational data over the same region by vertical velocity and SST in order to evaluate different versions of a GCM. Norris and Weaver (2001) produce histograms of the amount of cloud at different heights and optical depths from the International Satellite Cloud Climatology Project (ISCCP) in three vertical velocity categories over the mid-latitude oceans. Tselioudis *et al.* (2000) also present such cloud histograms, but binned by the pressure at sea level rather than vertical velocity. Following studies by, for example, Klein and Hartmann (1993) and Slingo (1980) which identify relationships between low cloud amount and lower tropospheric stability, Weaver and Ramanathan (1997) and Weaver (1999) composite cloud observations by vertical velocity and also by various measures of lower tropospheric stability.

These studies have generally investigated cloud processes using observational/re-analysis data and/or simulations of present-day climate from a GCM. There have been relatively few papers which have used such techniques to identify whether these relationships are important for determining the cloud response to climate change. Bony *et al.* (2004) and Williams *et al.* (2003) (hereafter W03) have proposed possible methodologies for evaluating cloud response to climate change in GCMs. The work by Bony *et al.* (2004) is described in a separate extended abstract (S. Bony: Use of observations to constrain cloud feedbacks and climate sensitivity) and hence, will not be repeated here.

W03 propose identifying key relationships between cloud changes in response to increasing greenhouse gases and changes in other atmospheric variables. If the same relationships exist in simulated spatio-temporal variability of the present day climate then the latter can be evaluated using satellite data, and the reliability of the cloud response assessed. In HadSM4 (Hadley Centre Slab Model version 4), W03 find that the high cloud response to a doubling of $CO_2$ over the tropical oceans is mainly associated with a change in the 500 hPa vertical velocity (more high cloud in areas of increased ascent/reduced descent and vice versa) (Fig 1a). This relationship is also present in spatio-temporal variability of present day climate, suggesting that the same fundamental processes may be responsible (Fig 1b). In this case, the variability in the present day simulation may be evaluated against observational data from the International Satellite Cloud Climatology Project (ISCCP) (Fig 1c). The model cloud amounts are from the ISCCP simulator (http://gcssdime.gis.nasa.gov/simulator.html), which produces special diagnostics to take account of cloud overlaps and replicate what is seen from space (Klein and Jakob, 1999; Webb *et al*, 2001), allowing direct comparison with the observational

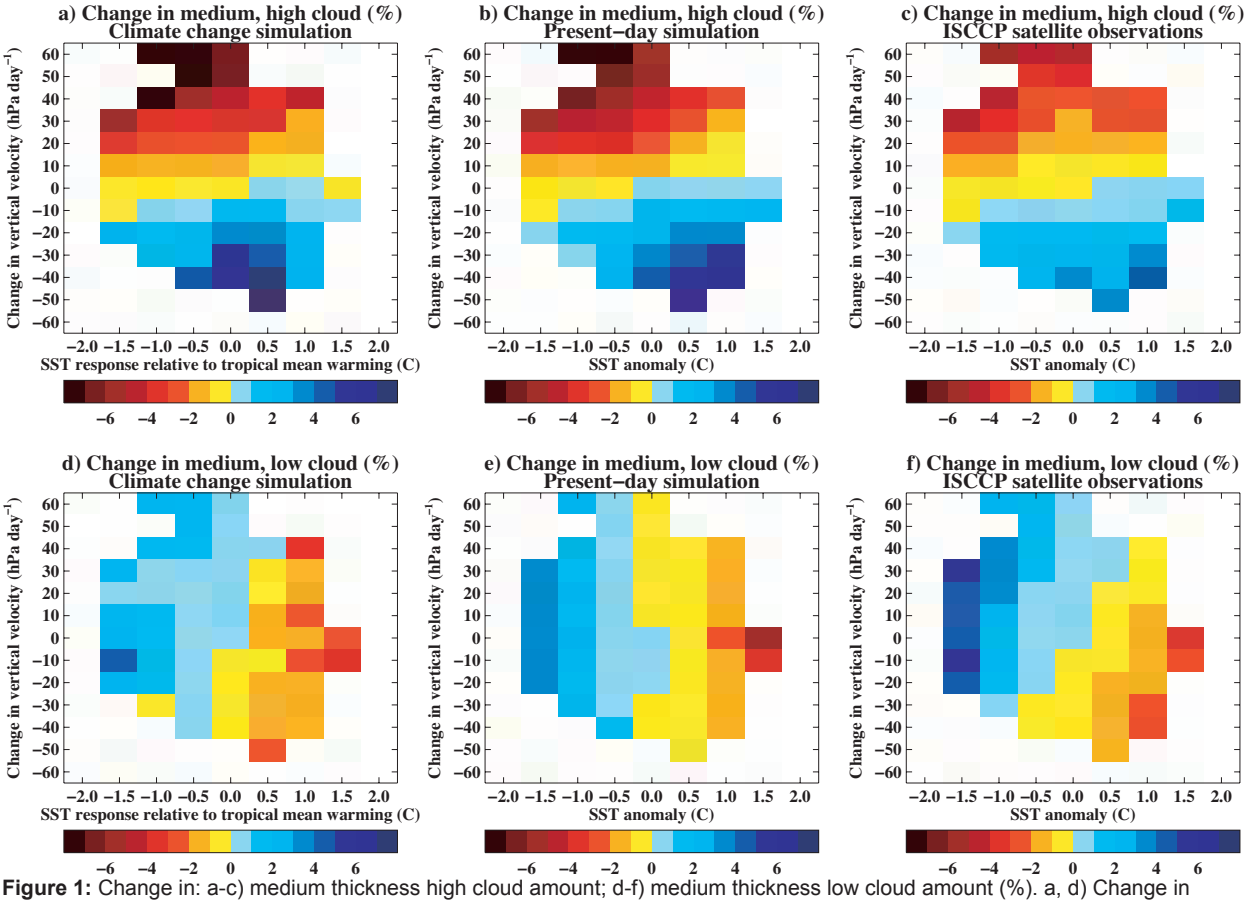


**Figure 1:** Change in: a-c) medium thickness high cloud amount; d-f) medium thickness low cloud amount (%). a, d) Change in cloud amount in response to doubling $CO_2$ in HadSM4 composited by the change in vertical velocity and change in SST relative to the tropical mean warming; b, e) Change in cloud amount in HadAM4 in response to spatio-temporal SST and vertical velocity anomalies; c, f) Change in ISCCP observed cloud amount composited by SST and vertical velocity anomalies from ECMWF re-analysis.

data. The basic relationship between high cloud and vertical velocity in the model may be seen in the observations, however the cloud response in the model appears to be a little too large in those regimes with the largest changes in vertical velocity. W03 also find a relationship between the change in low cloud and the change in SST relative to the change in tropical mean SST. In response to increased $CO_2$, there is a reduction in cloud over those regions which have warmed more than the tropical mean and an increase in low cloud where the warming is smaller than the tropical mean. The lowcloud response to SST and vertical velocity anomalies is similar in the present day simulation and again, compares well with observations, although the data suggest that there should be stronger relationship between low top cloud and vertical velocity than simulated by the model (Fig 1d-f). It should be noted that most points lie in the bins near the origin of these plots, hence the modest cloud response in this part of the domain may contribute more to the global mean change than the more extreme response in the peripheral bins.

Although the compositing shown in Fig 1 yields some success in relating cloud response to climate change over the tropical oceans to present day variability in the Hadley Centre GCM, in general, it is difficult to identify a small number of key dynamic and thermodynamic variables which together, define the climate change cloud response at a global scale.

Jakob and Tselioudis (2003) use a statistical clustering technique on ISCCP cloud histograms over the Tropical Western Pacific (TWP) to objectively identify cloud regimes. This offers the potential advantage over other compositing methodologies that explicit identification of a variable (or variables) to distinguish a regime is not required. Williams *et al.* (2004) (hereafter W04) extend the work of Jakob and Tselioudis (2003) by applying this technique to ISCCP histograms over four different geographical regions, which are known to contain different cloud regimes, and apply the same clustering to ISCCP simulator diagnostics in two versions of the the Hadley Centre GCM for present-day

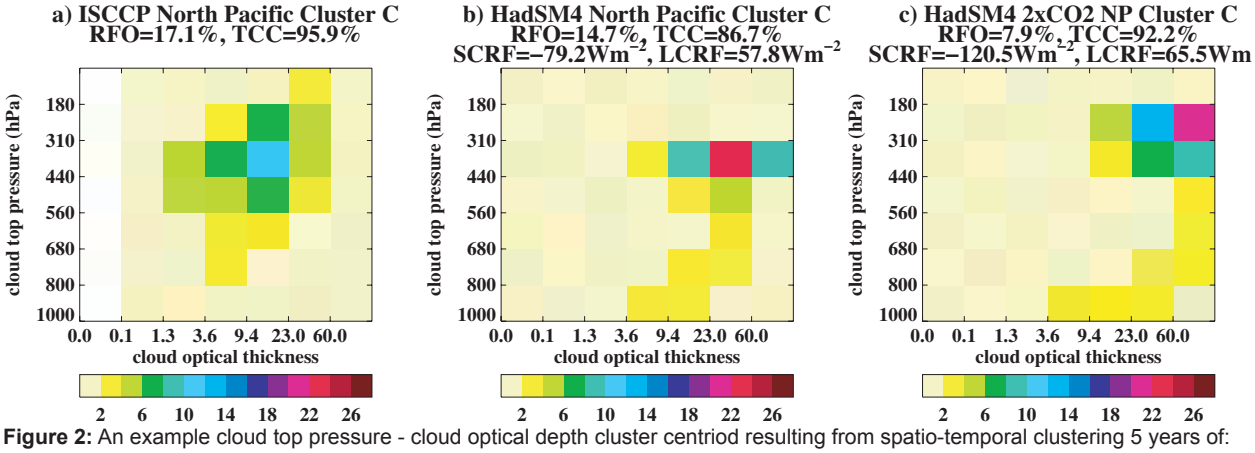


**Figure 2:** An example cloud top pressure - cloud optical depth cluster centriod resulting from spatio-temporal clustering 5 years of: a) daily ISCCP data; b) daily ISCCP simulator output from HadSM4 present day simulation; c) daily ISCCP simulator output from HadSM4 simulation with the $CO_2$ concentration doubled. In each case, the cluster shown is characteristic of the mid-latitude frontal cloud regime. Colours indicate cloud amount (%) in each cloud top pressure - optical depth category. Also shown is the relative frequency of occurrence (RFO) of the cluster, total cloud cover (TCC) of the cluster centroid and mean area weighted shortwave and longwave cloud radiative forcing (SCRF & LCRF) from the grid points included in each cluster.

and climate change simulations. W04 evaluate whether the GCM can accurately reproduce the characteristics of observed cloud regimes, and whether the simulated cloud response to climate is mainly due to a change in the frequency of occurrence of regimes or a change in the cloud properties of the regimes (or a combination of the two). The work is illustrated here by examining a particular regime over the North Pacific region. Clustering of the ISCCP data over the North Pacific yields five reliable clusters, one of these, which occurs 17% of the time (the third most common), contains predominantly high topped cloud which is optically thick (Fig 2a). This regime is associated with mid-latitude frontal systems. The HadSM4 GCM simulates this cluster reasonably well, although the cloud is a little too thick and the regime is simulated too infrequently (Fig 2b). In response to climate change, the cloud in this regime becomes optically thicker and the cloud tops increase in altitude. This leads to a strengthening of the average shortwave and, to a lesser extent, longwave cloud radiative forcing components for the cluster. However, the frequency of occurrence of the cluster is halved (Fig 2c). The response of this regime is consistent with the analysis of Carnell and Senior (1998) who find, for an earlier version of the Hadley Centre model, a reduction in the number of mid-latitude storms, but an increase in their intensity, when greenhouse gases are increased. For this regime, and for most of the clusters investigated by W04 in the different regions, it is found that both changes in the frequency of occurrence and a change in the cloud properties within a cloud regime contribute to the cloud response to climate change.

W04 find that the same basic processes occur in the response of the mid-latitude frontal regime (and several other clusters) in the other version of the model they examine (HadSM3), although a differing balance of the magnitude of response from the different regimes leads to net CRF changes of opposing sign over the North Pacific in the two models. It would be very interesting to determine whether such processes occurred generally in response to increased $CO_2$ in different GCMs, in which case the difference in net CRF response would simply be differences in the comparative magnitude of each process, or whether these responses are specific to the Hadley Centre model with other mechanisms determining the cloud response in other models. The Cloud Feedback Model Inter-comparison Project (CFMIP) (McAvaney and Le Treut (2003); http://www.cfmip.net) provides an ideal opportunity to test methodologies, such as the ISCCP clustering and other compositing techniques, in various GCMs. Through programmes such as CFMIP, which aim to evaluate several models against observations in a mechanistic framework, demonstrated to be related to climate change response, a greater understanding of simulated cloud radiative response to climate change might be gained and hopefully, uncertainty in climate sensitivity reduced.

## References

Bony, S., K.-M. Lau, and Y. C. Sud, 1997: Sea surface temperature and large scale circulation influences on tropical greenhouse effect and cloud radiative forcing. *J. Climate*, **10**, 2055–2077.

——, J.-L. Dufresne, H. Le Treut, J.-J. Morcrette, and C. A. Senior, 2004: On dynamic and thermodynamic components of cloud changes. *Clim. Dyn.*, **22**, 71–86 doi:10.1007/s00382–003–0369–6.

Carnell, R. E., and C. A. Senior, 1998: Changes in mid-latitude variability due to increasing greenhouse gases and sulphate aerosols. *Clim. Dyn.*, **14**, 369–383.

Cubasch, U., G. A. Meehl, G. J. Boer, R. J. Stouffer, M. Dix, A. Noda, C. A. Senior, S. C. B. Raper, and K. S. Yap, 2001: Projections of future climate change. *Climate change 2001: The scientific basis. Contribution of Working Group I to the Third Assessment Report of the Intergovernmental Panel on Climate Change*, Houghton, J. T., Y. Ding, D. J. Griggs, M. Noguer, P. van der Linden, X. Dai, K. Maskell, and C. I. Johnson, Eds., Cambridge University Press, 525–582.

Jakob, C., and G. Tselioudis, 2003: Objective identification of cloud regimes in the Tropical Western Pacific. *Geophys. Res. Let.*, **30**(21), doi:10,1029/2003GL018367.

Klein, S. A., and D. L. Hartmann, 1993: The seasonal cycle of low stratiform clouds. *J. Climate*, **6**(8), 1587–1606.

——, and C. Jakob, 1999: Validation and sensitivities of frontal clouds simulated by the ECMWF model. *Monthly Weather Review*, **127**(10), 2514–2531.

McAvaney, B. J., and H. Le Treut, 2003: The cloud feedback intercomparison project: (CFMIP). In CLIVAR Exchanges - supplementary contributions. **26**, March.

Norris, J. R., and C. P. Weaver, 2001: Improved techniques for evaluating GCM cloudiness applied to the NCAR CCM3. *J. Climate*, **14**, 2540–2550.

Ringer, M., and R. Allan, 2004: Evaluating climate model simulations of tropical cloud. *Tellus. A*, In press.

Slingo, J. M., 1980: A cloud parametrization scheme derived from GATE data for use with a numerical model. *Q. J. R. Meteorol. Soc.*, **106**, 747–770.

Tselioudis, G., Y. Zhang, and W. B. Rossow, 2000: Cloud and radiation variations associated with northern midlatitude low and high sea level pressure regimes. *Journal of Climate*, **13**(2), 312–327.

Weaver, C. P., and V. Ramanathan, 1997: Relationships between large-scale vertical velocity, static stability, and cloud radiative forcing over Northern hemisphere extratropical oceans. *J. Climate*, **10**, 2871–2887.

——, 1999: The interactions among cyclone dynamics, vertical thermodynamic structure and cloud radiative forcing in the North Atlantic summertime storm track. *J. Climate*, **12**, 2625–2642.

Webb, M., C. Senior, S. Bony, and J. J. Morcrette, 2001: Combining ERBE and ISCCP data to assess clouds in the Hadley Centre, ECMWF and LMD atmospheric climate models. *Clim. Dyn.*, **17**, 905–922.

Williams, K. D., M. A. Ringer, and C. A. Senior, 2003: Evaluating the cloud response to climate change and current climate variability. *Clim. Dyn.*, **20**, 705–721 doi:10.1007/s00382–002–0303–3.

——, C. A. Senior, A. Slingo, and J. F. B. Mitchell, 2004: Towards evaluating cloud response to climate change using objective identification of cloud regimes. *Clim. Dyn.*, Submitted.

# Annex 1: Report on the Joint WCRP CFMIP/IPCC Expert Meeting on 'Climate Sensitivity and Feedbacks'

Catherine Senior[1], Bruce Wielicki[2], Bryant McAvaney[3] and George Boer[4]
[1] *Hadley Centre, Met Office, U.K.*
[2] *NASA Langley Research Centre, Virginia, USA*
[3] *Laboratoire de Meteorologie Dynamique du CNRS, Paris, France*
[4] *Canadian Centre for Climate Modelling and Analysis, University of Victoria, Canada*

## Background

An expert meeting on 'Climate Sensitivity and feedbacks' was held at the Met Office in Exeter, U.K from April 19-22nd, 2004. The meeting was jointly arranged by IPCC WG1 and the WCRP CFMIP (Cloud Feedback Inter-comparison project: http\\www.cfmip.net), and acted both as a first meeting of CFMIP and as an expert meeting for IPCC WG1 to develop scientific questions relevant to the intergovernmental workshop on Climate Sensitivity, July 26th-29th in Paris. The Exeter meeting had as its main focus the role of clouds and cloud feedbacks in determining climate sensitivity. The meeting had 3 major sessions on 'Feedback Methods', 'Cloud: Validation and feedbacks' and 'CFMIP results and Plans'. In addition a number of key speakers gave presentations at a Royal Meteorological Society meeting on 'Climate Sensitivity and Feedbacks' held during the meeting. On the final day of the meeting, three breakout groups were asked to discuss topics that had arisen during the meeting. These topics were chosen to be issues on which we might be able to make recommendations to IPCC WG1 as ways forward to addressing some of the key scientific questions raised in the IPCC WG1 Workshop on Climate Sensitivity 'Scope and Aims' document. Below we summarise the topics of the breakout groups and the recommendations put forward.

## Summary of Breakout Group (BOG) discussions

### *1. BOG1: Climate Feedback Metrics.*

During the meeting, a number of speakers had talked about the possibility of constraining climate sensitivity using a basket of measures (or metrics) aimed at validating present day climate. BOG1 started by reviewing the utility of current experimental design (notably from the CFMIP project) for such a purpose and looked at what data would be needed to allow the necessary metric tests. The focus was particularly on clouds, although it was recognized that such an approach could be broadened as required. A number of climate model ensembles (the so-called QUMP ensemble at the Hadley Centre (Murphy et al, 2004), the climateprediction.net ensemble (Stainforth et al, 2004) and the forthcoming CFMIP ensemble are available (or will be soon) and BOG1 propose a way forward for using such ensembles that aims to relate errors in model simulations (when compared to observations) to uncertainty in climate prediction. The ultimate goal being to reduce uncertainty in climate sensitivity through application of such carefully constructed metrics to a range of models.

### *2. BOG2: CFMIP*

Those involved in CFMIP discussed the plans for the project with particular reference to IPCC WG1, and highlighted a number of key areas. A recommendation was made that the CFMIP data be used for research into developing climate metrics, notably related to clouds (stratocumulus and the link between upper tropospheric humidity and cirrus cloud were considered most urgent). Also it was recommended that the ISCCP-simulator (a software package that can be applied to model output in order to produce quantities that can be directly compared to quantities retrieved from the International Satellite Cloud Climatology

Project) be included in IPCC AR4, AMIP and CMIP runs. It will be recommended to groups involved in CFMIP to diagnose instantaneous radiative forcing (as will be available for AR4 experiments) and to use partial radiative perturbations for analyzing cloud feedbacks in addition to the more common approach of looking at changes in cloud radiative forcing. A novel area of research for CFMIP is developing methodologies (e.g. compositing and clustering) to evaluate aspects of clouds in models that can be shown to be important for cloud response to climate change. It is recommended that such techniques should be applied to a wider range of models, e.g. those in AMIP, CMIP and AR4. This could be best achieved if modeling groups who submit data to AR4 can be encouraged to also participate in CFMIP.

### *3. BOG3: Climate sensitivity and response*

The third BOG discussed the relative roles and importance of transient and equilibrium climate sensitivity particularly to policy makers. Recommendations were that modeling groups should provide the temporal evolution of the effective (or transient) climate sensitivity to IPCC AR4 and should be encouraged to analyse the spatial and temporal structure of the feedbacks under a range of IPCC forcings. There was discussion of the relationship between climate sensitivity, ocean heat uptake and temperature response and ways of constraining climate sensitivity and temperature response using the past behavior of the climate system. One approach is the use of climate perturbations that are comparatively well know. A recommendation was made that IPCC AR4 coupled models include the simulation of the climate perturbation associated with the Mount Pinatubo eruption, paying particular attention to the nature and timescale of the simulated response, the role of ocean heat uptake and the bounds that can be placed upon climate sensitivity. Another approach is the use of observed trends (both in the instrumental record and in palaeoclimate reconstructions) to constrain climate sensitivity. A recommendation was made that studies of past forced climate variations should be pursued but will require carefully developed datasets of forcing and response. Finally constraining temperature evolution was discussed, as for small changes this is primarily dependent on forcing and ocean heat uptake and only secondarily on climate sensitivity. This means that for the next few decades constraints on warming are more likely to be inferred from warming in the recent past than those on climate sensitivity itself. Further into the future, as warming increases, sensitivity becomes a controlling factor. Hence it was recommended that a vigorous program of extending and synthesizing the instrumental record should be undertaken.

Further details of the discussion and recommendations of the three breakout groups are given in the attached reports for each breakout group

## DRAFT BOG 1: Climate Feedback Metrics

## Recommendations

### *1. Overall Modelling Simulation Strategy*

The BOG 1 reviewed CFMIP experimental design with the goal of identifying ways of leveraging this experimental activity to address our charge. Questions that were discussed but not fully addressed included whether these experiments should be equilibrium-like experiments or should include the observed natural and anthropogenic forcing record (i.e., a transient slab experiment). Group discussion favoured the equilibrium strategy which is also more consistent with the CFMIP experimental design. We noted, however, that an attempt should be made to allow some of the CFMIP runs to better simulate an ENSO forcing by imposing spatial Q-flux patterns.

We concluded that the same cloud/climate metrics would be needed from the range of studies proposed for AMIP (C20C using observed SST and forcing), CFMIP, as well as the fully coupled IPCC runs. We recommend that the same set of data (at a minimum) be collected as planned for the CFMIP, with the

selected additions shown below in item 2. There is a concern that the ISCCP cloud pressure/optical depth statistics might not be included in the IPCC runs and we strongly recommend this data be included for study.

We noted that each of the different simulation methods brings different strengths and weaknesses in evaluating climate simulations versus observations. AMIP simulations provide more accurate boundary conditions such as ENSO, but break the surface energy budget feedbacks. CFMIP slab runs bring in the surface flux feedbacks, but are weak for ENSO events and are missing most ocean physics. Fully coupled IPCC 20th century runs enable the full ocean/atmosphere interaction but have limited numbers of simulations. We also considered the QUMP (Murphy et al, 2004) and climateprediction.net (Stainforth et al, 2004) efforts for large ensembles of Perturbed Physics Ensembles (PPEs). These are considered a key element of mapping errors in model simulations to uncertainty in climate sensitivity. These are dealt with in item 3 below.

In summary, tests of climate models versus observations will be required in a wide range of time/space scales and methods to handle the complete range of climate feedbacks. Ensembles of model runs will be key to determining natural variability, since all comparisons to observations are to a single realization of the Earth's climate system. Significance of climate metrics for model minus observations must have both observational error statistical distributions as well as model climate noise statistical distributions. Both must be defined at the relevant range of time/space scales to handle a complete range of climate feedbacks. While many "necessary" climate model tests are known, there currently exists no set of "sufficient" climate model tests. This remains a critical and active area of research, and this report is a further step toward a complete set of model tests.

### *2. Model Run Data Needed for Metrics: AMIP, CFMIP, IPCC*

We reviewed the CFMIP planned variables and time/space scales being saved and considered whether these were adequate for cloud feedback studies in general. While the general specifications looked very good, we had a few key additions:

a) Aerosol information if the model uses aerosols in the run. Properties should include visible optical depth, aerosol layer mean height, aerosol type/species, particle size and assumed single scatter albedo. If type/species specify all optical properties but optical depth, then these can be specified once for each type/species

b) 3-hourly sampling for the diurnal average variables is needed to study diurnal cycles of cloud. It would be sufficient to provide 3 hourly variables for the seasonal months of January, April, July, and October in 4 sample years. The selection of months and years is done to minimize data volume while retaining sufficient samples of diurnal cycle and inter-annual variability.

c) Note that ISCCP cloud pressure/optical depth cloud statistics are required at all time/space scales included in the planned CFMIP data

### *3. Relating Model Metrics to Climate Sensitivity*

One of the major shortcomings of all climate prediction assessments has been the inability to objectively and unambiguously relate the errors in model simulations (as judged by comparisons to observations) to uncertainty in climate sensitivity, i.e.

Climate Sensitivity Uncertainty = Function (Model Error versus Observations)

One of the problems immediately obvious (and why this has not been accomplished to date) is that climate model error metrics vary with a) model variable b) spatial scale c) time scale d) single variable errors versus multiple correlated variable errors. The fundamental nonlinear nature of the climate system guarantees that this function is unlikely to be simple. To date attempts have been ad-hoc and have varied widely depending on physical feedback mechanism, variable, time and space scale. What is needed is a more general approach.

QUMP and climateprediction.net offer a new opportunity to attack this outstanding problem in climate assessment and climate science. A strategy was discussed by the working group and will be explored in the coming year. A brief description and outline of steps is given below.

The methodology is based on the following concept. Consider any two climate models with different physics (could be parameterization, resolution, etc). Each model is run for control climate (fixed boundary conditions) and for perturbed boundary conditions. The example we will use here is the slab ocean runs for fixed $CO_2$ and for doubled $CO_2$. Consider each model as a real planet with perfectly known physics (the model formulation) and perfectly known observations (model output fields). The key is to consider planet 1 as a model of planet 2. We in essence use the climate sensitivity of model 1 to be a predictor of climate sensitivity for model 2. Since the models have different physics, the prediction will have error. But we can also compare the perfect observations of planet 2 (model 2 output) to the prediction of model 1. There are also errors in these fields. Analogy here is that we want to learn how to use differences in model 1 minus model 2 output fields (climate metrics) to predict the sensitivity difference of model 1 minus model 2. Model 2 is the real earth, Model 1 is the prediction model of Model 2. The next key is to vary all of the uncertain physical parameterizations in the climate system within reasonable ranges. This might be 50 tuneable parameters, each varied both one at a time and in combination, so that 100s to 1000s of different physical models are generated. The tuneable parameters are be chosen to be broad and to encompass most if not all of the known climate issues: surface physics, ocean physics, atmosphere physics, ice sheet physics, sea ice physics, chemistry, etc. We now have 1000s of planets, each somewhat like Earth, but each with different climate feedbacks. If we run each of these models in a fixed $CO_2$ and doubled $CO_2$ version, we also have the $CO_2$ doubling sensitivity of each planet (model). We call this a Physics Parameter Ensemble (PPE). When selected as individual pairs each model pair is used to get one realization of a real planet and a model trying to predict the sensitivity of that planet. Note that the climate sensitivity we are trying to predict does not have to be restricted to global average temperature. We could use any climate metric as the desired sensitivity output: Europe summer precipitation, ENSO magnitude, storm track shifts, etc. We will use the example here of doubling of $CO_2$ temperature climate sensitivity.

### *3.1 Step 1: Run the PPE ensemble in fixed CO2 and doubled CO2*

These runs must vary a wide range of physical parameterizations. In initial tests, the Hadley Centre has run 58 PPE samples and has begun studying the application of a broad Climate Prediction Skill (CPS) of about 30 parameters. They have saved a fairly complete set of climate diagnostics from this run. Climateprediction.net has run a much larger set of PPE experiments (1000s) but has much more limited climate diagnostics. They are now working to improve this set in future simulations submitted. Ultimately the types of metrics described in item 2 of this report will be desired. Because of the large number of model runs involved, a subset of these will be necessary initially.

### *3.2 Step 2: Select a set of climate skill metrics and train a neural net to relate Climate Prediction Skill to climate sensitivity difference*

Select each possible pair of climate model runs. Use all of the climate prediction skill metrics (order 30 to begin with) for each model pair as input to the neural net. Output is the climate sensitivity difference

between the two models. As discussed earlier, this mimics normal climate prediction, but where model 2 becomes the "Earth" and model 1 is the model trying to predict the "Earth's" (model 2) sensitivity. The difference in sensitivity between the two models is the error in its prediction of sensitivity. The climate metrics differences between the two models are the error in the "observations of Earth" (model 2 output fields) versus the prediction (model 1 output fields). Do this for all model pairs. There will be 1000s to millions of such pairs depending on the total number of models M in the PPE set.

**Model *i* predicts Model *j***

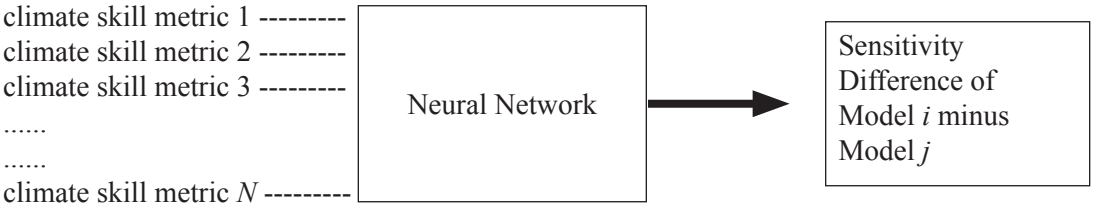


Once the neural net is complete, test its accuracy in prediction of sensitivity difference between each model pair. If this accuracy is sufficient then the set of climate metrics is deemed useful, note the uncertainty of the prediction (PDF of error in sensitivity difference prediction) and move to step 3. If the prediction is not useful (say 100% 1sigma uncertainty in sensitivity difference between model i versus model j) then the set of climate metrics was insufficient. Note that in using the climate metrics, a neural net will automatically give heavier weight to more important metrics, lower weight to less important metrics, and will allow for correlations between metrics. These are all key characteristics of moving beyond a simple linear sum of errors in all parameters and time/space scales. In all cases, the key to a robust neural net prediction is a large ensemble of tests, a complete set of climate sensitivity variations, and a good set of climate metrics.

### *3.3 Step 3: Test Neural Network against an independent set of models: CFMIP slab runs.*

Since all of the PPE runs were built on parameterization changes in the UKMO climate model, it is important to verify the neural net performance against an independent set of climate models with very different approaches to parameterization. The CFMIP slab runs of fixed $CO_2$ and doubled $CO_2$ provide this independent test. Test all pairs of CFMIP model runs using the neural net developed in step 2, to predict their sensitivity differences. The accuracy of this prediction should be compared against the training set accuracy in step 2. If accuracy is similar and still within goals, proceed to step 4. If not, will need to run a large ensemble of PPE simulations using varying climate models, not just the UKMO model. Then repeat step 2.

An additional useful test of the rigor of the neural net climate sensitivity predictions is to perform a set of solar constant change experiments with the same CFMIP slab climate models. The neural net can be used to predict the model climate sensitivities in a manner similar to the primary $CO_2$ doubling experiment.

### *3.4 Step 4: Use fully coupled 20th Century IPCC runs with and without anthropogenic forcing*

Use model pairs as in step 3 to test prediction capability of neural net for changing climate sensitivity between each pair of models. If this is not successful, may need to run a PPE set of fully coupled models to add in deep ocean physics. If it is successful, then move to step 5.

### *3.5 Step 5: Evaluate Uncertainty in IPCC model sensitivity*

Determine the climate metrics comparing the IPCC 20th century runs and actual Earth observations. Note

that this is the first actual use of observations in this evaluation process. All other training and testing of the neural net has used model simulations as alternative Earth/model pairs. Their purpose was to demonstrate the accuracy and rigor of the neural net system to relate climate metric differences to climate sensitivity differences. We now use actual observations of the Earth versus one of the climate models to set the climate metrics that are input to the neural net. The neural net then converts differences between model and observed Earth to predict the difference in climate sensitivity between model and Earth. Do this step for all IPCC model runs. For each model you will have its climate sensitivity as well as a prediction of the difference between the model and the true Earth sensitivity. For K model IPPC runs, there will be K predicted sensitivity and differences. There is also a known "noise" from step 4 in the ability to use the climate metrics to predict sensitivity differences. This allows a statistical test of what level all K models are consistent with a range of the true Earth climate sensitivity. We may find that a narrow range of Earth climate sensitivities would be consistent with all of the model predictions: this then would be the most likely range of sensitivity. It should be possible to predict the true Earth climate sensitivity range as a function of different percentiles of likelihood. If step 4 shows good predictability of the climate sensitivity uncertainty, but step 5 shows an inconsistent range of sensitivity plus uncertainty from the models, this result would point toward the likelihood of some unrealized physical process in the real Earth system that was not included in any of the PPE simulation variations of climate feedback processes.

### *3.6 Effect of Observational Noise and Climate System Internal Natural Variability.*

The neural network development intrinsically includes internal climate noise, at least as far as it is reasonably simulated by the climate models. The analysis proposed here can also be used, however, to test the effect of observation error on the neural net prediction of climate uncertainty. A brute force method is to Monte Carlo added noise onto the climate skill metrics, but there are more elegant ways to do this within the framework of a neural network approach.

### *3.7 Neural Networks and Other Analysis Tools*

Neural networks are only one type of statistical tool that could be applied to evaluate the relationships discussed in sections 3.1 to 3.6. The results are not guaranteed to be unique, especially if the set of training cases is too small or if the set covers only a small subset of the range of application (lack of completeness). The suggested tests in 3.3 and 3.4 are designed to highlight such difficulties if they occur, but other statistical methods should also be evaluated, and in the end might prove more effective. Neural networks are used in the discussion here as a suggested initial approach with broad capabilities.

There is also concern that a neural network approach is a "black box" with reduced insight into the key physical relationships. This criticism suggests that alternative linear and nonlinear approximations to the full climate system must be examined in parallel with statistical approaches. But the criticism can also be reduced by selection of climate variable metrics in 3.2 based on known physical forcing and feedback mechanisms in the climate system. The major challenge for any successful method is obtaining relationships that are valid in the fully coupled nonlinear climate system. The strongest evidence and physical insight will come from convergence of results from multiple approaches. The neural network approach described here has the potential to significantly advance this critical effort.

### *3.8 Can the Earth's True Climate Sensitivity be Outside the Uncertainty Range Determined in Section 3.5?*

Yes, but it is less likely than current uncertainty estimates. To date, our climate sensitivity uncertainty estimates have relied primarily on the range in sensitivity of the current range of climate models. But the

uncertainties in sensitivity predicted in section 3.5 are based in addition on the differences between the model runs and our actual observations: i.e. the bigger the differences the bigger the uncertainty. This is a new constraint on climate sensitivity that has not previously been available. For example, consider what would happen in the situation where all models are missing some fundamental cloud feedback mechanism that a) occurs in nature and b) is a large part of total cloud feedback. In this case, the true climate sensitivity might lie outside the range of any of the current climate models. The process in sections 3.1 to 3.5 adds an additional requirement, that the missing feedback c) doesn't affect significantly the observational metrics we used to test the models. Item c) is the new constraint we add in the current process in section 3.5. Past uncertainty estimates have not been able to explicitly incorporate model minus observation metrics. If the climate metrics used in 3.1 through 3.5 are physically based observational metrics for each feedback (in this case the relevant cloud properties and radiative fluxes) then a missing feedback should show up as large observation/model error, and as a result in a larger climate sensitivity uncertainty. While still not perfect, a climate feedback sufficient to cause the true climate sensitivity to be outside the range of the uncertainty estimate would now have to pass all three tests a) through c).

## DRAFT BOG 2 – CFMIP (Cloud Feedback Model Intercomparison Project)

### Recommendations

#### *1. Metrics*

An incomplete list of priority metrics on the basis of currently known modelled responses: a) a metric to determine stratocumulus (and other types of boundary layer cloud) response is most urgent. b) metrics that can help investigate the link between upper tropospheric humidity and cirrus

Recommend: Use of output of CFMIP by others as research into metrics methodologies continues.

Recommend: ISCCP simulator be installed in IPCC AR4 models (and CMIP and AMIP).

#### *2. Radiative Forcing*

CFMIP will request modelling groups to diagnose radiative forcing (from $2xCO_2$ only), using the instantaneous change double radiation call approach. The forcing should be diagnosed at TOA, surface and 200 mb, and split into SW and LW, up and down, clear-sky and all sky net fluxes. At a bare minimum at-least-5-year means of the geographical distribution should be provided. This should be linked to the WCRP (GEWEX Radiation Panel) Intercomparison of Radiation codes in Climate Models (ICRCCM).

Participants are also encouraged also to calculate the surface, TOA and 200 mb "Hansen"/"relaxed" forcing (double $CO_2$ but keep SST constant; Hansen et al., 1997).

Recommend: Instantaneous radiative forcing required from all participating CFMIP models (slab ocean experiment)

Recommend: Connection with WRCP ICRCCM radiation intercomparison programme.

#### *3. Radiative Changes*

Partial radiative perturbation (PRP) analysis indicates more cleanly what causes what radiative changes, but cloud radiative forcing (CRF) change is more related to observations. CFMIP encourages participants to use both, everyone is urged to keep in mind the differences between them. CFMIP will recommend standards for the detail (e.g. RH as well as q, double substitution, zonal means / maps). The use of simple models to interpret changes in CRF in the absence of PRP diagnostics will be tested using the models

with PRP diagnostics. Alternative definitions of CRF which do not suffer from the cloud masking effect in the clear-sky fluxes will be sought.

Recommend: Individual modelling groups to perform PRP analysis “in house” using standardised techniques.

### *4. Compositing and Clustering*

A novel area of research for CFMIP is developing methodologies (e.g. compositing

and clustering by cloud types) to evaluate aspects of clouds in models that can be demonstrated to be important for the cloud response to climate change and hence, climate sensitivity. It is recognised that there is a need to explore links between different parts of the hydrological cycle – CFMIP should aim to develop techniques in this area e.g. storm/precipitation compositing (George Tselioudis, personal communication)

Recommend: Compositing techniques should be applied to model results submitted to AMIP and CMIP and IPCC AR4.

Recommend: Develop compositing techniques that represent the variations of combinations of cloud types that are associated with distinct meteorological states.

Recommend: AR4 participants should submit results to CFMIP.

### *5. Other Issues*

Recommend: Reinforce that the atmospheric model used for CFMIP should be the same as that used for AMIP and CMIP.

Recommend: CFMIP should provide feedback to the GEWEX Cloud System Study (GCSS) on systematic problems in areas important for cloud response, and should also advise on experimental design for climate change studies using Cloud Resolving Models.

Advantage of idealised +/-2K runs (as well as backward compatibility) is being able to compare models’ response with same warming, but it is an unrealistic one. Imposing structured SST changes (e.g. using the CMIP mean or median) would maintain that advantage while reducing the unrealism and so is recommended for the future. It could also be used for ensembles of perturbed physics, as discussed in BOG1.

Recommend: From CMIP create ensemble mean structured SST mean change and test as an alternative method to slab ocean models for evaluation cloud feedbacks.

## DRAFT BOG3: Climate sensitivity and response

## Recommendations

### *1. Effective and equilibrium climate sensitivity*

*Climate sensitivity* is generally defined as the global mean (indicated by angular brackets) surface temperature change $\langle T'_{2x} \rangle$ experienced by the climate system, or a model of the system, after it has attained a new equilibrium after a doubling of atmospheric $CO_2$ concentration (IPCC2001). The $CO_2$ perturbation to the radiation stream is measured by the *radiative forcing* $\langle f_{2x} \rangle$ and the *equilibrium*

*sensitivity parameter* $s_e$ links the forcing to the temperature response as

$$<T'_{2x}> = s_e <f_{2x}> \quad (1)$$

To the extent that the sensitivity parameter is approximately constant and independent of the nature and pattern of the radiative forcing, (1) provides a way of estimating the global mean temperature response from the magnitude of the forcing and thus broadly characterizes the system. The global climate sensitivity is also used for scaling results, for calibrating simpler models, for estimating the temperature effects of different radiative forcings, and for comparing the behaviour of different models.

While the climate sensitivity of a particular model is comparatively robust, values of climate sensitivity differ by as much as a factor of two among models (e.g. IPCC2001, Fig 9.18) implying that projections of global warming can also differ by that factor for the global mean and by larger amounts locally. It is important to understand why this is the case, to probe the robustness of the sensitivity over a range of forcings, and to understand the connection between temperature response and sensitivity as the system evolves in response to radiative forcing.

The *equilibrium* climate sensitivity in (1) may be diagnostically linked to a more general *effective* climate sensitivity via the energy budget (Murphy, 1995). In a more general approach, the forcing $f(\lambda,\varphi,t)$ and the temperature response $T'(\lambda,\varphi,t)$ are functions of location and time and are linked through the vertically integrated energy budget equation (Boer and Yu, 2003a), as

$$dh'/dt = A' + R' = A' + g + f = A + \Lambda T' + f \quad (2)$$

Where $X' = X - X_0$ is the difference from the control or current climate, $dh'/dt$ the heat storage (mainly in the ocean), $A'$ the change in the convergence of horizontal heat transport and $R' = g + f$ the radiative perturbation which is decomposed into the radiative forcing $f$ and the radiative *feedback* $g = \Lambda T'$ expressed also as a function of local temperature response and a feedback parameter $\Lambda(\lambda,\varphi,t)$. The connection with (1) follows by averaging as $dh'/dt = \hat{\Lambda} <T'> + <f>$, with, $\hat{\Lambda} = <\Lambda T'>/<T'>$, or alternatively as

$$<T'> = -<f - dh'/dt>/\hat{\Lambda} = s<f - dh'/dt> \rightarrow s_e <f> \quad (3)$$

$$s = <T'>/<f - dh'/dt> \rightarrow s_e \quad (4)$$

where the arrow indicates the limit as equilibrium is approached. All terms, including the effective sensitivity parameter $s(t) = 1/\hat{\Lambda}(t)$ are nominally functions of time. When the system reaches a new equilibrium, $<dh'/dt> \rightarrow 0$, the effective sensitivity $s$ becomes the equilibrium sensitivity, $s_e$. The evolution of effective sensitivity is seen in some (Senior and Mitchell, 2000, Boer and Yu, 2003b) but not all (Watterson, 2000) climate models and it is important to understand the cause, magnitude, and implications of this evolution as it applies to the climate system.

In this context, the usual equilibrium $2xCO_2$ sensitivity is a broad, 1st order, and very visible measure of the response of the climate system to a given forcing which indirectly conveys some information on regional patterns of change and which is useful for calibrating simpler models. It is, however, a heavily averaged parameter and attention should be directed also toward the geographical pattern and temporal evolution of the feedback $g$ and the normalized feedback parameter $\Lambda_l = g/<T'>$ together with the associated effective global sensitivity $s(t)$ in order to more completely understand and characterize the behaviour of the system and its evolution.

***R*1**. It is recommended that climate modelling groups calculate the temporal evolution of the global effective sensitivity $s(t)$ as part of their standard diagnostic information (including providing it as part of

the IPCC data). The geographical pattern and evolution of the forcing *f*, feedback *g* and of the feedback parameter $\Lambda_l$, including its components, are all important and should be diagnosed and displayed.

The purpose includes documenting the evolution of sensitivity with climate state and providing information on the nature and magnitude of the feedbacks operating in climate models under the range of IPCC (and other) forcing scenarios.

### 2. Climate sensitivity and temperature change

Climate sensitivity and the evolution of temperature are closely related aspects of the climate system and its behaviour under global warming. For the globally averaged system in (3-4) and assuming that $\langle dh'/dt \rangle \approx \kappa \langle T' \rangle$, i.e. that the system is not in equilibrium and that rate of storage of heat in the deep ocean depends on the temperature change, then to first order

$$\delta\langle T' \rangle \approx \left( \frac{s}{1+\kappa s} \right) \delta\langle f \rangle \text{ whence } \delta\langle T' \rangle_2 \approx \left( \frac{\delta\langle f \rangle_2}{\delta\langle f \rangle_1} \right) \delta\langle T' \rangle_1 \tag{5}$$

for *s* and κ constant or slowly varying. Thus the temperature change for a given forcing depends non-linearly on both the sensitivity and the rate of storage of heat in the ocean, but the temperature change in the future is related to the temperature change in the past by the ratio of the forcing changes.

### 3. Constraining climate sensitivity

Constraints on climate sensitivity based on the past behaviour of the climate system are of considerable interest to the IPCC. Constraints may consist of a range of possible $\langle T'_{2x} \rangle$ values as, for instance, the 1.5 to 4.5°C range of the IPCC reports or, preferably, the probability distribution *p(s)* which reflects the uncertainty in a more quantitative way. Gregory et al. (2003) obtain an estimate of *p(s)* by estimating the values of each of $\langle T' \rangle$, $\langle f \rangle$ and $\langle dh'/dt \rangle$ together with a measure of uncertainty from observations and other information. Taking these to represent means and standard deviation of normally distributed variables, the usual calculus of probabilities gives the probability distribution of a function of these variables namely of sensitivity *s* from (4).

The form of (4) implies that *p(s)* will be asymmetric with a fairly sharp cut off for low values of *s* and a longer tail for larger values of *s*. This general structure is seen in a range of other studies (e.g. Forest et al., 2000; Andronova and Schlesinger, 2001; Forest et al., 2001; Harvey and Kaufman, 2002; Knutti et al., 2002; Forest et al., 2002; and Knutti et al., 2003) that infer *p(s)* from the behaviour of models of the climate system constrained by the observational record. The general approach in these, and other studies, is to constrain the climate sensitivity, and other parameters including the radiative forcing, by fitting model results to observed changes. The 90% confidence interval from studies such as these typically encompasses the IPCC sensitivity range of 1.5 to 4.5°C.

The instrumental record thus provides the possibility of inferring constraints on climate sensitivity which depend, however, on the accurate estimation of the forcing and the successful attribution of observed warming among the several external forcings including GHGs, volcanoes and solar change. The uncertainty in the forcing and in the nature and magnitude of the natural variability of the system together with different model behaviours lead to somewhat different estimates of *s* and of *p(s)* and this leads to the following recommendation.

***R2.*** Constrains on system sensitivity may be tightened by the study of particular climate perturbations where the forcing and the response are comparatively well known. It is recommended that IPCC coupled

model experiments include the simulation of the climate perturbation associated with the Pinatubo eruption with special attention to the nature and timescale of the response, the role of ocean uptake, and the bounds that can be placed on climate sensitivity.

The same general approaches may be used to investigate climate sensitivity based on forced climate variations that occurred in periods preceding the instrumental observational record. Studies such as those of Hoffert and Covey (1992) and Hegerl et al. (submitted) take this approach. This requires that suitable and reliable non-instrumental, i.e. proxy, temperature and other information is available together with information on climate forcing. This need motivates the following suggestion.

***R3.*** Studies of past forced climate variations directed toward constraining sensitivity should be pursued. This depends on the availability of forcing and response data sets which must be vigorously but carefully developed.

Finally, model behaviour indirectly gives information on the range of $s$ and the distribution $p(s)$ in so far as the models are representative of the climate system. One approach is to consider the collection of model sensitivities from complex climate models as a random sample from the population of climate models embodying our current understanding of the climate system. These results, as embodied in Figure 9.18 of IPCC2001 for instance, may be used to estimate $p(s)$ under this assumption. A related approach, discussed in detail in Section 1, investigates $p(s)$ by perturbing model parameters.

### *4. Constraining temperature evolution*

Climate sensitivity by itself does not determine the evolution of temperature for a given IPCC forcing scenario. One of the results of IPCC2001 (Chapter 9) was to show that many models reasonably successfully simulate the observed 20th century global warming even though climate sensitivities differ by a factor of 2 or more. The modelled temperatures subsequently diverge as the simulations proceed into the 21st century, however. Thus for early times, when $T'$ is small, its evolution is initially determined by $f$ and by ocean heat uptake and only secondarily by feedback strength/sensitivity.

For the next few decades, constraints on warming can likely be more directly inferred from the past climate record than from the sensitivity itself since from (5) future temperature change is related to past temperature change by the ratio of the changes in forcing. This contrasts with the inferred sensitivity which depends in a non-linear way on both ocean heat uptake and the observed temperature trend. Of course this depends on the comparative constancy of sensitivity and ocean heat uptake.

In subsequent decades, as warming increases, feedback/sensitivity becomes a controlling determinant of the simulated warming in models and the real system. Some constraints are nevertheless possible based on the past record as investigated, for instance by Allen et al. (2000, 2003), Stott and Kettleborough (2002), Sokolov et al., (2003), Knutti et al., (2003) among others.

The continued study of the physical processes determining both sensitivity and the temperature record is important. Particular attention should be paid to ocean heat uptake and those data sets that aid the specifications of past forcing and permit the attribution of the climate perturbations to these forcings.

***R4***. A vigorous program of extending and synthesizing the instrumental record should be undertaken. In particular, new variables should be analyzed and the temporal and spatial coverage of the usual variables such as temperature should be extended into the bodies of both the atmosphere and the ocean in a bid to constrain sensitivity and temperature.

## References


Allen, M., Wm. Ingram and D. Stainforth, 2002: Constraints on future changes in climate and the hydrologic cycle. *Nature*, **419**, 224-232.

Allen, M. P. Stott, J. Mitchell, R. Schnur and T. Delworth, 2000: Quantifying the uncertainty in forecasts of anthropogenic climate change. *Nature*, **407**, 617-620.

Andronova, N.G. and M.E. Schlesinger, 2001: Objective estimation of the probability density function for climate sensitivity. *J. Geophys. Res*., **106**, 22605-22611.

Boer, G.J. and B. Yu, 2003a: Climate sensitivity and response. *Clim. Dyn*., **20**, 415-429.

Boer, G.J. and B. Yu, 2003b: Climate sensitivity and climate state. *Clim. Dyn*., **21**, 167-176.

Forest, C.E, M.R. Allen, P.H.Stone, A.P. Sokolov, M.R. Allen and M.D. Webster, 2002: Quantifying uncertainties in climate system properties with the use of recent climate observations. *Science*, **295**, 113-117.

Forest, C.E, M.R. Allen, A.P. Sokolov and P.H.Stone, 2001: Constraining climate model properties using optimal fingerprint detection methods. *Clim. Dyn*., **18**, 277-295.

Forest, C.E, M.R. Allen, P.H.Stone, and A.P. Sokolov, 2000: Constraining uncertainties in climate models using climate change detection techniques. *Geophys. Res. Lett*. **27**, 569-572.

Gregory, J.M., et al., 2002: An observationally based estimate of the climate sensitivity. *J. Clim.*, **15**, 3117-3121.

Hansen, J., M. Sato, and R. Ruedy, 1997: Radiative forcing and climate response, J. Geophys. Res., 102(D6), 6831-6864.

Harvey, L.D. and R.K. Kaufmann, 2002: Simultaneously constraining climate sensitivity and aerosol radiative forcing. *J. Clim.*, **15**, 2837-2861.

Hegerl G. C., T. J. Crowley, and Wm. Hyde, 2004: Estimating climate sensitivity from paleo-data. To be submitted

Hoffert, M.I. and C. Covey, 1992: Deriving global climate sensitivity from paleoclimate reconstructions. *Nature*, **260**, 573-576.

Knutti, R., T. Stocker, F. Joos and G.-K. Plattner, 2002: Constraints on radiative forcing and future climate change from observations and climate model ensembles, *Nature* **416**, 719-722.

Knutti, R., T. Stocker, F. Joos and G.-K. Plattner, 2003: Probabilistic climate change projections using neural networks. *Clim. Dyn*., **21**, 257-272.

Murphy, J.M., 1995: Transient response of the Hadley Centre coupled ocean-atmosphere model to increasing carbon dioxide: Part III. Analysis of global-mean response using simple models. *J. Clim*., **8**, 57-80.

Murphy J M. *et al.,* 2004: Quantification of modelling uncertainties in a large ensemble of climate change simulations. *Nature,* to appear.

Senior, C.A. and J. Mitchell, 2000: The time-dependence of climate sensitivity. *Geophys. Res. Lett*., **27**, 2685-2689.

Senior, C.A., Wielicki, B.A., McAvaney, B. and Boer, G. J., Report on the joint WCRP CFMIP/IPCC expert meeting on 'Climate Sensitivity and Feedbacks'. Briefing material for Paris meeting

Sokolov, P, C.E. Forest, and P. H. Stone, 2003: Comparing oceanic heat uptake in AOGCM transient climate change experiments. *J. Clim*., **15**, 1573-1582.

Stainforth, D.A. *et al*., 2004: Evaluating uncertainty in the climate response to changing levels of greenhouse gases. Submitted to *Nature*.

Stott, P. and J. Kettleborough, 2002: Origins and estimates of uncertainty in predictions of twenty-first century temperature rise, *Nature*, **416**, 723-726.

Watterson, I.B., 2000: Interpretation of simulated global warming using a simple model. *J. Clim.*, **13**, 202-215.

## Annex 2: Letter to Modeling Groups Regarding the Radiative Forcing Intercomparison Project

Dear IPCC participant,

We would like to invite you to participate in an intercomparison of the radiative forcings due to specified changes in radiatively active species. The goals of this exercise are to facilitate the comparison of GCMs included in the IPCC AR4 and to establish new benchmark calculations for this purpose. The chief objective is to determine the differences in forcing caused by the use of different radiation codes in the GCMs used for IPCC climate change simulations. The intercomparison results and analyses will be tabled at the IPCC Climate Sensitivity Workshop, to be held in Paris during July 2004.

The two types of species to be evaluated are (i) well-mixed gases and (ii) sulfate aerosols. We will collect calculations from two types of radiative transfer models: the parameterizations used in GCMs, and line-by-line (LBL) models. We are soliciting participation from the global modeling groups in WGCM participating in IPCC and from a number of LBL modelers.

For the purposes of this initial intercomparison, we are seeking just the instantaneous changes in clear-sky fluxes. While the relevant quantity for climate change is all-sky forcing, the introduction of clouds would greatly complicate the initial intercomparison exercise. If the initial comparison shows that participating models are yielding similar clear-sky values, we will consider extending the comparison to all-sky forcings. In addition, we are recommending that the calculations omit the effects of stratospheric thermal adjustment to forcing using Fixed Dynamical Heating (FDH). This omission will facilitate comparison of fluxes from LBL codes and GCM parameterizations, and it will exclude differences arising from differences in dynamical heating rates from various GCMs. Therefore, for the purposes of this exercise we define "flux" to mean "flux for clear-sky conditions" and "forcing" to mean "instantaneous changes in fluxes without stratospheric adjustment".

In order to establish a common baseline, we will specify the background atmospheric state for all the experiments using a thermodynamic profile for present-day conditions. The AFGL midlatitude summer atmospheric profile (MLS) will be used in all the calculations. We will provide versions of the MLS profile at low and high vertical resolution for the GCM and LBL calculations, respectively. If the LBL integrations with the high-resolution profiles prove prohibitively expensive, the LBL groups may use the low-resolution profiles. More information on the profiles follows below. Unless otherwise specified, all experiments should use the same vertical profiles of temperature T, water vapor mass-mixing ratio, and ozone mass-mixing ratio. The only exception is experiment (4), which is based upon profiles of T and $H_2O$ extracted from an integration of the GFDL atmospheric GCM coupled to a mixed layer model for $2xCO_2$ concentrations. In experiment (5), we will also use vertical profiles of modeled sulfate concentrations for pre-industrial and present-day conditions. The GCM and sulfate data have been kindly provided by Tony Broccoli and Oliver Boucher.

The sets of calculations below will yield the following:

1. Forcing for $CO_2$ change (experiments 1 and 2);
   a. Present – preindustrial
   b. $2xCO_2$ - $1xCO_2$
2. Forcing for changes in the major well-mixed GHGs (present – preindustrial; experiment 3);
3. The effect of water vapor changes on the forcing by $CO_2$ (experiment 4); and
4. Forcing due to sulfate aerosols (experiment 5)

The results we would like to collect from each participating group for each experiment are:

1. Net shortwave and longwave clear-sky flux at top of model
2. Net shortwave and longwave clear-sky flux at 200 mb (a surrogate for the tropopause)
3. Net shortwave and longwave clear-sky flux at the surface.

The LBL groups are also welcome to submit their calculations of spectrally resolved fluxes corresponding to the basic products. The LBL groups should use spectral ranges of 100 to 2500 $cm^{-1}$ for the longwave and 2000 to 57600 $cm^{-1}$ for the shortwave. The GCM groups should use the standard spectral ranges for their respective radiative parameterizations.

For all the shortwave calculations, please use the following boundary conditions:

1. A Lambertian surface with a spectrally flat albedo = 0.1
2. The zenith angle = 53 degrees
3. Total input insolation = 1360 $Wm^{-2}$

For all the longwave calculations, please assume that the surface has a spectrally flat emissivity equal to 1.

## EXPERIMENTS/CALCULATIONS:

1. Pre-industrial for $CO_2$:
   a. Constant volume mixing ratio for $CO_2$ = 287 ppmv (1860 value)

Note: No effects from other radiatively active species, except for absorption by the default $H_2O$ and $O_3$ and molecular Rayleigh scattering.

2. Present-day and doubled $CO_2$
   a. Repeat (1a), except $CO_2$ = 369 ppmv (2000 value).
   b. Repeat (1a), except $CO_2$ = 574 ppmv ($2xCO_2$, i.e., 2x preindustrial value).

3. Well-mixed GHGs
   a. Repeat (1a), but with additional well-mixed gases at pre-industrial values:
      i. $CH_4$ = 806 ppbv
      ii. $N_2O$ = 275 ppbv
      iii. CFC11 = 0 pptv
      iv. CFC12 = 0 pptv
   b. Repeat (1a), but with additional well-mixed gases at Year 2000 values:
      i. $CH_4$ = 1760 ppbv
      ii. $N_2O$ = 316 ppbv
      iii. CFC11 = 267 pptv
      iv. CFC12 = 535 pptv

4. $CO_2$ feedback experiment
   a. Repeat (2b), but use the GFDL profile in place of the AFGL MLS profile.

5. Direct sulfate forcing (shortwave only)
   a. Repeat (1a), but with a pre-industrial profile of sulfate
   b. Repeat (1a), but with a present-day profile of sulfate.

The vertical profiles are available from the PCMDI anonymous ftp site/website XXX[1]. We will establish a mechanism for uploading results from the experiments shortly.

Sincerely,

W. Collins and V. Ramaswamy

[1]Fill in value.

## Annex 3: Provisional List of Participants

**Patricio ACEITUNO**
Department of Geophysics
University of Chile
Casilla 2777
Santiago
CHILE
Phone: +56 2 696 8790
Fax: +56 2 696 8686
Email: aceituno@dgf.uchile.cl,
patricio_aceituno@yahoo.es

**Epiphane Dotou AHLONSOU**
Division of Climatology
Service Météorologique National
B.O. Box 379
Cotonou
REPUBLIC OF BENIN
Phone: +229 30 14 13
Fax: +229 30 08 39
Email: meteo@leland.bj

**Filipe AIRES**
Laboratoire de Météorologie Dynamique du CNRS
École Polytechnique
F 91128 Palaiseau Cedex
FRANCE
Phone: +33 (0) 1 69 33 45 34
Fax: +33 (0) 1 69 33 37 58
Email: filipe.aires@lmd.polytechnique.fr

**Abdelkader ALLALI**
Ministry of Agriculture, Rural Development & Forestry
DPV. BP 1387
Rabat Chellah
MOROCCO
Phone: +212 65 601170
Fax: +212 37761557
Email: allali@mailcity.com, allali@lycos.com

**Richard ALLAN**
Environmental Systems Science Centre (ESSC)
University of Reading
Harry Pitt Building
3 Earley Gate, Whiteknights
Reading, RG6 6AL
UNITED KINGDOM
Phone: +44 (0) 118 378 8741, ext 7762
Fax: +44 (0) 118 378 6413
Email: rpa@mail.nerc-essc.ac.uk

**Myles ALLEN**
Atmospheric, Oceanic and Planetary Physics (AOPP)
Department of Physics
University of Oxford
Parks Road
Oxford, OX1 3PU
UNITED KINGDOM
Phone: +44 1865 272085/095
Fax: +44 1865 272923
Email: myles.allen@physics.oxford.ac.uk

**Caspar AMMANN**
Climate and Global Dynamics Division
National Center for Atmospheric Research (NCAR)
PO Box 3000
Boulder, CO 80307-3000
USA
Phone: +1 303 497 1705
Fax: +1 303 497 1348
Email: ammann@ucar.edu

**Natasha ANDRONOVA**
Department of Atmospheric Sciences
University of Illinois @ Urbana-Champaign
105 S.Gregory St.
Urbana, IL 61801
USA
Phone: +1 217 333 3819
Fax: +1 217 244 4393
Email: natasha@atmos.uiuc.edu

**Howard BARKER**
Meteorological Service of Canada
Cloud Physics Research Division
4905 Dufferin Street
Downsview, ON M3H 5T4
CANADA
Phone: +1 416 739 4909
Fax: +1 416 739 4211
Email: howard.barker@ec.gc.ca

**George BOER**
Canadian Centre for Climate Modelling and Analysis
Meteorological Service of Canada
University of Victoria
PO Box 1700, STN CSC
Victoria, B.C., V8W 2Y2
CANADA
Phone: +1 250 363 8226
Fax: +1 250 363 8247
Email: george.boer@ec.gc.ca

**Sandrine BONY**
Laboratoire de Météorologie Dynamique du CNRS
l'Université Pierre et Marie Curie
Case postale 99
4, place Jussieu
F 75252 Paris Cedex 05
FRANCE
Phone: +33 1 44 27 50 14
Fax: +33 1 44 27 62 72
Email: Sandrine.Bony@lmd.jussieu.fr

**Pascale BRACONNOT**
Laboratorie des Sciences du Climat et de
l'Environnement
L'Orme des Merisiers
CEA Saclay Bat. 709
91191 Gif-sur-Yvette cédex
FRANCE
Phone: +33 1 69 08 77 21
Fax: +33 1 69 08 77 16
Email: pasb@lsce.saclay.cea.fr

**Anthony BROCCOLI**
Department of Environmental Sciences
Cook College
Rutgers University
14 College Farm Road
New Brunswick, NJ 08901-8551
USA
Phone: +1 732 932 8644
Fax: +1 732 932 9817
Email: broccoli@envsci.rutgers.edu

**Robert CESS**
Institute for Terrestrial and Planetary Atmospheres
Marine Sciences Research Center
Stony Brook University
Nicolls Road
Stony Brook, NY 11794-5000
USA
Email: rcess@notes.cc.sunysb.edu

**John CHARLERY**
Department of Computer Science
Mathematics and Physics
University of the West Indies
Cave Hill Campus
BARBADOS
Phone: +1 246 417 4368/4000
Fax: +1 246 417 4597
Email: jcharlery@uwichill.edu.bb

**CHEN Dehui**
China Meteorological Administration
46 Zhongguancun Nandajie
Haidian, Beijing 100081
CHINA
Phone: +86 10 684 06662
Fax: +88 10 621 74797
Email: chendh@cma.gov.cn

**Jens Hesselbjerg CHRISTENSEN**
Danish Meteorological Institute
Lyngbyvej 100
DK-2100 Copenhagen Ø
DENMARK
Phone: +45 3915 7428
Fax: +45 3915 7460
Email: jhc@dmi.dk

**William COLLINS**
National Center for Atmospheric Research (NCAR)
Boulder, CO 80307-3000
USA
Phone: +1 303 497 1381
Fax: +1 303 497 1324
Email: wcollins@ucar.edu

**Matthew COLLINS**
Hadley Centre for Climate Prediction and Research
Met Office
FitzRoy Road
Exeter, EX1 3PB
UNITED KINGDOM
Phone: +44 1392 884110
Fax: +44 870 9005050
Email: matthew.collins@metoffice.com

**Robert COLMAN**
Bureau of Meteorology Research Centre
G.P.O.box 1289k
Melbourne, Victoria 3001
AUSTRALIA
Phone: +61 3 9669 4520
Fax: +61 3 9669 4660
Email: r.colman@bom.gov.au

**Thomas CROWLEY**
Department of Earth and Ocean Sciences
Duke University
Box 90227
Durham, NC 27708
USA
Phone: +1 919 681 8228
Fax: +1 919 929 1057
Email: tcrowley@duke.edu

**Michel DÉQUÉ**
Meteo-France CNRM/GMGEC/EAC
42 Avenue G. Coriolis
31057 Toulouse Cedex
FRANCE
Phone: +335 61 07 93 82
Fax: +335 61 07 96 10
Email: deque@meteo.fr

**Martin DIX**
CSIRO Atmospheric Research
Private Bag No. 1
Aspendale Victoria 3195
AUSTRALIA
Phone: +61 3 9239 4533
Fax: +61 3 9239 4444
Email: Martin.Dix@csiro.au

**Hervé DOUVILLE**
Meteo France CNRM
42 Avenue G. Coriolis
31057 Toulouse
FRANCE
Phone: +33 5 61 07 96 25
Fax: +33 5 61 07 96 10
Email: herve.douville@meteo.fr

**Jean-Louis DUFRESNE**
Laboratoire de Météorologie Dynamique du CNRS
l'Université Pierre et Marie Curie
Case postale 99
4, place Jussieu
F 75252 Paris Cedex 05
FRANCE
Phone: +33 1 44 27 50 14
Fax: +33 1 44 27 62 72
Email: dufresne@lmd.jussieu.fr

**Seita EMORI**
Integrated Modeling Research Program
Frontier Research System for Global Change
16-2, Onogawa
Tsukuba, Ibaraki, 305-8506
JAPAN
Phone: +81 45 778 5614
Fax: +81 45 778 5496
Email: emori@jamstec.go.jp

**David FISHER**
Geological Survey of Canada
Terrain Sciences Division
Natural Resources Canada
601 Booth St
Ottawa, Ontario K1A 0E8
CANADA
Phone: +1 613 996 7623
Fax: +1 613 996 5448
Email: fisher@nrcan.gc.ca

**Donald FORBES**
Geological Survey of Canada
Bedford Institute of Technology
1 Challenger Drive (PO Box 1006)
Dartmouth, NS B2Y 4 A2
CANADA
Phone: +1 902 426 7737
Fax: +1 902 426 4104
Email: dforbes@nrcan.gc.ca

**Piers FORSTER**
Department of Meteorology
University of Reading
Earley Gate, PO Box 243
Reading RG6 6BB
UNITED KINGDOM
Phone: +44 (0) 118 931 6020
Fax: +44 (0) 118 931 8905
Email: p.m.forster@reading.ac.uk

**Raquel FRANCISCO**
PAGASA, Weather Bureau
1424 Quezon Avenue
Quezon City
PHILIPPINES
Phone: +632 9204052; 632 9294065
Fax: +632 9294065
Email: raquelfrancisco2001@yahoo.com

**Pierre FRIEDLINGSTEIN**
Institut Pierre Simon Laplace (IPSL)
Laboratoire des Sciences du Climat et de
l'Environnement (LSCE)
CEA Saclay, L'Orme des Merisiers, Bat 701
91191 Gif sur Yvette
FRANCE
Phone: +33 1 69 08 87 30
Fax: +33 1 69 08 77 16
Email: pierre@lsce.saclay.cea.fr

**Qiang FU**
Atmospheric Sciences
University of Washington
ATG Building, Room 320
Box 351640
Seattle, WA 98195-1640
USA
Phone: +1 206 685 2070
Fax: +1 206 543 0308
Email: qfu@atmos.washington.edu

**Carlos GAY GARCÍA**
Centro de Ciencias de la Atmosfera
Universidad Nacional Autonoma de Mexico (UNAM)
Circuito Exterior, Ciudad Universitaria
CP 04510
D.F. MEXICO
Phone: +525 5622 4076
Fax: +525 56160789
Email: cgay@servidor.unam.mx

**Michael GHIL**
Department of Atmospheric Sciences and Institute of Geophysics and Planetary Physics
University of California, Los Angeles
Box 951565 - 7127 Math Sciences
Los Angeles, CA 90024-1565
USA
Phone: +1 310 206 8225
Fax: +1 310 206 3051
Email: ghil@atmos.ucla.edu

**Filippo GIORGI**
Physics of Weather and Climate Group
Abdus Salam International Centre for Theoretical Physics (ICTP)
P.O. Box 586
34100 Trieste
ITALY
Phone: +39 40 2240 425
Fax: +39 40 224 163 / 0449
Email: giorgi@ictp.trieste.it

**Jonathan GREGORY**
Department of Meteorology
University of Reading, Earley Gate
PO Box 243
Reading RG6 6BB
UNITED KINGDOM
Phone: +44 118 378 7376
Fax: +44 118 378 8316
Email: j.m.gregory@reading.ac.uk, Jonathan.Gregory@metoffice.com

**Alex HALL**
Department of Atmospheric Sciences
University of California, Los Angeles
Box 951565
Los Angeles, CA 90095
USA
Phone: +1 310 206 5253 (office); 1 310 206 5257 (lab)
Fax: +1 310 206 5219
Email: alexhall@atmos.ucla.edu

**Gabriele HEGERL**
Division of Earth and Ocean Sciences
Nicholas School for the Environment and Earth Sciences
Duke University
Box 90227
Durham, NC 27708
USA
Phone: +1 919 684 6167
Fax: +1 919 684 5833
Email: hegerl@duke.edu, ghegerl@nc.rr.com

**Isaac HELD**
NOAA Geophysical Fluid Dynamics Laboratory
P.O. Box 308
Princeton, NJ 08542
USA
Phone: +1 609 452 6512
Fax: +1 609 987 5063
Email: Isaac.Held@noaa.gov

**Trond IVERSEN**
Department of Geophysics
University of Oslo (UiO)
P.O. Box 1022 Blindern
0315 Oslo
NORWAY
Phone: +47 22 85 58 21
Fax: +47 22 85 52 69
Email: trond.iversen@geo.uio.no

**Eystein JANSEN**
University of Bergen
Department of Earth Sciences and Bjerknes Centre for Climate Research
Allégaten 55
N-5007 Bergen
NORWAY
Phone: +47 5558 3491
Fax: +47 5558 4330
Email: eystein.jansen@geo.uib.no

**Fortunat JOOS**
Physikalisches Institut - Klima- und Umweltphysik
University of Bern
Sidlerstrasse 5
3012 Bern
SWITZERLAND
Phone: +41 (0) 31 631 4461
Fax: +41 (0) 31 631 87 42
Email: joos@climate.unibe.ch

**Sylvie JOUSSAUME**
National Institute for Sciences of the Universe (INSU)
CNRS
B.P. 287
3, rue Michel-Ange
75766 Paris cedex 16
FRANCE
Phone: +33 1 44 96 43 80
Fax: +33 1 44 96 50 05
Email: sylvie.joussaume@cnrs-dir.fr

**Jean JOUZEL**
Institut Pierre Simon Laplace
Université Versailles Saint Quentin
Batiment d'Alembert
5 boulevard d'Alembert
78280 Guyancourt
FRANCE
Phone: +33 1 39255816
Fax: +33 1 39255822
Email: Jouzel@lsce.saclay.cea.fr, jzipsl@ipsi.jussieu.fr

**Eigil KAAS**
Climate Research Division
Danish Meteorological Institute
Lyngbyvej 100
DK-2100 Copenhagen
DENMARK
Phone: +45 39 15 74 24
Fax: +45 39 15 74 60
Email: ek@dmi.dk

**Lucka KAJFEZ-BOGATAJ**
University of Ljubljana
Biotechnical Faculty
Jamnikarjeva 101
1000 Ljubljana
SLOVENIA
Phone: +386 61 123 1161
Fax: +386 61 123 1088
Email: lucka.kajfez.bogataj@bf.uni-lj.si

**Vladimir KATTSOV**
Voeikov Main Geophysical Observatory
7 Karbyshev St.
St Petersburg 194021
RUSSIA
Phone: +7 812 247 8668
Fax: +7 812 247 8661
Email: kattsov@main.mgo.rssi.ru

**Richard KERR**
Science Magazine
1200 New York Avenue, N.W.
Washington, DC 20005
USA
Phone: +1 202 326 6587
Fax: +1 202 371 9227
Email: rkerr@aaas.org

**Tahl KESTIN**
IPCC WGI TSU
NOAA Aeronomy Laboratory
DSRC R/AL/8
325 Broadway
Boulder, CO 80305
USA
Phone: +1 303 497 4487
Fax: +1 303 497 5628
Email: tahl@ucar.edu

**Jeff KIEHL**
National Center for Atmospheric Research (NCAR)
PO Box 3000
Boulder, CO 80307
USA
Phone: +1 303 497 1350
Fax: +1 303 497 1348
Email: jtkon@ucar.edu

**Masahide KIMOTO**
Center for Climate System Research
University of Tokyo
4-6-1 Komaba, Meguro-ku, Tokyo 153-8904
JAPAN
Email: kimoto@ccsr.u-tokyo.ac.jp

**Stefan KINNE**
Max Planck Institute for Meteorology
Bundesstraße 55
20146 Hamburg
GERMANY
Phone: +49 40 41173 383
Fax: +9 40 41173 298
Email: kinne@dkrz.de

**Akio KITOH**
Meteorological Research Institute
Japan Meteorological Agency
1-1 Nagamine, Tsukuba, Ibaraki 305-0052
JAPAN
Phone: +81 298 53 8594
Fax: +81 298 55 2552
Email: kitoh@mri-jma.go.jp

**Reto KNUTTI**
Climate and Environmental Physics
Physics Institute
University of Bern
Sidlerstrasse 5
CH-3012 Bern
SWITZERLAND
Phone: +41 31 631 34 02
Fax: +41 31 631 87 42
Email: knutti@climate.unibe.ch

**Won-Tae KWON**
Climate Research Laboratory
Meteorological Research Institute (METRI)
Korean Meteorological Administration
460-18, Shindaebang-dong, Dongjak-gu
Seoul 156-720
KOREA
Phone: +82 2 846 2852
Fax: +82 2 846 2853
Email: wontk@metri.re.kr

**Hervé LE TREUT**
Laboratoire de Météorologie Dynamique du CNRS
l'Université Pierre et Marie Curie
Case postale 99
4, place Jussieu
F 75252 Paris Cedex 05
FRANCE
Phone: +33 1 4427 8406
Fax: +33 1 4427 6272
Email: letreut@lmd.jussieu.fr

**Laurent LI**
Laboratoire de Météorologie Dynamique du CNRS
l'Université Pierre et Marie Curie
Case postale 99
4, place Jussieu
F 75252 Paris Cedex 05
FRANCE
Phone: +33 1 44 27 84 09
Fax: +33 1 44 27 62 72
Email: li@lmd.jussieu.fr

**Scott LONGMORE**
IPCC WGI TSU
NOAA Aeronomy Laboratory
DSRC R/AL/8
325 Broadway
Boulder, CO 80305
USA
Phone: +1 303 497 4492
Fax: +1 303 497 5628
Email: longmore@ucar.edu

**Jason LOWE**
Hadley Centre for Climate Prediction & Research
(Reading Unit)
Met Office
Department of Meteorology
University of Reading
Earley Gate
PO Box 243
Reading, RG6 6BB
UNITED KINGDOM
Phone: +44 (0) 118 378 5612
Fax: +44 (0) 118 378 5615
Email: jason.lowe@metoffice.com

**LUO Yong**
National Climate Centre
China Meteorological Administration
46 Zhongguancun Nandajie
Haidian, Beijing 100081
P. R. CHINA
Phone: +86 10 6840 6488
Fax: +86 10 6217 6804
Email: yluo@cma.gov.cn. jakeluo@hotmail.com

**Victor MAGAÑA RUEDA**
Centro De Ciencias De La Atmosfera
Ciudad Universitaria
Universidad Nacional Autonomia De Mexico
Mexico City 04510
MEXICO
Phone: +525 5622 4088
Fax: +525 5616 0789
Email: victormr@servidor.unam.mx

**Syukuro MANABE**
Program in Atmospheric and Oceanic Sciences
Princeton University
P.O.Box CN710
Sayre Hall, Forrestal Campus
Princeton, NJ 08544-0710
USA
Phone: +1 609 258 2790
Fax: +1 609 258 2850
Email: manabe@splash.princeton.edu

**Martin MANNING**
IPCC WGI TSU
NOAA Aeronomy Laboratory
DSRC R/AL/8
325 Broadway
Boulder, CO 80305
USA
Phone: +1 303 497 4479
Fax: +1 303 497 5628
Email: mmanning@al.noaa.gov

**Valérie MASSON-DELMOTTE**
Laboratoire des Sciences du Climat et de l'Environnement
Bat 709 L'Orme des Merisiers
CEA Saclay
F-91 191 Gif sur Yvette cédex
FRANCE
Phone: +33 1 69 08 77 15
Fax: +33 1 69 08 77 16
Email: masson@lsce.saclay.cea.fr

**Bryant MCAVANEY**
Bureau of Meteorology Research Centre
GPO Box 1289K
Melbourne, VIC 3001
AUSTRALIA
Phone: +61 3 9669 4134
Fax: +61 3 9669 4660
Email: b.mcavaney@bom.gov.au

**Mack MCFARLAND**
DuPont Fluoroproducts
CRP 702-2330A
4417 Lancaster Pike
Wilmington, DE 19805
USA
Phone: +1 302 999 2505
Fax: +1 302 999 2816
Email: mack.mcfarland@usa.dupont.com

**Gerald MEEHL**
National Center for Atmospheric Resarch (NCAR)
PO Box 3000
Boulder, CO 80307
USA
Phone: +1 303 497 1331
Fax: +1 303 497 1133
Email: meehl@ucar.edu

**Valentin MELESHKO**
Voeikov Main Geophysical Observatory
Karbyshev Street 7
St. Petersburg, 194021
RUSSIA
Phone: +7 812 247 4390
Fax: +7 812 247 8661
Email: meleshko@main.mgo.rssi.ru

**Ronald MILLER**
NASA Goddard Institute for Space Studies
2880 Broadway
New York, NY 10025
USA
Phone: +1 212 678 5577
Fax: +1 212 678 5552
Email: rmiller@giss.nasa.gov

**Emannuel MPETA**
Tanzania Meteorological Agency
P.O. Box 3056
Dar es Salaam
TANZANIA
Phone: +255 22 211031/2110227
Fax: +255 22 2110231
Email: empeta@meteo.go.tz

**Richard Kombezgani MUGARA**
Zambia Meteorology Department
PO Box 30200
10101 Lusaka
ZAMBIA
Phone: +260 1 252 627
Fax: +260 1 252 728/251 889
Email: zmd@zamnet.zm

**James MURPHY**
Hadley Centre for Climate Prediction & Research
Met Office
FitzRoy Road
Exeter, EX1 3PB
UNITED KINGDOM
Phone: +44 1392 886658
Fax: +44 1392 885681
Email: james.murphy@metoffice.com

**Akira NODA**
Meteorological Research Institute
Japan Meteorological Agency
1-1 Nagamine, Tsukuba, Ibaraki 305-0052
JAPAN
Phone: +81 298 538 608
Fax: +81 298 552 552
Email: noda@mri-jma.go.jp

**Toru NOZAWA**
National Institute for Environmental Studies (NIES)
16-2 Onogawa, Tsukuba, Ibaraki, 305-8506
JAPAN
Phone: +81 298 50 2530
Fax: +81 298 50 2960
Email: nozawa@nies.go.jp

**Bartolomé ORFILA-ESTRADA**
Instituto Nacional de Meteorología (INM)
Ministerio de Medio Ambiente
C/ Leonardo Prieto Castro, 8
28040 Madrid
SPAIN
Phone: +34 91 5819 804
Fax: +34 91 5819 767
Email: orfila@inm.es

**Bette OTTO-BLIESNER**
National Center for Atmospheric Research (NCAR)
PO Box 3000
Boulder, CO 80307
USA
Phone: +1 303 497 1723
Fax: +1 303 497 1348
Email: ottobli@ucar.edu

**Jonathan OVERPECK**
Institue for the Study of Planet Earth
University of Arizona
715 N. Park Ave. 2nd Floor
Tucson, AZ 85721
USA
Phone: +1 520 622 9065
Fax: +1 520 792 8795
Email: jto@u.arizona.edu

**Beenay PATHACK**
Meteorological Services
St Paul Road, Vacoas
MAURITIUS
Phone: +230 6965626
Fax: +230 6861033
Email: meteo@intnet.mu, bpathack@mail.gov.mu

**Serge PLANTON**
Météo-France CNRM
42 Avenue G. Coriolis
31057 Toulouse Cedex
FRANCE
Phone: +33 5 61 07 93 76
Fax: +33 5 61 07 96 10
Email: serge.planton@meteo.fr

**Manuel PONDECA**
Department of Physics
Eduardo Mondlane University
Maputo
MOZAMBIQUE
Phone: +258 1 493376
Fax: +258 1 493377
Email: mspondeca@zebra.uem.mz,
Manuel.Pondeca@noaa.gov

**Stefan RAHMSTORF**
Potsdam Institute for Climate Impact Research (PIK)
PO Box 601203
14482 Potsdam
GERMANY
Phone: +49 331 288 2688
Fax: +9 331 288 2600
Email: rahmstorf@pik-potsdam.de

**Jouni RÄISÄNEN**
Department of Physical Sciences
University of Helsinki
FIN-00014
FINLAND
Phone: +358 9 191 50872
Fax: +358 9 191 50860
Email: jouni.raisanen@helsinki.fi

**V. RAMASWAMY**
NOAA Geophysical Fluid Dynamics Laboratory
Princeton University - Forrestal Campus
PO Box 308
Princeton, NJ 08542-0308
USA
Phone: +1 609 452 6510
Fax: +1 609 987 5063
Email: v.ramaswamy@noaa.gov

**David RANDALL**
Department of Atmospheric Science
Colorado State University
Fort Collins, CO 80523-1371
USA
Phone: +1 970 491 8474
Fax: +1 970 491 8693
Email: randall@atmos.colostate.edu

**Sarah RAPER**
Alfred Wegener Institute
Columbusstrasse
D-27568 Bremerhaven
GERMANY
Phone: +49 47148311363
Fax: +49 47148311149
Email: sraper@awi-bremerhaven.de, s.raper@uea.ac.uk

**Alan ROBOCK**
Department of Environmental Sciences
Rutgers University
14 College Farm Road
New Brunswick, NJ 08901-8551
USA
Phone: +1 732 932 9478
Fax: +1 732 932 8644
Email: robock@envsci.rutgers.edu

**Rémy ROCA**
Laboratoire de Météorologie Dynamique du CNRS
Ecole Normale Supérieure
24, Rue Lhomond
F 75231 Paris Cedex 05
FRANCE
Phone: +33 1 44 32 22 41
Fax: +33 1 43 36 83 92
Email: roca@lmd.polytechnique.fr

**Erich ROECKNER**
Max-Planck-Institut für Meteorologie
Bundesstr. 55
20146 Hamburg
GERMANY
Phone: +49 40 41173 368
Fax: +49 40 41173 298
Email: roeckner@dkrz.de

**Jean-François ROYER**
Météo France CNRM
42 ave. G. Coriolis
31057 Toulouse Cedex
Phone: +33 5 61 07 93 77
Fax: +33 5 61 07 96 10
Email: Jean-francois.Royer@meteo.fr

**Robert SAUSEN**
Institute of Atmospheric Physics
Deutsches Zentrum für Luft- und Raumfahrt e.V. (DLR)
GERMANY
Phone: +49 8153 28 2500
Fax: +49 8153 28 1841
Email: robert.sausen@dlr.de

**Michael SCHULZ**
Laboratoire des Sciences du Climat et de
l'Environnement
Bat 70
91191 Gif-sur-Yvette Cedex
FRANCE
Phone: +33 1 69087731
Fax: +33 1 69087716
Email: schulz@cea.fr

**Cath SENIOR**
Hadley Centre for Climate Prediction and Research
Met Office
FitzRoy Road
Exeter EX1 3PB
UNITED KINGDOM
Phone: +44 1344 856 895
Fax: +44 1344 854 898
Email: cath.senior@metoffice.com

**Madan SHRESTHA**
Department of Hydrology & Meteorology
G.P.O. Box 406
Kathmandu
NEPAL
Phone: +977 1 4262411/4262974
Fax: +977 1 4262348
Email: madanls@hotmail.com, mlshrestha@dhm.gov.np

**Frank SIROCKO**
Universitat mainz
Institut fur Geowissenschaften
55900 Mainz
GERMANY
Phone: +49 6121 39 22714
Email: sirocko@mail.uni-mainz.de

**Silvina SOLMAN**
National Council of Research and Development of Argentina -CIMA (CONICET-UBA)
Ciudad Universitaria
Pabellon II
Piso 2
1428 Buenos Aires
ARGENTINA
Phone: +54 11 4787 2693
Fax: +54 11 4788 3572
Email: solman@cima.fcen.uba.ar

**Susan SOLOMON**
Co-Chair, WGI
NOAA Aeronomy Laboratory
DSRC R/AL/8
325 Broadway
Boulder, CO 80305-3328
USA
Phone: +1 303 497 3483
Fax: +1 303 497 5686/5628
Email: solomon@al.noaa.gov

**Richard SOMERVILLE**
Scripps Institution of Oceanography
University of California, San Diego
Mail Code: 0224
9500 Gilman Drive
La Jolla, CA 92093-0224
USA
Phone: +1 858 534 4644
Fax: +1 858 534 8561
Email: rsomerville@ucsd.edu

**Asgeir SORTEBERG**
Bjerknes Centre for Climate Research
c/o Geophysical Institute
University of Bergen
Allégaten 70
5007 Bergen
NORWAY
Phone: +47 555 82693
Fax: +47 555 89883
Email: asgeirs@gfi.uib.no

**Jayaraman (J.) SRINIVASAN**
Centre for Atmospheric and Oceanic Sciences and Indian Institute of Science
Bangalore 560012
INDIA
Phone: +91 80 22933068/23600450
Fax: +91 80 23600865
Email: jayes@caos.iisc.ernet.in, jayes@mecheng.iisc.ernet.in

**Thomas STOCKER**
Klimamodellierung
Physikalisches Institut - Klima- und Umweltphysik
Universität Bern
Sidlerstrasse 5
3012 Bern, BE
SWITZERLAND
Phone: +41 31 631 44 62
Fax: +41 31 631 87 42
Email: stocker@climate.unibe.ch

**John STONE**
Meteorological Service of Canada
Environment Canada
10, Wellington St.
Hull, PQ K1A 0H3
CANADA
Phone: +1 819 997 3805
Fax: +1 819 994 8854
Email: john.stone@ec.gc.ca

**Ron STOUFFER**
NOAA Geophysical Fluid Dynamics Laboratory
Princeton University - Forrestal Campus
P.O. Box 308, US Route 1
Princeton, NJ 08542
USA
Phone: +1 609 452 6576
Fax: +1 609 987 5063
Email: Ronald.Stouffer@noaa.gov

**Akimasa SUMI**
Center for Climate System Research
University of Tokyo
4-6-1 Komaba, Meguro-ku, Tokyo 153-8904
JAPAN
Phone: +81 3 5453 3951
Fax: +81 3 5453 3964
Email: sumi@ccsr.u-tokyo.ac.jp

**Olivier TALAGRAND**
Laboratoire de Météorologie Dynamique du CNRS
Ecole Normale Supérieure
24, Rue Lhomond
F 75231 Paris Cedex 05
FRANCE
Phone: +33 1 44 32 22 45
Fax: +33 1 43 36 83 92
Email: talagran@lmd.ens.fr

**Melinda TIGNOR**
IPCC WGI TSU
NOAA Aeronomy Laboratory
DSRC R/AL/8
325 Broadway
Boulder, CO 80305
USA
Phone: +1 303 497 7072
Fax: +1 303 497 5628
Email: tignor@ucar.edu

**George TSELIOUDIS**
NASA Goddard Institute for Space Studies & Columbia University Department of Applied Physics
2880 Broadway
New York, NY 10025
USA
Phone: +1 212 678 5578
Fax: +1 212 678 5552
Email: gtselioudis@giss.nasa.gov

**Rob VAN DORLAND**
Royal Netherlands Meteorological Institute (KNMI)
PO Box 201
3730 AE, De Bilt
THE NETHERLANDS
Phone: +31 30 2206 775
Fax: +31 30 2210 407
Email: dorlandv@knmi.nl

**Evgeny VOLODIN**
Institute for Numerical Mathematics
Russian Academy of Science
Gubkina 8
Moscow 119991
GSP-1
RUSSIA
Phone: +7 095 9383904
Fax: +7 095 9381821
Email: volodin@inm.ras.ru

**Andrew WEAVER**
School of Earth and Ocean Sciences
University of Victoria
PO Box 3055
Victoria BC, V8W 3P6
CANADA
Phone: +1 250 472 4001
Fax: +1 250 472 4004
Email: weaver@uvic.ca, wlewis@uvic.ca

**Keith WILLIAMS**
Met Office
FitzRoy Road
Exeter EX1 3PB
UNITED KINGDOM
Phone: +44 (0)1392 886905
Fax: +44 (0)1392 885681
Email: keith.williams@metoffice.com

**Richard WOOD**
Hadley Centre for Climate Prediction & Research
Met Office
FitzRoy Road
Exeter EX1 3PB
UNITED KINGDOM
Phone: +44 (0)1392 886641
Fax: +44 (0)1392 885681
Email: richard.wood@metoffice.com

**Jun-Ichi YANO**
Laboratoire de Meteorologie Dynamique du CNRS
l'Université Pierre et Marie Curie
Case postale 99
4, place Jussieu
F 75252 Paris Cedex 05
FRANCE
Phone: +33 1 44 27 84 04
Fax: +33 1 44 27 62 7
Email: jun-ichi.yano@lmd.jussieu.f